1-1-2012

Silec: A New Tool to Study Mitochondrial and Metabolic Disease

Sankha Subhra Basu
University of Pennsylvania, sbasu@mail.med.upenn.edu

Silec: A New Tool to Study Mitochondrial and Metabolic Disease

Abstract
Coenzyme A (CoA) and CoA thioesters are central to numerous metabolic pathways. However, the inability to synthesize isotopically labeled CoA has limited analytical methods to measure these compounds. In this thesis, we developed Stable Isotope Labeling with Essential nutrients in Cell culture (SILEC), a method to generate isotopically labeled CoA derivatives by growing cells in a labeled CoA precursor, [$^{13}C^{15}N$]-pantothenate. Labeled CoA derivatives were used as internal standards in a stable isotope dilution liquid chromatography-mass spectrometry (LC-MS) method to measure changes in short chain acyl-CoA species. This assay was also adapted to include measurement of glutathione-CoA (CoASSG), a mixed disulfide increased in mitochondrial oxidative stress. Menadione significantly increased intracellular levels of CoASSG, and decreased levels of CoASH through the formation of CoA-menadione adduct. In addition, rotenone, an organic pesticide and potent complex I inhibitor, induced a dose-dependent decrease in succinyl-CoA and increase in beta-hydroxybutyryl-CoA (BHB-CoA) in multiple human cell lines, as well as inhibited glucose-derived acetyl-CoA and succinyl-CoA biosynthesis. This SILEC assay was further adapted for use in freshly isolated human platelets to assess metabolic changes in Friedreich's Ataxia (FA), an inherited mitochondrial disease caused by mutations in the frataxin gene. FA patients were found to have significantly decreased acetyl-CoA: succinyl-CoA ratio, consistent with an *in vitro* siRNA knockdown model of frataxin. Finally, platelets were demonstrated to serve as a powerful *ex vivo* metabolic and toxicologic challenge platform evidenced by treatment with propionate, rotenone and a number of stable isotope metabolic tracers. Together, these methods provide a paradigm for the discovery of novel biomarkers for metabolic and mitochondrial disease.

Degree Type
Dissertation

Degree Name
Doctor of Philosophy (PhD)

Graduate Group
Pharmacology

First Advisor
Ian A. Blair

Keywords
Coenzyme A, Mass Spectrometry, Metabolism, Mitochondria, Stable Isotope

Subject Categories
Analytical Chemistry | Biochemistry | Pharmacology

SILEC: A NEW TOOL TO STUDY MITOCHONDRIAL AND METABOLIC DISEASE

Sankha S. Basu

A DISSERTATION

in

Pharmacology

Presented to the Faculties of the University of Pennsylvania in Partial

Fulfillment of the Requirements for the Degree of Doctor of Philosophy

2012

Supervisor of Dissertation:

Signature: _____
Ian A. Blair, PhD, A.N. Richards Professor of Pharmacology

Graduate Group Chairperson:

Signature: _____
Vladimir Muzykantov, MD, PhD, Professor of Pharmacology

Dissertation Committee:
Trevor Penning, PhD, Professor of Pharmacology
Harry Ischiropoulos, PhD, Research Professor of Pediatrics
Jeff Field, PhD, Professor of Pharmacology
Alexander Whitehead, PhD, Professor of Pharmacology

To my parents,

whose sacrifices and inspiration made

this possible.

“Far better is it to dare mighty things, to win glorious triumphs, even though checkered by failure...than to rank with those poor spirits who neither enjoy nor suffer much, because they live in a gray twilight that knows not victory nor defeat.”

-Theodore Roosevelt

Acknowledgments

First, I would like to thank my thesis advisor, Dr. Ian Blair, whose continual encouragement has laid the foundation for my future as an independent investigator. I would also like to thank Dr. Stacy Gelhaus and Dr. Clementina Mesaros, who have helped me transition from molecular biology to analytical chemistry. In addition, I would like to thank Dr. Angela Wehr and Matthew Macdonald, who have helped provide scientific and personal support throughout my time in the lab. I would like to extend special thanks to Christine Shwed, who has been integral in not only improving the research environment, but whose tireless efforts have enriched our lab experience. Lastly, I would also like to thank all former and current members of the Blair Lab, whose research has been integral to much of the work presented in this thesis.

I would like to acknowledge a number of research collaborators. I would like to extend a special thanks to Eric Deutsch and Dr. David Lynch for their help on the frataxin and Friedreich's Ataxia studies, along with all volunteers who have provided platelets for these studies. I would like to thank Dr. Alec Schmaier, for his guidance in the platelet studies, Andrew Worth, for his help in developing the LC-MS organic acid method and Ellyn Boukus for her help with mass isotopomer distribution analysis. I would like to thank Dr. Ronald Carnemolla from Vladimir Muzykantov's lab for helping with the SILEC insect cell culture experiments, and Dr. Michael Schupp from Mitch Lazar's lab for providing mouse liver for the SILEC tissue experiments. Finally, I would like to thank Margie Maronski and Dr. Mark Dichter for providing cortical rat neurons for the rotenone studies.

I would like to thank my thesis committee members, Dr. Trevor Penning, Dr. Harry Ischiropoulos, Dr. Steve Whitehead and Dr. Jeff Field for their insights and guidance. In particular, I would like to thank Dr. Penning who served as my committee chair as well as a mentor in the field of toxicology. I would also like to thank Dr. Skip Brass and Maggie Krall for their support in providing a tremendous environment to grow as a physician-scientist. I would like to thank Barbara Zolotorow for her help in organizing the training grant, as well as the National Institutes of Health (NIH) for funding which made this research possible. Finally, I would like to thank my friends and family who have been tremendously supportive and patient during the graduate school process.

Abstract

SILEC: A NEW TOOL TO STUDY

MITOCHONDRIAL AND METABOLIC DISEASE

Sankha S. Basu

Ian A. Blair, PhD

Coenzyme A (CoA) and CoA thioesters are central to numerous metabolic pathways. However, the inability to synthesize isotopically labeled CoA has limited analytical methods to measure these compounds. In this thesis, we developed Stable Isotope Labeling with Essential nutrients in Cell culture (SILEC), a method to generate isotopically labeled CoA derivatives by growing cells in a labeled CoA precursor, [$^{13}C_3{}^{15}N$]-pantothenate. Labeled CoA derivatives were used as internal standards in a stable isotope dilution liquid chromatography-mass spectrometry (LC-MS) method to measure changes in short chain acyl-CoA species. This assay was also adapted to include measurement of glutathione-CoA (CoASSG), a mixed disulfide increased in mitochondrial oxidative stress. Menadione significantly increased intracellular levels of CoASSG, and decreased levels of CoASH through the formation of CoA-menadione adduct. In addition, rotenone, an organic pesticide and potent complex I inhibitor, induced a dose-dependent decrease in succinyl-CoA and increase in β-hydroxybutyryl-CoA (BHB-CoA) in multiple human cell lines, as well as inhibited glucose-derived acetyl-CoA and succinyl-CoA biosynthesis. This SILEC assay was further adapted for

use in freshly isolated human platelets to assess metabolic changes in Friedreich's Ataxia (FA), an inherited mitochondrial disease caused by mutations in the frataxin gene. FA patients were found to have significantly decreased acetyl-CoA: succinyl-CoA ratio, consistent with *in vitro* siRNA knockdown model of frataxin. Finally, platelets were demonstrated to serve as a powerful *ex vivo* metabolic and toxicologic challenge platform evidenced by treatment with propionate, rotenone and a number of stable isotope metabolic tracers. Together, these methods provide a paradigm for the discovery of novel biomarkers for metabolic and mitochondrial disease.

Table of Contents

List of Tables

List of Illustrations

Abbreviations

ACP	Acyl carrier protein
AD	Alzheimer's disease
aKG	α-ketoglutarate
BHB	β-hydroxybutyrate
BHB-CoA	β-hydroxybutyryl-CoA
CID	Collision-induced dissociation
CoA	Coenzyme A
CoASSG	Glutathione-CoA
csFBS	Charcoal-dextran stripped FBS
dFBS	Dialyzed FBS
DMEM	Dulbecco's modified eagle medium
DMSO	Dimethyl sulfoxide
ESI	Electrospray ionization
$FADH_2$	Flavin adenine dinucleotide (reduced)
FAO	Fatty acid oxidation
FBS	Fetal bovine serum
GSH	Glutathione
GSSG	Oxidized glutathione
HBSS	Hank's Buffered Salt Solution
H358	Human bronchioalveolar carcinoma cells
Hepa 1c1c7	Murine hepatoma cells
HepG2	Human hepatocellular carcinoma cells
HMG-CoA	3-hydroxymethyl-3-glutyryl-CoA

HP	High performance
ISC	Iron sulfur cluster
LC	Liquid chromatography
M#	Mass isotopomer (M+#)
MS	Mass spectrometry
MNQ	Menadione
mtDNA	Mitochondrial DNA
NADH	Nicotinamide adenine dinucleotide (reduced)
nDNA	Nuclear DNA
NMR	Nuclear magnetic resonance
OXPHOS	Oxidative phosphorylation
PD	Parkinson's disease
PRP	Platelet-rich plasma
S2	Drosophila Schneider cells
SH-SY5Y	Human derived neuroblastoma cells
SILAC	Stable Isotope Labeling by Amino acids in Cell culture
SILAP	Stable Isotope Labeled Proteome
SILEC	Stable Isotope Labeling by Essential nutrients in Cell culture
SPE	Solid phase extraction
SRM	Selective reaction monitoring
SSA	Sulfosalicylic acid
TCA	Trichloroacetic acid
uFBS	Undialyzed FBS

Chapter 1: The metabolic role of CoA and developments in the analytical measurement of CoA derivatives

Despite the discovery of mitochondria more than one hundred years ago, biological advances over the past half-century have been largely defined by the discovery of DNA, the foundation of genetic theory, and the elucidation of the human genome. [1, 2] The parallel development of mitochondrial biology has been largely overshadowed until recently, as both scientists and clinicians have begun to appreciate the wider role mitochondria play not only in metabolism, but also in the pathogenesis of a wide variety of human diseases.[3-5] The ability to rigorously and quantitatively measure changes in mitochondrial metabolites is critical in understanding mitochondrial pathology and finding biomarkers for many of these diseases.[6] A brief introduction is provided for the reader to better appreciate the research presented in this thesis.

1.1 Mitochondria and metabolic disease

Mitochondria are specialized eukaryotic organelles that provide many of the bioenergetic requirements of the cell.[7] Unlike most organelles, mitochondria contain an inner and outer membrane. Enclosed within the inner membrane is the mitochondrial matrix, the location of various metabolic processes such as the Krebs cycle, fatty acid oxidation (FAO), and oxidative phosphorylation (OXPHOS) (Figure 1.1). Eukaryotic cells contain hundreds to thousands of mitochondria with a wide range of OXPHOS capacity, depending on the energy requirements of the tissue.[8, 9] Also, unlike other organelles, mitochondria contain their own DNA (mtDNA), which is distinct from nuclear DNA (nDNA).[10] This peculiarity of mitochondria is explained by the generally

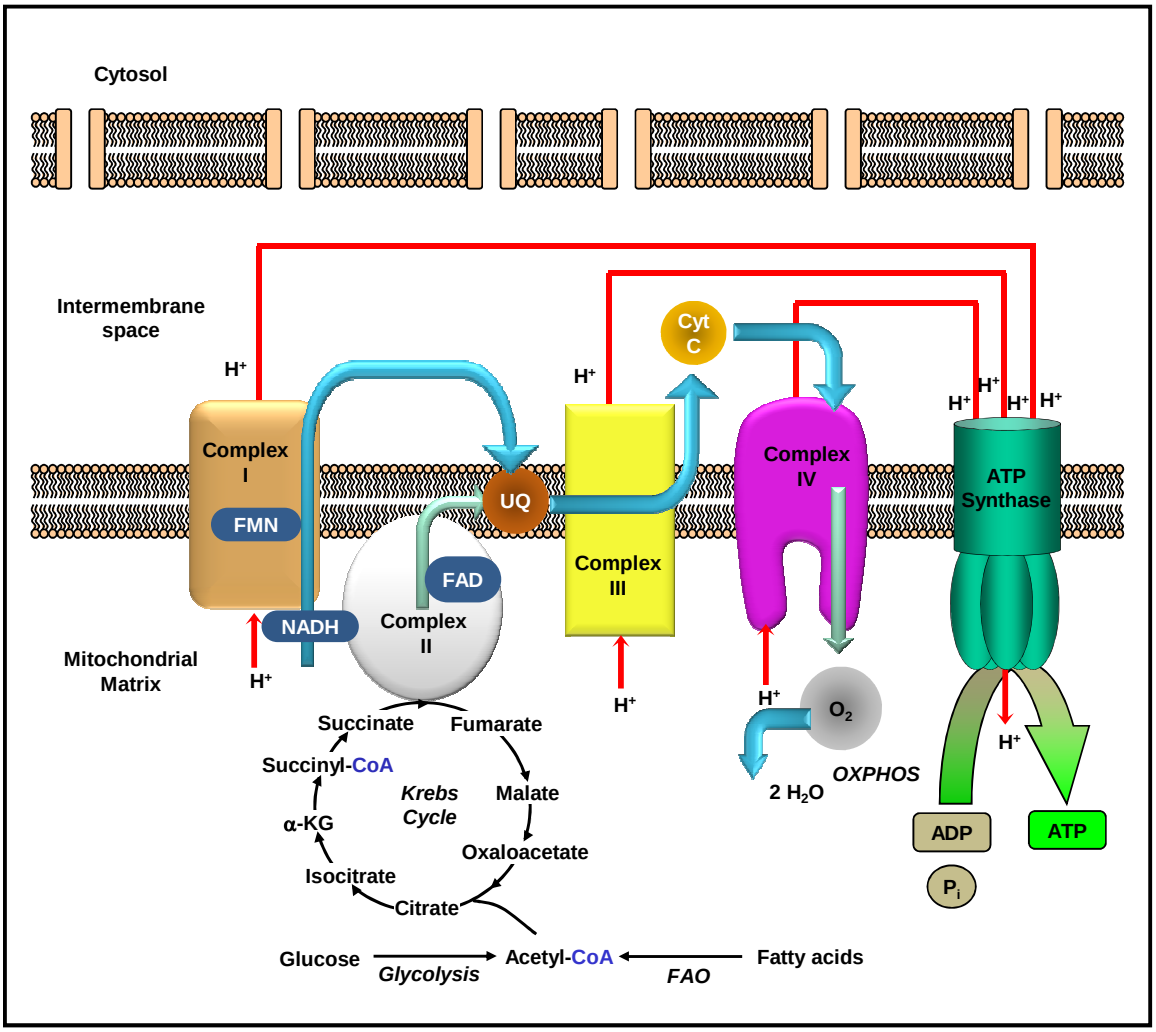

Figure 1.1 Electron transport chain and oxidative phosphorylation. OXPHOS is accomplished by a set of five enzymatic complexes (I-V). Complex I is normally the point of entry for the majority of electrons in the respiratory chain that eventually cause sequential 1-electron reductions of molecular oxygen to water. In addition, complex I translocates protons generated by the Krebs cycle from the mitochondrial matrix to the intermembrane space. This establishes the electrochemical gradient required for ATP biosynthesis. Complex I (NADH dehydrogenase) and complex II (succinate dehydrogenase) use NADH and $FADH_2$, respectively, to reduce ubiquinone. This subsequently reduces cytochrome C (complex III) and complex IV, ultimately reducing molecular oxygen to form water. Cumulatively, complexes I-IV generate a proton gradient in the mitochondrial intermembrane space, which reenter the matrix through ATP synthase (Complex V) to form ATP from ADP. In this way, chemical energy from carbon sources is converted into ATP, the universal energy currency used in the cell.

accepted endosymbiotic theory of mitochondrial origin, which proposes that mitochondria were originally OXPHOS-capable eubacteria that formed a symbiotic relationship with another microorganism providing increased energy efficiency in exchange for structural and nutritional advantages.[7] It is believed that these eubacteria eventually evolved to become the modern-day eukaryotic mitochondria. Plant chloroplasts, which also contain their own DNA, are believed to have arisen through a similar mechanism.[11] It has been suggested that this mitochondrial evolutionary origin itself may be a factor in the pathogenesis of various diseases.[12]

A number of genetic diseases have been linked to mutations in mtDNA.[4] Although mtDNA contains only 13 genes,[13] compared to the greater than 30,000 genes in nDNA, mutations in these genes can lead to debilitating tissue-specific diseases, most notably several optic neuropathies.[14] Curiously, all mitochondria are inherited from the egg rather than the sperm so mitochondrial diseases have a unique maternal inheritance pattern.[15] Due to the central role of mitochondria in metabolism and bioenergetics, it is not surprising that mitochondrial dysfunction often leads to pathologic features in tissues with higher metabolic energy demands.[16] In addition to diseases with mitochondrial inheritance, mitochondrial dysfunction has been implicated in diabetes,[17] heart disease,[18] cancer,[19] Alzheimer's disease (AD),[20] Parkinson's disease (PD),[21] autism,[22] and numerous other neurological and metabolic diseases.[23, 24] In addition, many environmental toxins, pesticides in particular, are thought to exhibit their toxicity through inhibition of mitochondrial function.[25, 26] As a result, environmental insults, particularly in the context of genetic predispositions may be the etiological factor of many diseases of idiopathic origin. There is also mounting evidence clinical manifestations such as

idiosyncratic adverse drug reactions may also involve metabolic and mitochondrial toxicity.[27] Central to many of these processes is the molecule coenzyme A (CoA).

1.2 Coenzyme A (CoA)

CoA is a ubiquitous intracellular thiol and coenzyme common to all forms of life,[28] serving both metabolic and detoxification functions, ranging from fatty acid metabolism to xenobiotic acetylation.[29] In fact, it is estimated that CoA is used by 4% of all cellular enzymes.[30] CoA is composed of three components: an ATP moiety, a cysteinyl group, and a pantethine group, which originates from pantothenate (vitamin B5). In addition to CoA, pantothenate is utilized in the synthesis of the prosthetic group in acyl-carrier protein (ACP).[31] Plants, fungi and many prokaryotes are capable of synthesizing pantothenate from its constituent amino acids, valine and aspartate (Figure 1.2).[32, 33] Animals, however, are not capable of *de novo* pantothenate synthesis and as a result, require it in their diet.[34] From pantothenate, CoA is synthesized through five enzymatic steps.[35] The first enzyme, pantothenate kinase, which converts pantothenate to pantethine-phosphate, is the rate-determining step of CoA biosynthesis.[36] Pantothenate deficiency is rare in humans, but can manifest clinically in neurological, gastrointestinal and metabolic symptoms, all of which can be reversed by pantothenate supplementation.[37]

CoA primarily functions as an acyl carrier molecule, through a thioester linkage between the acyl group and the free thiol of CoASH (reduced CoA). There are numerous CoA-derivatives, including a thioester for most individual fatty acids (a comprehensive list is provided in the appendix, Table A.1). One important class of acyl-CoA species is

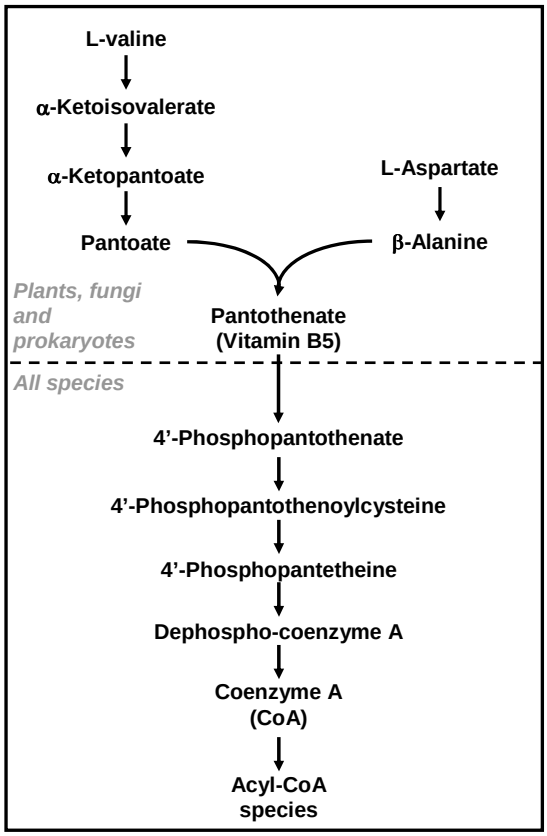

Figure 1.2 Pantothenate and CoA biosynthesis. As illustrated here, plants, fungi and many prokaryotes are capable of de novo pantothenate synthesis from valine and aspartate, while other organisms require it as an essential nutrient. Pantothenate is subsequently converted to CoA through the sequential action of five enzymes. CoA can then be incorporated into various acyl-CoA thioesters. Previously published in Basu, Blair. *Nat Protocols*, 2011.

the short chain acyl-CoA thioester class, the measurement of which is the focus of this thesis. Figure 1.3 illustrates the role of some of these compounds in relation to the Krebs cycle. Of all short chain acyl-CoA species, acetyl-CoA is most prominent due its diverse functions. Pyruvate formed by glycolysis is converted irreversibly by pyruvate dehydrogenase into acetyl-CoA, which condenses with oxaloacetate to form citrate, serving as a carbon entry point in the Krebs cycle. Each turn of the cycle produces reducing equivalents in the form of NADH and $FADH_2$, which are used in OXPHOS to produce ATP (Figure 1.1). Another important CoA thioester is succinyl-CoA, a Krebs cycle intermediate formed from α-ketoglutarate (aKG) by the action of aKG dehydrogenase. Succinyl-CoA is then converted by succinyl-CoA synthetase into succinate, which along with $FADH_2$ is utilized by succinate dehydrogenase (complex II) to reduce ubiquinone and generate fumarate (Figure 1.1). As compared to glycolysis, in which a single glucose molecule can produce a net of 2 ATP, the coupled action of the Krebs cycle and OXPHOS produces 36-38 ATP from a single molecule of glucose, thereby providing a tremendous increase in energy efficiency. This improvement is particularly striking in the case of β-oxidation of fatty acids (FAO). In FAO, fatty acids which are often transported or stored as triglycerides are broken down through a sequential process. In each cycle, the fatty acyl-CoA is shortened by two carbons, which are released as acetyl-CoA and a new acyl-CoA thioester, two carbons shorter than the original, is formed. The carbons from acetyl-CoA can then enter the Krebs cycle as previously described, while the shortened acyl-CoA can undergo another round of oxidation. The penultimate CoA thioester formed from even chained fatty acids is BHB-CoA. The complete oxidation of a single palmitate molecule can provide 108 ATP. On

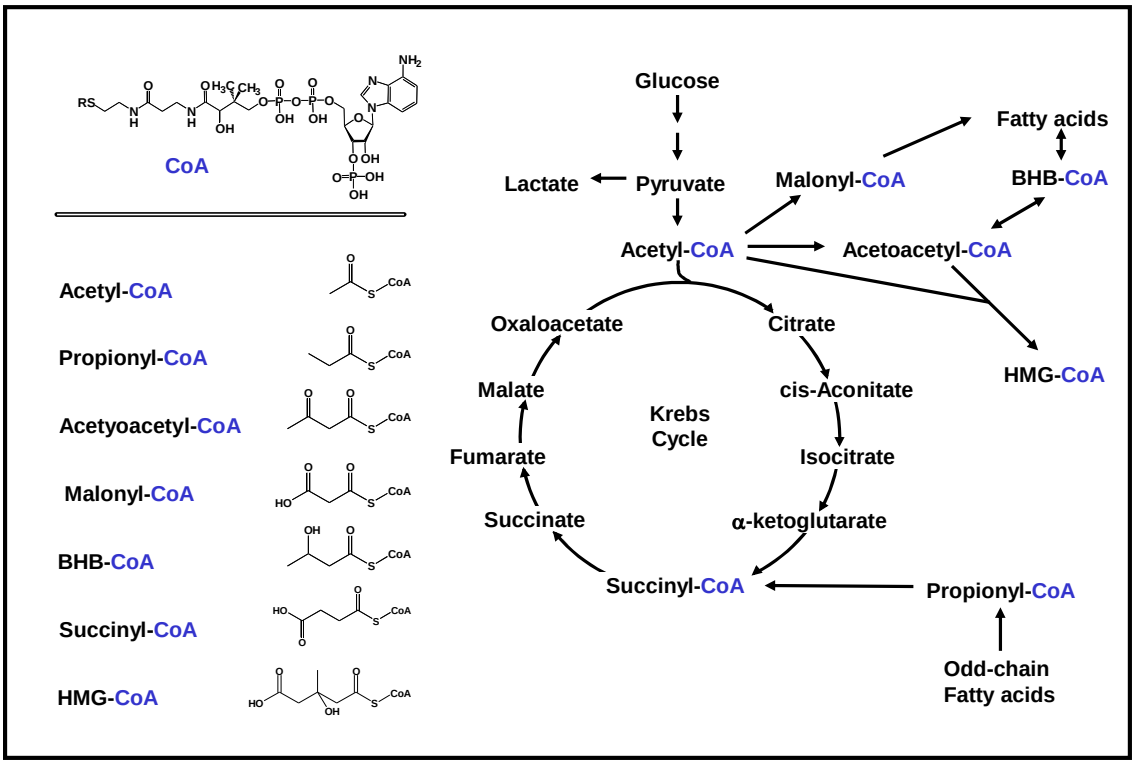

Figure 1.3 Short chain acyl-CoA thioesters and the Krebs cycle. The structure of CoA and various important CoA thioesters (blue) and their relative position in relation to the Krebs cycle are illustrated.

the other hand, acetyl-CoA can be converted to malonyl-CoA as the first step in fatty acyl synthesis. In the case of odd chain fatty acids, the last acyl-CoA thioester is propionyl-CoA, which contains three carbons. This can subsequently enter the Krebs cycle through succinyl-CoA. 3-hydroxymethyl-3-glutyryl-CoA (HMG-CoA) is another critically important short chain acyl-CoA thioester involved in several metabolic pathways including ketogenesis and cholesterol synthesis. In fact, HMG-CoA synthase is the rate limiting enzyme of ketogenesis,[38] a metabolic state in which ketone bodies are produced by the liver to serve as alternative energy sources to glucose for the brain, and is induced by starvation or high protein and low carbohydrate diets. HMG-CoA reductase is the rate limiting enzyme in cholesterol synthesis and is the target of the widely prescribed statin class of drugs (HMG-CoA reductase inhibitors).[39] Although these are only a few of the many CoA thioesters, we have primarily focused on these particular species due to their critical importance in metabolism.

In addition to functioning as a fatty acyl-carrier, CoA is used in several other capacities as well, including playing a prominent role in detoxification. One such role is serving as a cofactor in phase II acetylation, where the acetate from acetyl-CoA is activated and transferred to the metabolite. In fact, it was the acetylation properties of CoA that led to its initial discovery by Fritz Lipmann in 1945,[40] (the "A" in CoA was used to represent "activation of acetate").[41] Also, like glutathione (GSH), CoASH can react with xenobiotic compounds and electrophiles.[42, 43] It has also been shown that CoASH is the major reducing intracellular thiol in *Staphylococcus Aureus*, likely due to the fact that these bacteria do not contain GSH.[44] For this reason, along with the structural elucidation of the enzymes in CoA synthesis,[34] there has been a renewed

interest in this biosynthetic pathway for potential antimicrobial drug targets.[33] Interestingly, the mixed disulfide glutathione-CoA (CoASSG) has also been shown to form *in vivo*,[45-48] though its exact role and mechanism of formation remains unclear.[49-52] However, it has been shown that the ratio of CoASSG: CoASH is increased in settings of mitochondrial oxidative stress such as hyperoxia[53, 54] and seizures,[55] indicating that like GSSG:GSH ratio, which is used as a marker of *cellular* oxidative stress, CoASSG: CoASH ratio may serve as an indicator of *mitochondrial* oxidative stress. Still, new roles for CoA continue to be discovered, as is exemplified by the recent discovery of CoA-linked RNA adducts[56] as well as CoA-electrophile adducts.[43] The expansive roles of CoA as well as studies showing that levels of CoA species are perturbed in many pathological settings including diabetes,[57, 58] as well as various inherited metabolic disorders,[59-64] has revitalized efforts to develop methods to measure these species.

1.3 Measuring CoA

Given that CoA-activated compounds can differ so dramatically in their chemical properties, the class of CoA species to be measured must be considered first. These can be broken down as follows: reduced CoA (CoASH), acyl-CoA thioesters, CoA-disulfides, and other CoA-activated compounds, which may include a broad number of CoA adducts bound to exogenous or endogenous electrophiles. Although there is a continuum in the length of the carbon tails of acyl-CoA thioesters, these can be basically broken down into short- (up to 5 carbons), medium- (up to 10 carbons), long- (up to 20 carbons) and very long-chain (more than 20 carbons) acyl-CoA species. Due to differences in chemical and physical properties of these different acyl-CoA species, different classes of CoA

derivatives require different extraction methods. In general, short chain acyl-CoA species are acid soluble and if a biological sample is sonicated or homogenized in a strong acid solution, the acid soluble short chain acyl-CoA species can be extracted.[65, 66] This can be accomplished by using sulfosalicylic acid (SSA), perchloric acid or trichloroacetic acid (TCA). In general, a 10% TCA solution was the most optimal for short chain acyl-CoA extraction.[67] After acid extraction, these short chain acyl-CoA species can be further purified using solid phase extraction (SPE) or repeated ether extraction to remove the TCA. SPE extraction was generally favorable for both ease and cost factors.[67] For medium, long and very long chain acyl-CoA molecules, performing a liquid-liquid extraction with an organic solvent is ideal.[68-70]

Also, the source of CoA is important as well. CoA molecules can be measured from whole cells (or tissues), or from isolated mitochondria. While the ability to isolate and study viable mitochondria set the foundation for much of our understanding of mitochondrial biology,[71] the act of isolating mitochondria can generate oxidative stress leading to artifactual changes attributed to sample processing.[72] More importantly, when developing biomarker studies to measure CoA changes, whole tissues or cells (such as fibroblasts or blood cells) need to be extracted since CoA species are intracellular. Further isolation of mitochondria from these cells would not only introduce oxidative stress, but would also be laborious and clinically impractical. Therefore, whole cell assays were the chosen method in our work.

Like mitochondria, the discovery of CoA also preceded the discovery of the double helix. CoA was first described by Fritz Lipmann in 1945, for which he was eventually awarded the Nobel Prize in Medicine in 1953.[41] Over the next forty years, a

significant amount of research was focused on the identifying, separating and accurately measuring acyl-CoA thioesters in biological systems. The majority of methods developed through these decades focused on high performance (HP) liquid chromatography (LC) coupled with ultraviolet (UV) detection.[65, 66, 73] CoA species exhibit a characteristic UV absorption at 254 nm. Since all CoA thioesters contain the CoA moiety, they can be readily detected if properly separated. However, because UV detection is used, complete baseline separation is required for measurement of CoA species. To accomplish this for short-chain acyl-CoA species, high concentrations of phosphate buffer were needed to successfully separate a broad number of these species.[65] Additional LC-UV methods were also made for other CoA derivatives. One problem with such methods is lack of specificity due to co-eluting peaks. More importantly, however, even the best methods had a sensitivity which was generally in the high picomolar to single-digit nanomolar range. While this may be adequate from larger pieces of animal tissue containing abundant CoA species, this is inadequate for practicable *in vitro* analysis or clinical studies involving much smaller amounts of biological material. Over the next two decades, significant technogical improvements in mass spectrometry (MS) have allowed not only increased specificity but also dramatic improvements in sensitivity of CoA analysis. These LC-MS methods have been used in the measurements of short chain acyl-CoA species,[67, 74-76] as well as medium and long chain acyl-CoA species.[68-70] Although MS methodology has notable advantages in sensitivity and specificity, it also can present variable precision and accuracy, especially with electrospray ionization (ESI).[77, 78] Stable isotope dilution mass spectrometry can be used to overcome this problem.

1.4 Stable isotope dilution MS

LC-selected reaction monitoring (SRM)/MS provides a highly sensitive and specific platform to measure a broad range of analytes in a variety of complex biological matrices.[79] In addition, advancements in high resolution mass MS[80, 81] as well as the development of more dynamic software platforms[82-84] have provided scientists the capability of measuring thousands of different analytes in a single run, making MS the optimal methodology for robust high-throughput metabolomic and proteomic analyses.[85, 86] Nonetheless, appropriate internal standards are critical for the success of any MS-based method, particularly when measuring endogenous metabolites in biological samples, due to matrix effects on analyte stability, extraction, and ionization efficiency.[77, 78, 87-90] To account for these effects, an internal standard that faithfully reproduces the biological and chemical properties of the analyte of interest is needed.[91] Stable isotope analogs represent the best internal standards for MS-based analyses because they have the same biological and physicochemical properties as the analyte of interest, but can still be distinguished by a mass spectrometer.[91]

1.5 Stable Isotope Labeling with Amino acids in Cell culture (SILAC)

Difficulty in chemically synthesizing stable isotope analogs of complex biological molecules has spurred the development of techniques to generate these standards in biological systems.[92-94] In the case of proteins, a method called SILAC has been developed (Figure 1.4).[95] After generation of isotopically labeled cells, one of two possible experimental modalities can be used. In the "classical" SILAC approach, an

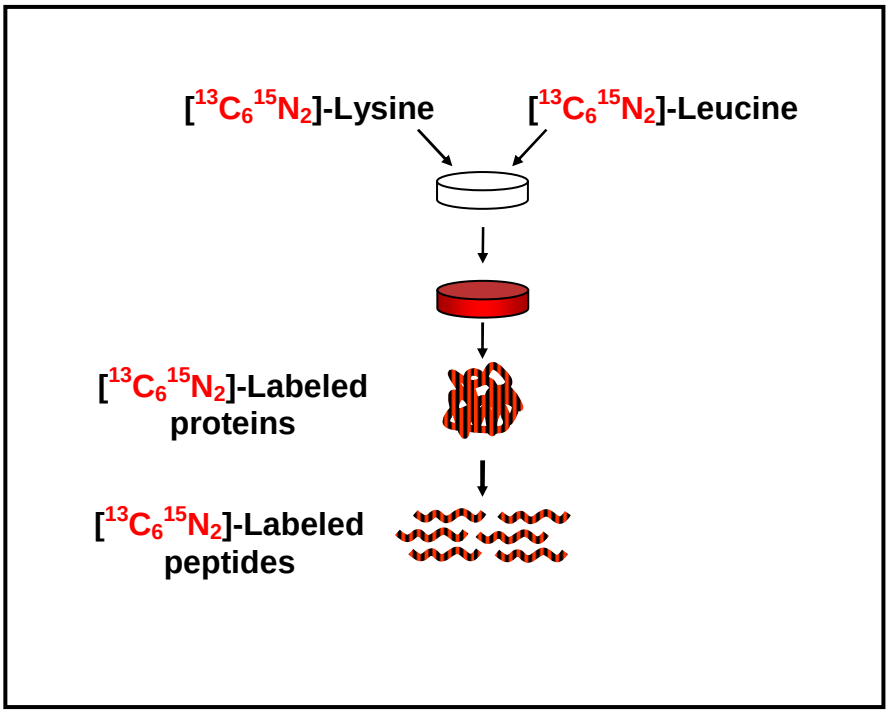

Figure 1.4 Stable Isotope Labeling with Amino acids in Cell culture (SILAC). In this method, cells are grown in the presence of a stable isotope-labeled essential amino acid such as lysine or leucine, with the unlabeled form specifically omitted. The inability to synthesize these essential amino acids *de novo* results in their exclusive uptake and incorporation into cellular proteins. After serial passages in this media, greater than 99% of these residues are labeled. These can then be used for stable isotope dilution MS.

equal number of labeled and unlabeled cells are subjected to different stimuli, mixed, processed together and analyzed by MS.[95] Alternatively, the labeled cells can be lysed to produce a stable isotope labeled proteome internal standard (SILAP),[96] which can then be spiked into different experimental samples to normalize the measured analytes for relative quantitation.[97-99] The advantage of the latter approach is the ability to apply these standards to both *in vitro* or *in vivo* samples, as well as avoiding any biological perturbations introduced by growing the cells in labeled amino acids.

Like proteins, CoA and other endogenous metabolites have been difficult to chemically synthesize and consequently labeled analogs for many of these compounds are not commercially available. In the following chapter, we present a novel methodology to generate isotopically labeled CoA internal standards.

Chapter 2: The development of Stable Isotope Labeling by Essential Nutrients in Cell Culture (SILEC) for preparation of labeled CoA and its thioesters

2.1 Abstract

While CoA and acyl-CoA thioester derivatives are central players in numerous metabolic pathways, the lack of a commercially available isotopically labeled CoA limits the development of rigorous stable isotope dilution MS-based methods. In this chapter, we adapted SILAC methodology to biosynthetically generate stable isotope labeled CoA and CoA-thioester analogs for use as internal standards in an LC-SRM/MS assay. This was accomplished by incubating murine hepatoma cells (Hepa 1c1c7) in media in which pantothenate, a CoA precursor, was replaced with [$^{13}C_3{}^{15}N_1$]-pantothenate. Efficient incorporation into various CoA species was optimized to > 99% [$^{13}C_3{}^{15}N_1$]-pantothenate labeling after three passages. Charcoal-dextran stripped FBS (csFBS) was found to be optimal for serum supplementation due to its lower contaminating unlabeled pantothenate content. In addition, a method to generate specific CoA derivatives was demonstrated by treating SILEC- labeled cells with propionate to generate [$^{13}C_3{}^{15}N_1$]-propionyl-CoA. Labeled cells were harvested, and stable isotope labeled CoA species were extracted and utilized as internal standards for CoA thioester analysis in cell culture as well as in mouse tissue. This SILEC methodology can serve as a paradigm for using vitamins and other essential nutrients to generate stable isotope standards that cannot be readily synthesized.

Portions of this chapter have been previously published (Basu et al. *Anal Chem*, 2011; Basu SS, Blair IA. *Nat Protocols*, 2011).

2.2 Introduction

CoA, a ubiquitous fatty acyl carrier plays a critical role in many metabolic and mitochondrial processes.[35, 100, 101] MS/MS represents the optimal platform for developing CoA analysis due to its sensitivity and specificity. Also, when subjected to collision-induced dissociation (CID), CoA derivatives exhibit a characteristic fragmentation pattern, breaking at the ATP moiety, resulting in product ions with a neutral loss of 507 amu (Figure 2.1A).[76, 102] Typical parent protonated molecular ions observed for endogenous CoASH and its derivatives in a constant neutral loss/MS experiment are presented in Figure 2.1B. The use of this type of analysis not only facilitates LC-SRM/MS method development, but also allows for more specific CoA discovery experiments. However, the lack of isotopically labeled CoA has limited the development of comprehensive stable isotope dilution MS/MS analysis of CoA-containing compounds.

In this chapter, our focus is in generating stable isotope labeled CoASH and short-chain acyl-CoA species, which would not only improve our ability to study metabolism,[53, 54, 58, 103] but also aid in the diagnosis of various metabolic diseases.[60-64, 104] The use of labeled standards is particularly important, since cellular thiols can be rapidly oxidized or react with both intracellular and extracellular molecules.[105-107] To biosynthetically generate labeled CoA standards, we developed SILEC, a method similar to SILAC, except that a labeled vitamin, pantothenate, is used instead of labeled amino acids.[93] Unlike plants, fungi, and most prokaryotes, animals are not capable of *de novo* pantothenate synthesis.[33] As a result, pantothenate is a dietary requirement and a necessary cell culture media supplement. After uptake, pantothenate is converted to CoA through five enzymatic steps.[35] By growing cells in the presence of [$^{13}C_3{}^{15}N$]-

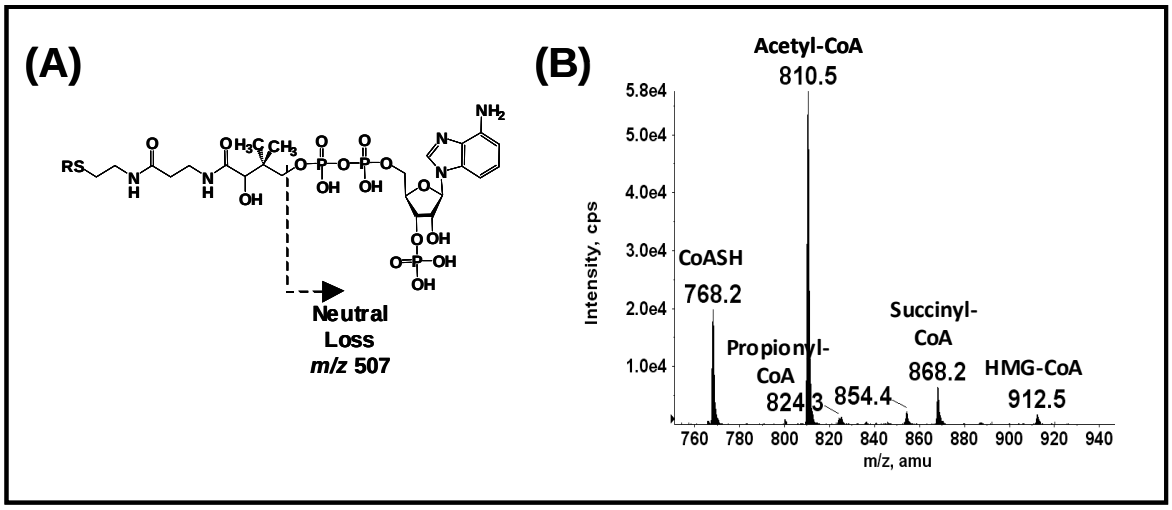

Figure 2.1 CoA structure and LC-constant neutral loss/MS analysis. (A) Generalized CoA structure, showing the CID-induced neutral loss of the ATP moiety (*m/z* 507). The substituent (R group) can include any thioester or derivative of CoA arising from endogenous or exogenous sources. (B) LC-constant neutral loss/MS scans (*m/z* 507) of short chain acyl-CoA species extracted from unlabeled Hepa 1c1c7 murine hepatoma cells. The extraction was performed as described in the methods section. The precursor parent molecules of various short-chain acyl-CoA species are annotated in the spectrum.

pantothenate, the stable isotopes were incorporated into CoA (Figure 2.2) much as labeled lysine and leucine are incorporated into proteins using SILAC methodology. This allowed us not only to generate isotopically labeled CoASH, but also a wide variety of acyl-CoA thioesters in a single biological system. In this chapter, we present the development of this method, with particular focus on optimization of growth conditions, scale-up, validation as well as preparation of specific CoA species, which were subsequently extracted and used as LC-MS internal standards *in vitro* as well as in mouse tissue. A detailed step-by-step protocol and troubleshooting guidelines are presented in the following chapter.

2.3 Materials and Methods

2.3.1 Chemicals and Reagents.

CoASH, acetyl-CoA, succinyl-CoA, HMG-CoA, propionyl-CoA, SSA, TCA and menadione were purchased from Sigma Aldrich (St. Louis, MO). RPMI 1640 pantothenate-omitted media was purchased from AthenaES (Baltimore, MD). Undialyzed FBS (uFBS), dialyzed FBS (dFBS), and charcoal-dextran stripped FBS (csFBS) were purchased from Gemini Bio-Products (West Sacramento, CA). All solvents used were Optima grade (Fisher Scientific, Pittsburgh, PA). [$^{13}C_3{}^{15}N_1$]-pantothenate was purchased from IsoSciences (King of Prussia, PA).

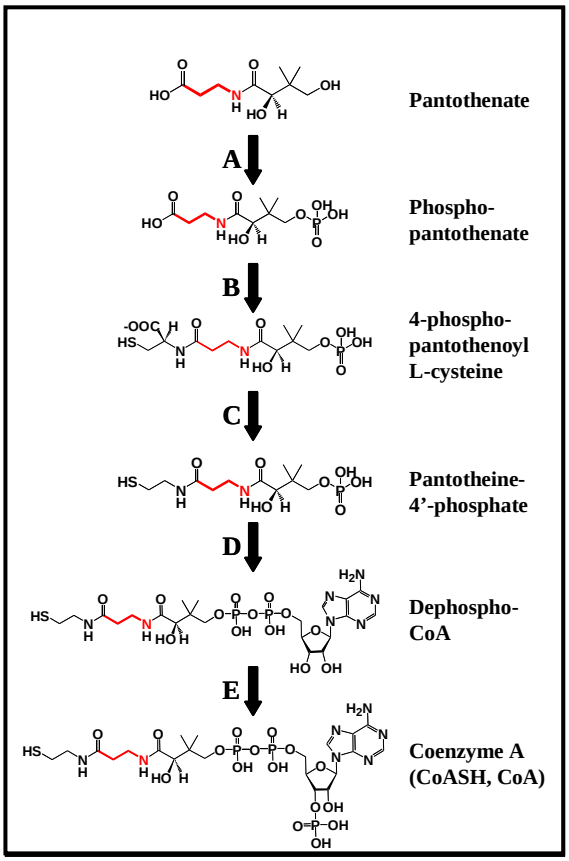

Figure 2.2 Incorporation of [$^{13}C_3$ $^{15}N_1$]-pantothenate into CoA. Enzymes: (A) Pantothenate kinase (rate-determining). (B) Phosphopantothenoyl cysteine synthetase. (C) Phosphopantothenoyl cysteine decarboxylase. (D) Phosphopantetheine adenylyltransferase. (E) Dephospho-CoA kinase. [^{13}C] and [^{15}N] atoms are marked in red.

2.3.2 Cell culture and extraction of short chain CoA thioesters.

Murine hepatocytes (Hepa 1c1c7, ATCC #CRL-2026) were maintained in RPMI 1640 media supplemented with 10% FBS, 2 mM L-glutamine, 100 units/mL penicillin and 100 μg/mL streptomycin at 37°C and 5% CO_2. Extraction of CoA species was performed using modifications to similar methods.[102, 108] Briefly, cells were washed twice with 10 mL of ice cold PBS. Cells were harvested by scraping into 1 mL of PBS. A 100 μL aliquot was saved for protein quantitation and the remainder was pelleted at 1000*g*. The cell pellet was resuspended in 1 mL ice cold 10% TCA and pulse-sonicated for 30 sec on ice using a sonic dismembranator (Fisher), followed by a 5 min centrifugation at 15000*g*. The supernatant was transferred to a fresh tube and the pellet was discarded. The supernatant was purified by SPE as follows: Oasis HLB 1cc (30 mg) SPE columns (Waters) were pre-conditioned with 1 mL methanol followed by equilibration with 1 mL water. The collected supernatant was applied, washed with 1 mL water and finally eluted using 3 subsequent applications of 0.5 mL methanol containing 25 mM ammonium acetate. Eluted compounds were dried down with nitrogen and resuspended in 100 μL 5% 5-SSA. Injections of 10 μL were made for LC-MS analysis.

2.3.3 LC-MS.

Analytes were separated using a reversed phase Phenomenex HPLC Luna C18 column (2.0 x 150 mm, pore size 5 μm) with 5 mM ammonium acetate in water as solvent A, 5 mM ammonium acetate in 95/5 acetonitrile/water (v/v) as solvent B and 80/20/0.1 (v/v/v) acetonitrile/water/formic acid as Solvent C. Gradient conditions were as follows: 2% B for 1.5 min, increased to 25% over 3.5 min, increased to 100% B in 0.5

min and held for 8.5 min, washed with 100% C for 5 min, before equilibration for 5 min. The flow rate was 200 μL/min. Samples were analyzed using an API 4000 triple quadrupole mass spectrometer (Applied Biosystems, Foster City, CA) in the positive ESI mode. Samples (10 μL) were injected using a Leap CTC autosampler (CTC Analytics, Switzerland) where they were maintained at 4°C, and data was analyzed with Analyst 1.4.1 software. The column effluent was diverted to the mass spectrometer from 8 min to 13 min and to waste for the remainder of the run. The mass spectrometer operating conditions were as follows: ion spray voltage (5.0 kV), compressed air as curtain gas (15 psi) and nitrogen as nebulizing gas (8 psi), heater (15 psi), and collision-induced dissociation (CID) gas (5 psi). The ESI probe temperature was 450°C, the declustering potential was 105 V, the entrance potential was 10 V, the collision energy was 45 eV, and the collision exit potential was 15 V. Isotopic labeling using [$^{13}C_3{}^{15}N_1$]-pantothenate resulted in labeled CoA and thioester derivatives with a mass shift of 4 amu. Transitions employed for LC-SRM/MS analyses are shown in Table 2.1.

2.3.4 Stable isotope labeling using [$^{13}C_3{}^{15}N_1$]-pantothenate.

Labeling of CoA and its thioesters was achieved using a procedure similar to SILAC except that [$^{13}C_3{}^{15}N_1$]-pantothenate was used instead of labeled amino acids.[92] Murine hepatocytes were cultured in RPMI media containing 1 mg/L [$^{13}C_3{}^{15}N_1$]-pantothenate and 10% serum (uFBS, dFBS, or csFBS). To monitor labeling efficiency, cells were harvested at each passage and processed as described above. The ratio of unlabeled to labeled CoASH was used to monitor labeling and to calculate absolute concentrations of pantothenate. To characterize pantothenate labeling, cells were grown

Compound	Parent *(m/z)*	Daughter *(m/z)*
CoASH	**768.1**	**261.1**
[$^{13}C_3$ $^{15}N_1$]-CoASH	**772.1**	**265.1**
Acetyl-CoA	**810.1**	**303.1**
[$^{13}C_3$ $^{15}N_1$]-Acetyl-CoA	**814.1**	**307.1**
Propionyl-CoA	**824.1**	**317.1**
[$^{13}C_3$ $^{15}N_1$]-Propionyl-CoA	**828.1**	**321.1**
Succinyl-CoA	**868.1**	**361.1**
[$^{13}C_3$ $^{15}N_1$]-Succinyl-CoA	**872.1**	**365.1**
HMG-CoA	**912.1**	**405.1**
[$^{13}C_3$ $^{15}N_1$]-HMG-CoA	**916.1**	**409.1**

Table 2.1 SRM transitions for short-chain CoA thioesters and stable isotope labeled analogues prepared by SILEC.

to confluence, washed and treated with the labeling media for 0, 1, 3, 6, 12, 18 or 24 h, followed by harvesting and extraction. CoA labeling and scale-up were optimized by varying the type of serum (uFBS, dFBS and csFBS) as well as the concentration of [$^{13}C_3{}^{15}N_1$]-pantothenate, supplemented into the labeling media. After scale-up (as described below), cells were harvested by scraping and sonication in 10% TCA. Acidified extracts containing stable isotope labeled CoA thioesters were pooled, aliquoted, frozen, stored at -80°C and thawed as needed.

2.3.5 Scale up of labeled CoA standards

Cells were split 1:5, collected, and processed each day for seven days. Although there was some minor variation among different CoA species, the peak level for each of the CoA species occurred on day 4 or 5 (appendix, Table A.2). Therefore, a two-step approach was employed. First, cells were grown in media supplemented with 10% csFBS and 1 mg/L [$^{13}C_3{}^{15}N_1$]-pantothenate for three passages. Second, the media was replaced on the third day of the final passage with media containing 3 mg/L [$^{13}C_3{}^{15}N_1$]-pantothenate and 3% csFBS. The incubation was continued overnight; cells were then harvested and processed the next day. This resulted in efficient labeling of all CoA species to > 99.5% labeling. Typically this was conducted using twenty plates or more.

2.3.6 Validation.

Cells from twenty plates were sonicated in 10% TCA (0.5 mL per plate), pooled and aliquoted into 3 fractions of 3 mL, which were subsequently stored at -80°C. Lysates from [$^{13}C_3{}^{15}N_1$]-pantothenate-labeled cells were prepared as described above and also

stored at -80°C. CoASH and short chain acyl-CoA standards were also stored in 5% SSA at -80°C. For the standard curve, CoA standards were thawed and diluted using 10% TCA, each with a final volume of 0.5 mL. One 3 mL cell lysate aliquot was thawed each day of the validation and divided into six 0.5 mL aliquots. Each of the standards as well as the fractions was mixed with 0.5 mL of the labeled CoA TCA lysate. Samples were processed as described above. Intra-day and inter-day validation was performed for each analyte.

2.3.7 Application of SILEC standards to cell culture using propionate treatment

Propionate incorporation into propionyl-CoA in Hepa 1c1c7 cells was used as a model for CoA metabolism.[109] Treatments were performed in 10 cm tissue culture dishes and cells were grown to 90% confluence and washed twice with PBS prior to treatment. Cells were treated in a minimal treatment media consisting of HBSS, supplemented with $CaCl_2$, $MgSO_4$, glucose and 25 mM HEPES buffer. Propionate stocks were prepared in HBSS at 1 M and diluted to a final treatment concentration of 10 mM. Control cells were treated with treatment media alone. Cells were treated for 1 h and processed as described above. Due to the wide disparity of CoA thioesters concentrations in treated compared with untreated cells, an optimal "customized" internal standard mixture was generated by combining the CoA extracts from untreated SILEC cells and an equal number of propionate-treated SILEC cells. This internal standard contained an acyl-CoA profile more applicable to both experimental groups. An equal amount of these extracts were added into both groups as well as the standard curve. Experimental cells were maintained as described previously.

2.3.8 Application of SILEC standards to mouse tissues

Snap frozen mouse livers were obtained from the Lazar lab. Liver sections (30-100 mg) from either fed or fasted (12 h) mice were stored at -80°C. 0.8 mL ice cold 10% TCA was added to each tube along with 0.2 mL SILEC standards. Samples were homogenized twice using a Tissuelyzer system (Qiagen) at 30 Hz, for 3 minutes, and subsequently centrifuged at 21000*g* to precipitate protein pellet. The acid extract was then purified using Oasis HLB SPE columns as previously described, except two washes with water were performed. Standard curve samples were processed in a similar fashion.

2.4 Results and Discussion

2.4.1 LC-SRM/MS and CoA extraction.

While multiple LC-MS methods have been developed to analyze CoA thioester species in plant[74, 110] and animal tissues,[70, 102] the focus of our study is using mammalian cell culture models, which often require increased sensitivity.[75, 111] CoA and short chain CoA thioesters were identified in cellular extracts using a constant neutral loss scan of *m/z* 507 amu corresponding to ATP (Figure 2.1). SRM transitions were developed for five unlabeled and labeled CoA thioesters (Table 2.1) in order conduct sensitive quantitative LC-MS analysis. However, the SILEC technique can be readily extended to any short, medium, or long chain acyl-CoA thioester by modifying the extraction procedure.[112] Due to the similarity of the various short-chain CoA thioesters, LC-SRM/MS analysis was employed for specific identification as well accurate and precise

quantification of the various CoA species without requiring absolute baseline separation as is required in HPLC-UV methods.[66, 113] CoA standards and acid extracted acyl-CoA molecules from hepatocytes were separated and quantified using LC-SRM/MS (Figure 2.3).

2.4.2 Stable isotope labeling with [$^{13}C_3{}^{15}N_1$]-pantothenate.

Stable isotope labeled CoA thioester derivatives were generated by growing cells in pantothenate-omitted media supplemented with [$^{13}C_3{}^{15}N_1$]-pantothenate. To verify and characterize the incorporation of labeled pantothenate into acyl-CoA species, cells were grown in labeled media, harvested at different times, and processed (Figure 2.4). Various CoA species and their heavy labeled isotopes were monitored to assess the relative amounts of labeling. The ratio of labeled to unlabeled CoA was consistent throughout all analyzed CoA thioesters. Labeled CoASH could be detected as early as 3 h, replacing approximately 4% of the CoASH in the cells every hour. After 12 h, there appeared to be a labeling "plateau", likely the result of an active or sequestered CoA pool unavailable for turnover.

Like SILAC methodology, labeling efficiency is dependent on the relative concentration of labeled to unlabeled substrate in the media. As such, minimizing unlabeled pantothenate in the media is critical for the production of pure isotopically labeled CoA standards. Since circulating vitamins represent a major source of contaminating unlabeled pantothenate in serum-supplemented cell culture, three different types of sera were tested: undialyzed (uFBS), dialyzed (dFBS) and charcoal-dextran stripped (csFBS). Although dFBS and csFBS are both often used in many cell culture

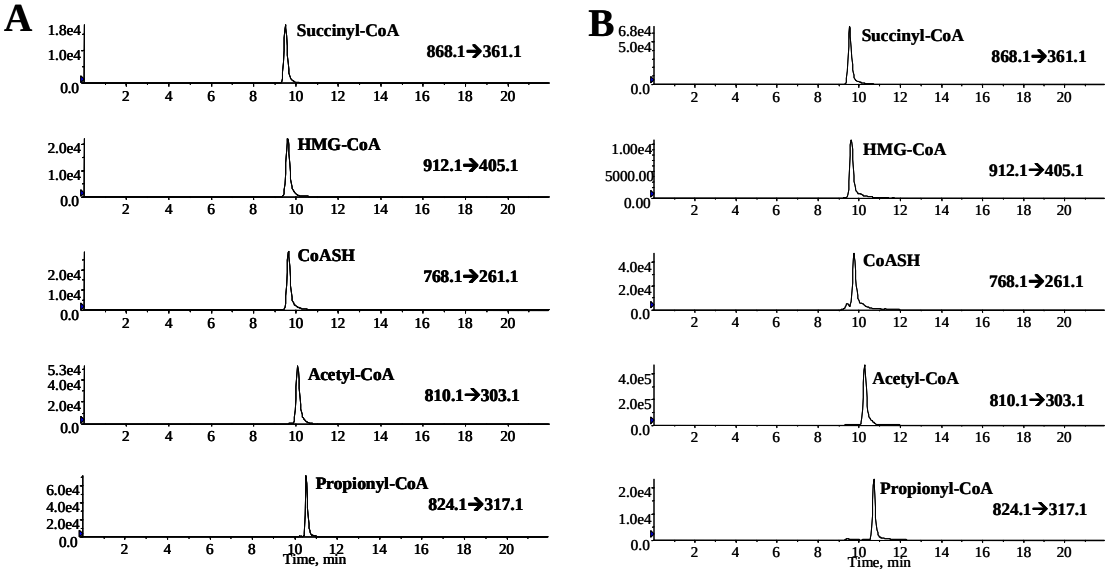

Figure 2.3 LC-SRM/MS chromatograms of short chain acyl-CoA thioesters. (A) CoA thioester standards (1 pmol each) and (B) acid extracted and SPE purified CoA species from Hepa 1c1c7 cells.

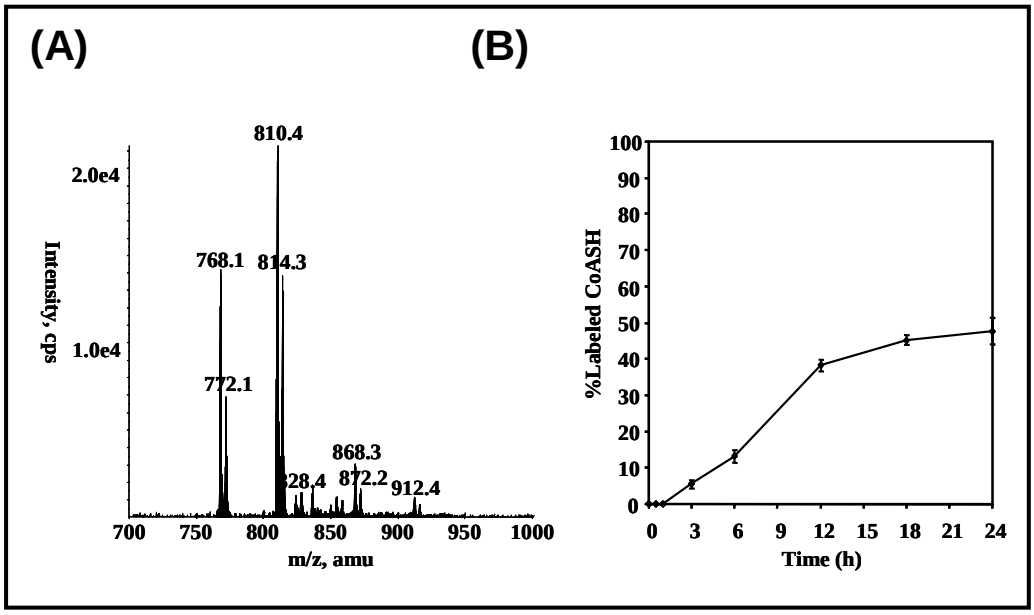

Figure 2.4 Stable isotope labeling of CoA thioesters in Hepa 1c1c7 cells grown in [$^{13}C_3{}^{15}N_1$]-pantothenate (1 mg/L). (A) LC-constant neutral loss/MS analysis with a neutral loss of *m/z* 507 from hepatocytes extracts after 24 h of pantothenate labeling. (B) Time course (24 h) of pantothenate incorporation into CoA.

applications to decrease inter-batch variation, dialysis uses only size filtration, while stripping serum with activated charcoal more specifically binds and depletes certain small molecules such as steroids,[114] peptide hormones, and vitamins.[115] We found that maximal labeling was achieved by the third passage with minimal increases in labeling with additional passages (Table 2.2). csFBS was determined to be the most efficient for our application due to its lower pantothenate content. The maximal achievable steady-state of labeled CoA represents the percentage of labeled pantothenate to total pantothenate in the media. By determining the percentage of CoA that is labeled within the cells, the concentration of unlabeled contaminating pantothenate was calculated and determined: uFBS (5.8mg/L), dFBS (0.21 mg/L) and csFBS (0.091mg/L) (Table 2.3).

2.4.3 Scale up and customization of stable isotope labeling of CoA and its thioesters.

To increase the purity of the labeled CoA standards, two techniques were employed: (A) increasing the amount of [$^{13}C_3{}^{15}N_1$]-pantothenate in the media, or (B) decreasing the amount of serum. Decreasing the serum concentration resulted in significantly slowed growth characteristics, while further increases in media supplementation of [$^{13}C_3{}^{15}N_1$]-pantothenate resulted in limiting returns on labeling. By utilizing a two-step approach using 10% csFBS initially followed by a final incubation with 3% csFBS, efficient scale-up was achieved while limiting the amount of labeled pantothenate that was required. A chromatogram demonstrating isotopically pure CoA internal standards is provided in the appendix (Figure A.1). To generate more of a particular labeled CoA thioester internal standard, we treated SILEC labeled cells with 10 mM propionate for 1 h. After incubation these cells were harvested and processed for

Serum	Passage # 1	2	3	4	5
uFBS	**59.3**	**59.8**	**55.9**	**58.7**	**63.4**
dFBS	**93.5**	**97.6**	**97.7**	**97.4**	**97.9**
csFBS	**94.6**	**98.4**	**98.9**	**99.0**	**99.1**

Table 2.2 Effect of different sera on stable isotope labeling of CoA (above) and determination of unlabeled pantothenate content in supplemented sera. Percentage of labeled CoASH in Hepa 1c1c7 cells serially passaged in pantothenate-omitted RPMI 1640 media supplemented with 1mg/L [$^{13}C_3{}^{15}N_1$]-pantothenate and 10% serum: uFBS, dFBS, csFBS.

$\%L_{max}$ = fraction of labeled CoA (max), experimentally determined (Table 2.2)
L = labeled supplemental pantothenate (1 mg/L)
U = unlabeled pantothenate (mg/L)

$$\%L\max = \frac{L}{L+U} \quad \rightarrow \quad \frac{1}{\%L\max} = 1 + \frac{U}{L} \quad \rightarrow \quad U = L * \left(\frac{1}{\%L\max} - 1 \right)$$

	$\%L_{max}$	L (mg/L media)	U (mg/L media)	U (mg/L serum)
uFBS	**63.4%**	**1.0**	**0.58**	**5.8**
dFBS	**97.9%**	**1.0**	**0.021**	**0.21**
csFBS	**99.1%**	**1.0**	**0.0091**	**0.091**

Table 2.3 Determination of unlabeled pantothenate in different batches of FBS and in the cell culture media prepared from them.

CoA thioesters. We found that there was a substantial increase in the amount of [$^{13}C_3{}^{15}N_1$]-propionyl-CoA in these cells (Figure 2.5)

Other approaches to generating heavy labeled CoA species are possible, though less optimal. Since CoA contains pantothenate, cysteine, and ATP, labeling with cysteine or a heavy labeled carbon source, would also result in labeled CoA. One limitation of cysteine labeling is that this can be synthesized *de novo*, which would result in decreased isotopic purity of the compound. Furthermore, since only a small fraction of cysteine or carbon from isotopic nutrient sources are incorporated into CoA, these methods are less efficient than the described method, where nearly all of the pantothenate is incorporated into CoA. Furthermore, preparation of [$^{13}C_3{}^{15}N_1$]-analogs avoids problems that can arise through the metabolic instability of deuterium and the separation of deuterium and protium analogs that occurs during LC-MS analysis.[116] Finally, methods using stable isotope CoA compounds with labeled acyl moieties are limited to those in which such labeled thioesters are available.[108] If a large number of CoA species are quantified, this would require labor-intensive preparation of each standard individually. Also, labeled CoASH could not be produced using this methodology. In contrast, biosynthetic generation of CoA thioesters provides simultaneous synthesis of every labeled thioester standard in a particular cell type in a naturally occurring profile in the appropriate concentration range to be used in the study. Moreover, different internal standard mixtures could be readily generated for specific applications by treating the labeled cells with a precursor fatty acid to reflect more appropriate thioester concentrations (Figure 2.5).

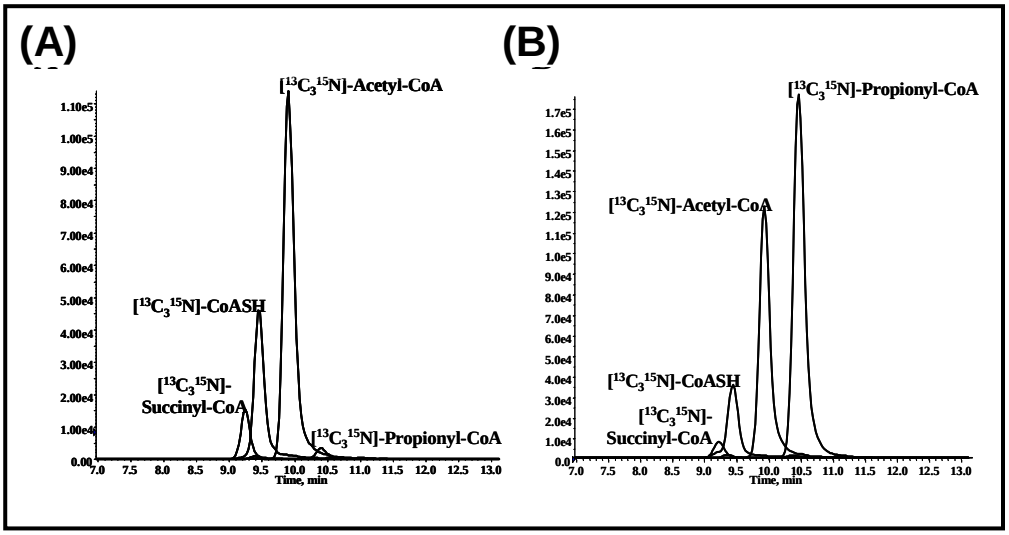

Figure 2.5 Preparation of a specific stable isotope labeled CoA thioester stable isotope standard. CoA extracts from stable isotope labeled cells (A) untreated and (B) treated with 10 mM propionate for 60 min.

2.4.4 Assay validation.

Validation was performed on various CoA thioesters using our SILEC-derived internal standards (Table 2.4). Extracted samples were quantified with and without SILEC standards. Specificity was also improved since the compounds were co-eluting with their standards. More importantly, it was found that using stable isotope analogs as internal standards provided a significant improvement in accuracy and precision when compared with non-identical internal standards (appendix, Table A.3). The approach more commonly employed involves using a non-labeled compound that is similar, but distinct, from the analyte of interest as the internal standard. There are several drawbacks to using this type of method. First, using an internal standard that is different than the analyte of interest presumes that both analyte and internal standard will behave equally throughout the assay. While this may be a reasonable assumption for closely related compounds, as compounds diverge chemically, they also will show a greater disparity in their behavior. Second, ESI is particularly susceptible to matrix effects, due to the limited amount of ionization that can occur at the source. These effects can lead to an under- or overestimation of certain compounds as they co-elute in a complex mixture.[77, 78, 90] Matrix effects are non-linear and can vary dramatically throughout a gradient run, particularly when analyzing tissue samples. Finally, analyte stability and loss during sample preparation can vary considerably for different CoA species. Therefore, the assumption that the measured analyte will have the same stability as the analog internal standard may also lead to over- or underestimation of the compound. Additionally, the stable isotope can act as a carrier for trace analytes and improve sensitivity.

	Linearity	Precision (RSD)		LOQ
	(R^2)	Intra-batch	Inter-batch	(pmol)
Acetyl-CoA	**0.9990**	**2.4%**	**2.6%**	**0.1**
Succinyl-CoA	**0.9996**	**5.6%**	**1.6%**	**0.2**
CoASH	**0.9966**	**6.8%**	**2.6%**	**0.1**
Propionyl-CoA	**0.9999**	**9.1%**	**13.9%**	**0.05**
HMG-CoA	**0.9939**	**7.1%**	**10.4%**	**0.2**

Table 2.4 Assay validation. Standard curves were generated by spiking increasing concentrations of different CoA standards with 0.5 ml of acid extracted CoA. Pooled frozen extracts from Hepa cells were thawed and mixed with internal standard mixture and extracted. Limit of quantitation (LOQ) was determined to be the level at which the signal-to-noise ratio was at least 5:1 compared to a blank.

2.4.5 Applications of SILEC standards to biological samples

Cells treated with 10 mM propionate for 1 h showed a 10-fold increase in propionyl-CoA levels as compared to control cells, with concomitant decreases in levels of acetyl-CoA, succinyl-CoA, and CoA (Figure 2.6). In addition to cell culture, SILEC internal standards improved the precision of CoA measurements from tissues as well. Livers from fasted vs. fed mice showed significant differences in various short chain acyl-CoA species. In particular, there was a significant decrease in the amount of acetyl-CoA and succinyl-CoA levels, and an increase in the propionyl-CoA levels. There was also an increase in CoASH, though this change was not statistically significant. These data are consistent with a recently published study in fed and fasted mice, except that acetyl-CoA levels were increased rather than decreased in their model. However, differences in diet, fasting conditions as well as mouse line may contribute to the differences between these studies.

2.5 Conclusions

A SILEC method has been developed for generating labeled CoA and CoA thioester standards by adapting SILAC methodology to utilize an essential vitamin and an endogenous biosynthetic pathway. Isotopically labeled substrates have been employed previously in tracer experiments to monitor cellular metabolic flux.[94] However, our study has focused on the optimization and scale-up of stable isotope labeled standards with low levels of the endogenous unlabeled analogs for use in quantitative assays. By using csFBS instead of dFBS or uFBS, more effective incorporation of pantothenate was achieved. The resulting SILEC methodology employing [$^{13}C_3{}^{15}N_1$]-pantothenate

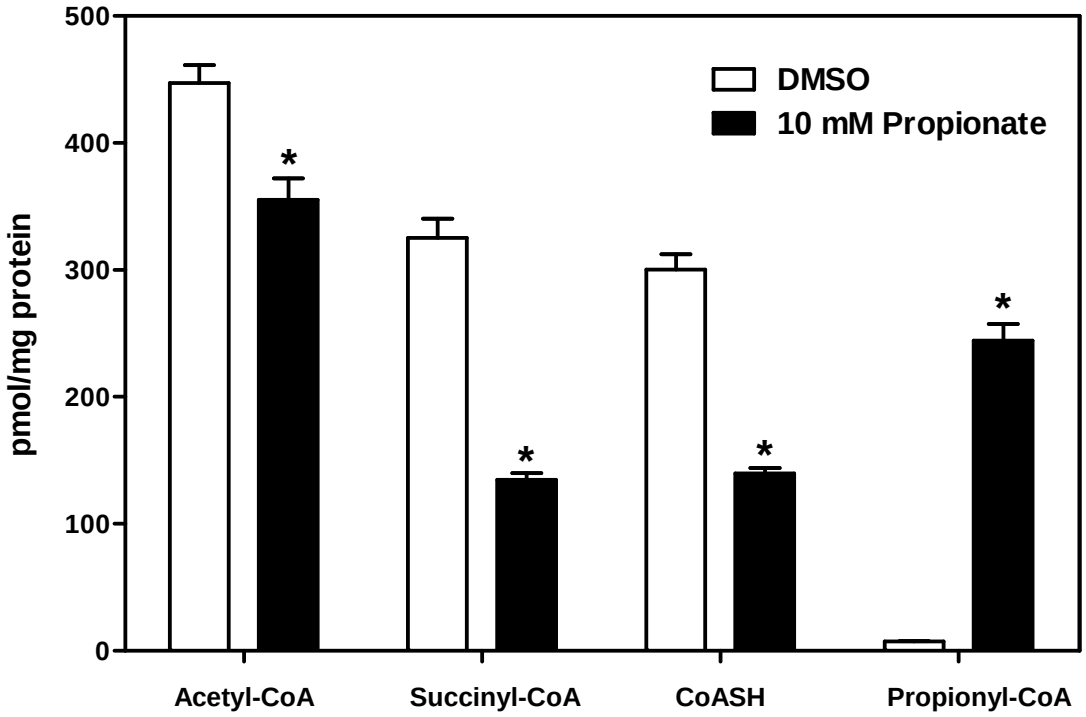

Figure 2.6 Changes in intracellular CoA thioester levels in Hepa 1c1c7 after propionate treatment: untreated (white), 10 mM propionate for 1 h (black). CoA thioesters extracted from control and treated SILEC-labeled cells were combined and used as stable isotope internal standards in measuring short chain acyl-CoA species. * $p<0.005$

	Fed	Fasted	p value
Acetyl-CoA	**26.1**	**12.8**	**2.E-04**
Succinyl-CoA	**9.2**	**5.3**	**5.E-04**
CoASH	**75.5**	**95.3**	**0.43**
Propionyl-CoA	**0.19**	**0.33**	**0.02**
HMG-CoA	**0.41**	**0.13**	**3.E-06**

Table 2.5 CoA-thioester levels in fed vs. fasting mice. Frozen mouse livers were processed for CoA levels using SILEC standards, n = 5 per group.

(instead of labeled amino acids used in SILAC methodology) made it possible to rigorously quantify short chain CoA thioesters in cell culture.

While our analysis was limited to short chain acyl-CoA species, this approach could be readily adapted to analyze medium or long chain CoA thioesters and other CoA-containing species with minor modifications to the extraction protocol.[112] Furthermore, by adapting the SILEC methodology, it could also be used to synthesize stable isotopes for metabolites that are derived from other isotopically labeled essential nutrients such as folates, riboflavin (vitamin B_2), and niacin (vitamin B_3). Stable isotope labeled metabolites from the extracts of these cells could subsequently be used as internal standards to more accurately quantify folate polyglutamates,[117] NAD,[118] or FAD.[119] Finally, the availability of labeled CoASH will facilitate the development of methodology for the quantification of this important mitochondrial thiol and its oxidized mixed disulfide derivatives such as glutathione-CoA.

Chapter 3: A practical protocol for the generation and application of SILEC mass spectrometry standards to biological samples

3.1 Abstract

SILEC was developed in Chapter 2 to generate isotopically labeled CoA and short-chain acyl-CoA thioesters, by modifying SILAC to include [$^{13}C_3{}^{15}N_1$]-pantothenate instead of the isotopically labeled amino acids. The lack of a *de novo* pantothenate synthesis pathway allowed for efficient and near-complete labeling of the measured CoA species. This chapter provides a step-by-step approach to generating SILEC labeled internal standards in mammalian and insect cells, as well as how to utilize them in stable isotope dilution MS-based analyses. Troubleshooting guidelines as well as a list of unlabeled and labeled CoA species are also included. This protocol represents a prototype for generating stable isotope internal standards from labeled essential nutrients such as pantothenate.

Portions of this chapter have been previously published (Basu SS, Blair IA. *Nat Protocols*, 2011).

3.2 Overview

SILEC methodology can be used to label CoA in any cell system that does not contain a robust *de novo* pantothenate synthesis pathway, including mammalian and insect cell lines, both of which are described in this protocol. Hepa 1c1c7 murine hepatoma cells were originally chosen due to their rapid growth rates in SILEC media, the abundance of short-chain acyl-CoA species of interest, and relative ease in scalability. In this chapter, we increase the breadth of the method developed in Chapter 2 by adapting SILEC labeling to Drosophila S2 cells, which have even shorter doubling times and grow in suspension, facilitating larger scale preparations of labeled standards. The purpose of this protocol is to provide a practical guide to generate stable isotope labeled short-chain acyl-CoA thioesters for use as internal standards in quantitative stable isotope dilution LC-MS assays.

3.2.1 Generation of labeled CoA

Biosynthetic generation of labeled CoA standards can be divided into four steps (Figure 3.1). The objective of the first step is to label the majority of the intracellular CoA while still generating enough cellular material to accommodate the proposed experiment. To accomplish this, cells are passaged 3-5 times in media containing 10% csFBS and 1mg/L [$^{13}C_3{}^{15}N$]-pantothenate, with unlabeled pantothenate specifically omitted. By the third passage, approximately 98-99% of the CoA in the cell are isotopically labeled. In the second step, the media is replaced overnight with ultra-labeling media containing a higher concentration of labeled pantothenate (2-3 mg/L) and a lower concentration of serum (0-5%). This both increases the concentration of labeled

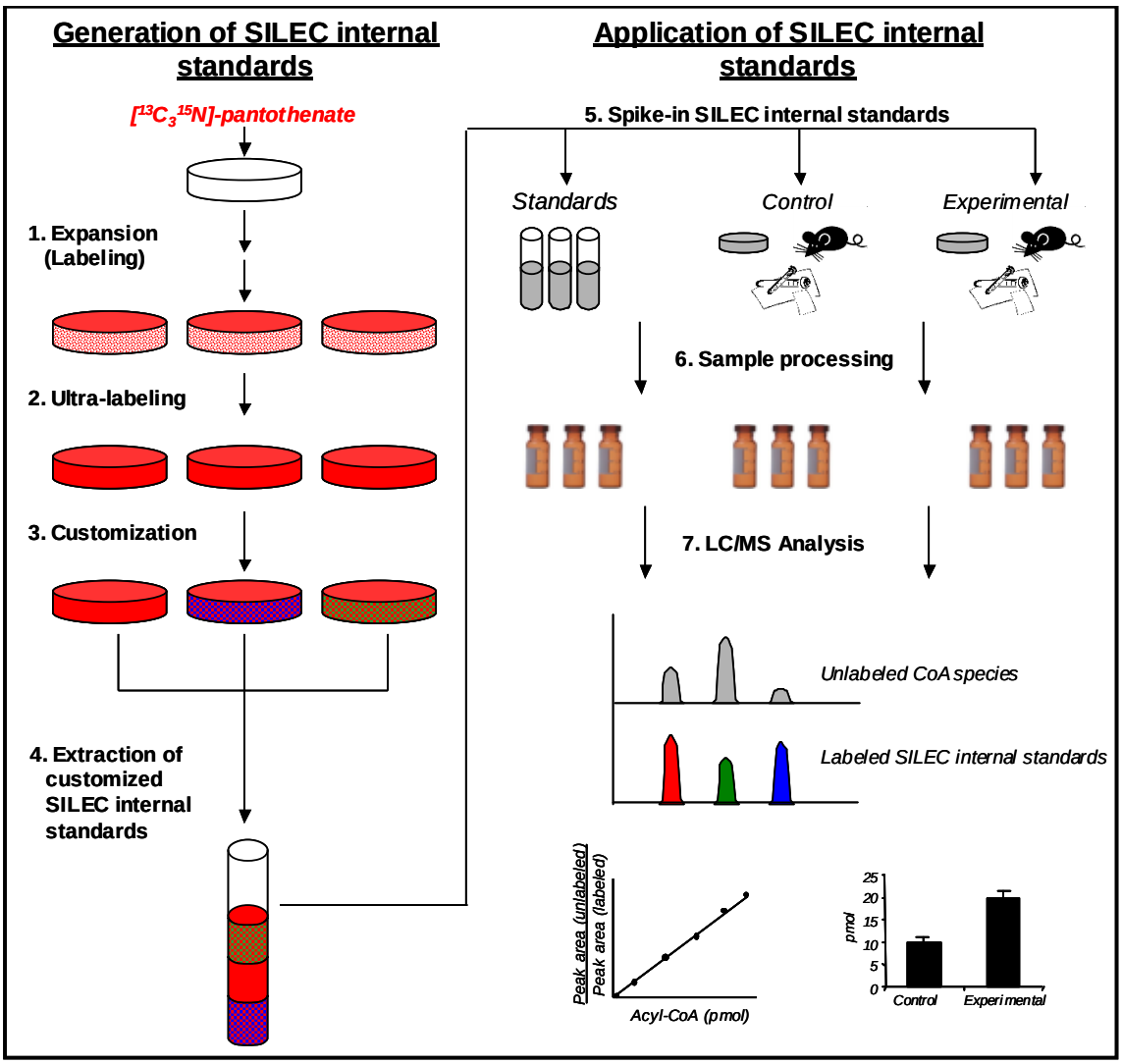

Figure 3.1 General scheme for Stable Isotope Labeling by Essential nutrients in Cell Culture (SILEC). (1) Expansion. Cells are serially passaged and expanded in the presence of labeled pantothenate. (2) Ultra-labeling. Media containing less serum and more labeled pantothenate is used to increase purity of labeled CoA. (3) Customization (optional). Labeled cells are subjected to different biological, pharmaceutical or toxicological exposures to modify the CoA derivative profile within the cells. (4) Extraction. Cells are lysed and pooled together to generate a SILEC CoA internal standard mix with a more global CoA profile. (5) SILEC spike-in. Equal amounts of SILEC internal standards are spiked into CoA standards, as well as *in vitro*, tissue or clinical samples. (6) Sample extraction. Standards and samples are subjected to the same sample extraction procedures. (7) LC-MS analysis. CoA species are separated and analyzed by LC-SRM/MS. Co-eluting SILEC standards are used to confirm the identity and normalize for the different CoA species.

pantothenate in the media, while decreasing the level of the contaminating unlabeled pantothenate from the serum. While serum-free culture could further decrease unlabeled pantothenate levels, such conditions can also negatively affect growth, viability and metabolic characteristics of cells in culture.[120-122] Therefore, an optimal level of serum must be determined to balance the benefits of increased labeling, while still maintaining cellular characteristics. At this point, the CoA species from a representative plate can be sampled to determine labeling efficiency and CoA profile using LC-neutral loss scan of *m/z* 507. If the desired CoA species can be identified and measured, the third step is not necessary. However, if one or more of the labeled CoA species of interest are below a reproducibly quantifiable level, a customization step may be necessary. This can be accomplished in multiple ways. First, labeled cells can be supplemented with a particular fatty acid, such as propionate or β-hydroxybutyrate (BHB) which is then taken up by the labeled cells to generate a higher percentage of that particular fatty acyl-CoA (Figure 3.2). In addition, cells can be subjected to different biological perturbations or toxicological insults to increase and decrease particular CoA species or to generate xenobiotic-CoA adducts such as menadione-CoA (Figure 3.3). The CoA species in these cells can then be extracted and pooled together to generate a SILEC reference metabolome, containing a more appropriate or more global CoA profile for the experiment. Alternatively, the cellular lysate can be hydrolyzed with a strong base, and the resulting [$^{13}C_3{}^{15}N_1$]-CoASH can be generated. This can be further purified and used to synthesize a particular CoA derivative.[73, 123-125]

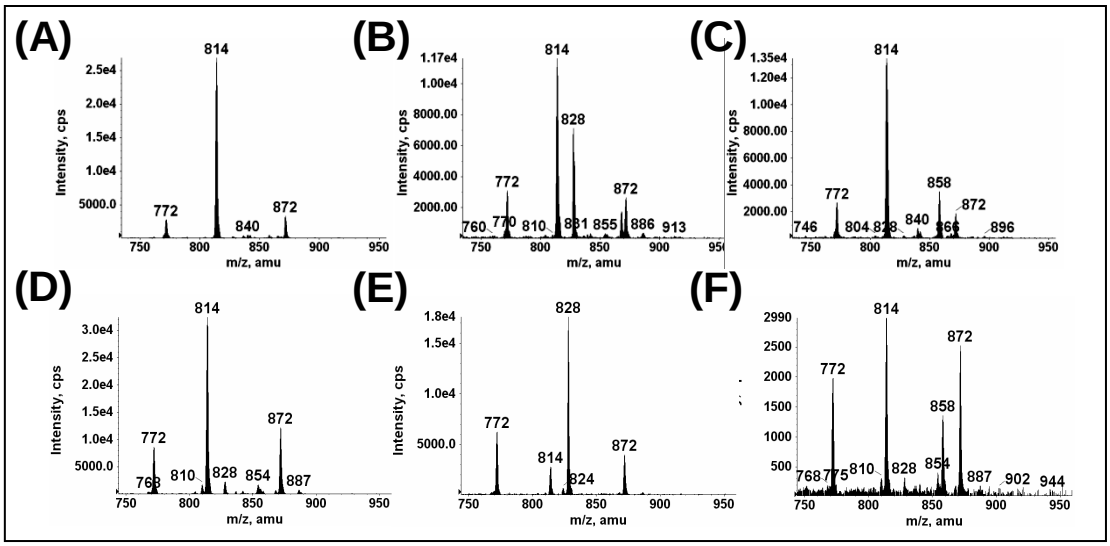

Figure 3.2 SILEC labeling and "customization" of CoA metabolome. (A-C) LC-neutral loss/MS scans (*m/z* 507) of acid extracted acyl-CoA species in SILEC-labeled Hepa 1c1c7 cells that were: (A) untreated, (B) treated with 10mM propionate for 1 h, or (C) treated with 10 mM BHB for 1 h. (D-F) LC-neutral loss/MS scans (*m/z* 507) of acid extracted acyl-CoA species in Drosophila S2 cells that were: (D) untreated, (E) treated with 10 mM propionate for 1 h, or (F) treated with 10 mM BHB for 1 h. The precursor ion masses of various labeled short chain acyl-CoA species can be identified: [$^{13}C_3{}^{15}N$]-acetyl-CoA (*m/z* 814), [$^{13}C_3{}^{15}N$]-succinyl-CoA (*m/z* 872), [$^{13}C_3{}^{15}N$]-CoASH (*m/z* 772), [$^{13}C_3{}^{15}N$]-propionyl-CoA (*m/z* 828), [$^{13}C_3{}^{15}N$]-BHB-CoA (*m/z* 858). These "customized" CoA extracts can be pooled together to generate a more comprehensive CoA profile.

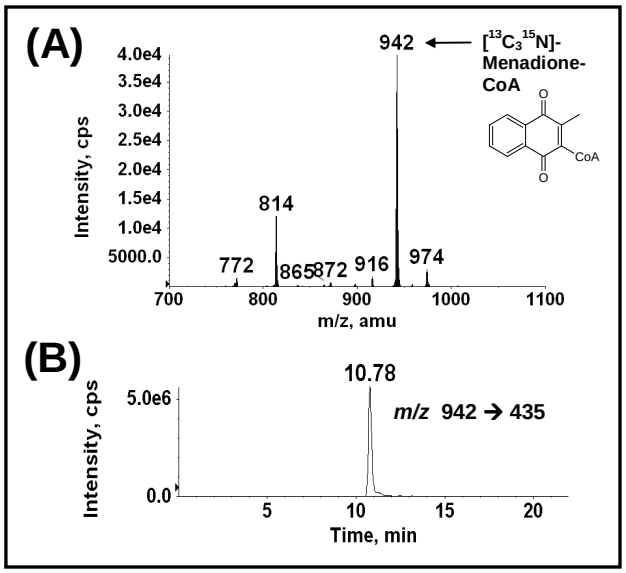

Figure 3.3 Biosynthetic generation of isotopically labeled menadione-CoA. (A) LC-neutral loss/MS scan (*m/z* 507) of acid-extracted CoA species from SILEC-labeled Hepa 1c1c7 cells treated with 20 μM menadione for 1 h. (B) LC-SRM/MS chromatogram of [$^{13}C_3{}^{15}N$]-menadione-CoA (*m/z* 942 → 435) derived from the same extract. Extraction and analysis were performed as specified. By spiking this extract into experimental samples, this isotopically labeled analyte can be used as an internal standard for quantifying unlabeled menadione-CoA.

3.2.2 Application of SILEC standards to biological samples

The cellular extracts containing the SILEC-labeled CoA internal standards can be applied to biological samples and used to normalize for the CoA species of interest (Figure 3.1). These biological samples can include cultured cells, tissue samples, or clinical samples of obtainable cells such as fibroblasts, lymphocytes or platelets. In each case, a constant amount of SILEC standards are spiked into the samples at an early point during sample processing; to scraped cells for *in vitro* experiments, to snap-frozen or lyophilized tissues for *in vivo* experiments or into purified cells such as lymphocytes or platelets for clinical studies. In addition to spiking the samples, the same amount of SILEC-labeled CoA internal standards are also spiked into known quantities of unlabeled CoA standards to generate a standard curve. Both biological samples and unlabeled CoA standards can then be extracted using SPE and analyzed by LC-MS. The peak area of each unlabeled standard is divided by the peak area of the corresponding SILEC internal standard analog to generate a standard curve of standards to peak area ratio. The same analysis is then performed on each sample and the peak area ratio is then used to calculate the amount of each of the CoA species in the sample. These amounts are then compared between experimental groups. This method is comparable to the SILAP or SILAC "spike-in" methods that have been described previously.[97, 99] The strength of using a stable isotope dilution MS method is not only in the specificity of CoA elution, but also that the labeled compounds will have the same stability as the unlabeled analyte of interest. Therefore, there would be a parallel degradation of the labeled internal standard that does not affect the ratio of unlabeled analyte to labeled internal standard. For this reason, absolute quantification of the labeled internal standards is unnecessary.

3.2.3 Additional considerations for modifying SILEC approach

Although this protocol specifically addresses the ability to generate isotopically labeled short chain acyl-CoA species, this can be modified to include other CoA species or adapted for other essential nutrients. There are several general aspects to consider if such an approach is taken. First, limitations of the SILEC approach are similar to those encountered with SILAC labeling in that a biological system is used to generate stable isotope standards. Although numerous labeled CoA species can be generated in a single system, batch-to batch variability persists even under well-controlled conditions. If using a starting material other than pantothenate such as folates, it is important to use media and the appropriate serum that does not contain that essential nutrient. Therefore, an omitted media along with a modified serum (such as csFBS or dFBS) is critical to generating isotopically pure standard. Finally, finding the appropriate cell line is also necessary for optimization. Since this is largely empirical, many cell lines likely need to be tested to optimize scale-up and production. A time-course should be established in order to determine the optimal time for harvesting from the chosen cell line, as was demonstrated in the Chapter 2.

3.3 Materials

- Cell line of choice (protocol written for Hepa 1c1c7 cells, ATCC #: CRL-2026 and Drosophila Schneider 2 cells, Invitrogen)
- Media:
    - Mammalian cells: pantothenate-omitted RPMI 1640 media (AthenaES, MD)
    - Insect cells: Schneider's media

- Hank's Buffered Salt Solution (HBSS)

- Phosphate-buffered saline (PBS)
- [$^{13}C_3{}^{15}N_1$]-pantothenate (Isosciences, PA)
- Charcoal-dextran stripped FBS (Gemini Biosciences, CA)
- 10 cm tissue culture dishes
- 75-cm^2 tissue culture flasks
- Cell scrapers
- Penicillin, streptomycin
- Glutamine
- Trichloroacetic acid (TCA)
- 5-Sulfosalicyilic acid (SSA)
- Potassium hydroxide (KOH)
- Oasis HLB 1cc (30 mg) SPE columns (Waters)
- 10 mL conical glass centrifugation tubes
- Nitrogen gas
- Methanol
- Ammonium acetate
- Acetonitrile and water (mass spectrometry grade)
- Formic acid

Instrumentation:

- Probe sonicator
- Microcentrifuge
- Vacuum manifold

- Nitrogen evaporator
- Refrigerated autosampler
- HPLC system with three pumps
- Triple quadrupole mass spectrometer (API 4000 or instrument of similar sensitivity)
- Computer with mass spectral computational software

Reagent Setup:

- Heat-inactivated csFBS. Thaw at 37°C and heat inactivate complement for 30 min at 55°C. Aliquot into 50 mL fractions and store at -20°C.
- [$^{13}C_3{}^{15}N$]-Pantothenate stocks. Prepare in double distilled (dd) H_2O at 1 mg/mL and store at -20°C.
- Unlabeled CoA standards. Prepare 5 mM stock solutions of acyl-CoA species in 5% aqueous SSA. Store in aliquots at -80°C. Thaw when needed and avoid repetitive freeze thaw cycles.
- SILEC Expansion media. *Mammalian cells*: Prepare pantothenate-free media containing 10% heat-inactivated csFBS, 2 mM L-glutamine, 100 I.U./ml penicillin, 100 μg/ml streptomycin and 1 mg/L [$^{13}C_3{}^{15}N$]-pantothenate. *Insect cells (S2):* Prepare Schneider's media containing 10% heat-inactivated csFBS, 2 mM L-glutamine, 100 I.U./ml penicillin, 100 μg/ml streptomycin and 3 mg/L [$^{13}C_3{}^{15}N$]-pantothenate.
- SILEC Ultra-labeling media. *Mammalian cells*: Prepare pantothenate-free media containing 3% heat-inactivated csFBS, 2 mM L-glutamine, 100 I.U./ml penicillin, 100 μg/ml streptomycin and 3 mg/L [$^{13}C_3{}^{15}N_1$]-pantothenate. *Insect cells (S2):*

Prepare Schneider's media containing 3% heat-inactivated csFBS, 2 mM L-glutamine, 100 I.U./ml penicillin, 100 µg/ml streptomycin and 10 mg/L [$^{13}C_3{}^{15}N$]-pantothenate.

- Customization of media. Prepare HBSS media supplemented with Ca^{2+}, Mg^{2+}, 1 g/L D-glucose, 25mM HEPES and the appropriate modifying compound (fatty acid, xenobiotic, etc.). For example, to generate labeled propionyl-CoA, add 10 mM propionic acid; for labeled BHB-CoA, add 10 mM BHB; for labeled menadione-CoA, add 20 µM menadione. All media should be filtered and can be stored at 4°C for up to 3 months. Warm media to 37°C prior to cell treatment for mammalian cells and to room temperature for insect cells.
- CoA extraction reagents.
    - Extraction solution: 10% (w/v) TCA in dd H_2O. Chill on ice prior to experiment.
    - Elution solution: 25mM ammonium acetate in methanol.
    - Resuspension solution: 5% (w/v) SSA in dd H_2O.
    - Hydrolysis solution: If pure [$^{13}C_3{}^{15}N_1$]-CoASH is being generated, prepare 40% (w/v) KOH in dd H_2O.
- LC-MS solvents. Prepare, sonicate and degas HPLC solvents prior to LC-MS analysis. Use solvents of mass spectrometry grade (Fisher *Optima* grade solvents are used for our analysis)
    - Solvent A: 5mM ammonium acetate in water
    - Solvent B: 95:5 ACN:H2O 5mM ammonium acetate in water
    - Solvent C: 80:20:0.1 ACN:H_2O:formic acid

3.4 Procedure

Generating labeled CoA standards

1. Thaw frozen cells directly into SILEC expansion media.
2. For Hepa 1c1c7 (adherent) cells, allow cells to reach confluency (3-4 days), wash two times with PBS, trypsinize and split 1:5 into SILEC expansion media. For S2 (suspension) cells, when cells have reached approximately $1x10^7$ cells/ml, split into a new flask containing SILEC expansion media at a concentration of $2x10^6$ cells.
3. Repeat step 2, passaging cells in SILEC expansion media three more times. At this point, CoA species should be greater than 98% labeled. If cell growth or morphological characteristics are significantly affected, see troubleshooting guide: *Perturbation of cell growth kinetics by SILEC media.*

Pause point: Harvest and freeze down one plate of labeled cells in SILEC expansion media containing 10% DMSO. These cells can be thawed to seed future SILEC expansions.

4. After the fourth passage, allow cells to reach confluency or $1x10^7$ cells/mL.
5. *Ultra-labeling step:* Wash cells with 10 mL PBS and replace with SILEC Ultra-labeling media and incubate for 24 h.

Testing of SILEC labeling

Short chain acyl-CoA acid extraction:

6. Harvest one plate of cells by scraping gently into media and spin down at 1000*g*.

7. Resuspend cells in 1 mL ice-cold extraction solution (10% TCA)
8. Sonicate cells for 30 sec on ice in a pulsatile manner.
9. Spin sonicated cell lysate at 15000*g* for 5 min to precipitate protein pellet.

Solid phase extraction (SPE):

10. Using a vacuum manifold, condition Oasis HLB SPE columns with 1 mL of methanol.
11. Equilibrate with 1 mL water.
12. Load acid extracted lysate (supernatant) to columns.
13. Wash column with 1 mL water.
14. Elute CoA compounds into fresh tube by applying three subsequent applications of 0.5 mL elution solution.
15. Dry samples under nitrogen.
16. Re-suspend in 50 μL of 5% SSA.

LC-MS analysis: (see Chapter 2 for specific LC-MS parameters)

17. Using the LC-MS specifications in Figure 2, perform a CID neutral loss scan of 507 amu, scanning a parent mass range of *m/z* 750 to *m/z* 1200. Sample injections of 10 μL should be used for analysis.
18. Characterizing CoA SILEC Profile: Generate a *m/z* list from the neutral loss scan and compare them against a *m/z* list of CoA species (Appendix), and prepare a SRM experiment for each of these parent ions and their respective product ions. The singly charged protonated molecule should be used for the parent CoA while

the associated product ion of 507 amu lower than the parent protonated molecule should be used. For example: acetyl-CoA has a parent protonated molecule of *m/z* 810.1 and a product ion at *m/z* 303.1 while [$^{13}C_3{}^{15}N_1$]-acetyl-CoA has a parent protonated molecule of *m/z* of 814.1 and a product ion at *m/z* 307.1

19. Determining labeling efficacy: Re-inject and analyze the sample using the LC-SRM/MS method, monitoring both the labeled and unlabeled channels to determine the amount of unlabeled CoA remains for each acyl-CoA.
20. Confirmation of acyl-CoA species: To confirm the identity of the labeled CoA species, spike extracted SILEC standards with a mixture of the CoA thioesters of interest (1 pmol each) and repeat the LC-SRM/MS analysis. The labeled and unlabeled compounds should co-elute. This is particularly important when multiple peaks arise or if there are multiple isobaric CoA species with similar parent and product ions.

Harvesting

21. If there are certain CoA species you are interested in that are not represented in the mixture, further steps may need to be taken (see "Generating customized SILEC standards"). In the case of incomplete labeling, systematic troubleshooting may be necessary (See troubleshooting section: *Incomplete labeling*). If one or more CoA thioesters of interest are not represented, continue on to step 23 to generate "customized" SILEC standards. If labeling is complete (> 99% labeling) and CoA profile is satisfactory, perform CoA extraction for all plates (steps 7-10).

22. Pool together acid soluble SILEC extracts, label batch and freeze at -80°C in 10 mL aliquots.

Pause point: The pooled acid soluble extracts contain the SILEC standards that will later be spiked into cell or tissue samples. These standards can be stored indefinitely at -80°C, but should be spiked into a new standard curve for each analysis. Avoid repetitive freeze-thaw cycles.

Generating customized SILEC standards

23. (Continued from step 21) Wash half of the plates 2X with PBS.
24. For the washed plates, replace with customization media and incubate washed plates in treatment media for 1 h.
25. Test labeling using steps 17-20
26. After incubation, harvest and extract CoA from all plates (steps 7-10) and pool together. This pooled extract should contain a SILEC CoA profile with increased levels of the species of interest.

CRITICAL STEP: It should be noted that using exogenous biological and toxicological stimuli to change the CoA profile in a given cell types is largely empirical and needs to be optimized for different cell systems and conditions. Prior to scaling up, optimization can be performed in unlabeled cells, though should be confirmed in labeled cells as well.

Producing purified [$^{13}C_3{}^{15}N$]-CoASH

27. (Continued from step 5) After overnight incubation in ultra-labeling media, perform steps 6-9 for all plates and pool together acid soluble lysates, which contain CoASH and short chain acyl-CoAs.
28. Adjust pH of lysate to ~13 with 40% KOH w/v. (Add 500 μL KOH to 5 mL TCA extract) and incubate at room temperature for 1 h.
29. Adjust pH of lysate to 6 with formic acid.
30. Purify labeled CoA using either preparative HPLC (monitor UV wavelength 254) or SPE extraction using previously described procedures.
31. Dry down hydrolyzed extract, which contain purified [$^{13}C_3{}^{15}N$]-CoASH. This product can now be used to chemically synthesize a particular CoA derivative.[73, 123-125]

Utilizing SILEC standards for CoA analysis

32. Thaw an adequate amount of previously generated acid-extracted SILEC CoA internal standard mixture. Generally, 1 mL of internal standard mixture is needed for every 5 samples. After thawing, mix thoroughly by vortex-mixing and leave on ice.

CRITICAL STEP: It is important to determine the amount of labeled SILEC CoA standard needed prior to the experiment. If multiple batches are necessary for a single experiment, these batches must first be pooled together prior to application to samples/standard curve. Due to the biosynthetic nature of SILEC generation, there can be significant batch-to-batch variability and likewise, using different batches of

labeled internal standards in different samples of the same experiment can lead to erroneous measurements.

33. To prepare standard curve samples: thaw and mix equal concentrations of unlabeled CoA standards of interest creating a master mix, and perform two-fold serial dilutions, from 1 µM down to approximately 10 nM, in extraction solution (10%TCA). Mix 50 µL of each dilution with 0.75 mL extraction solution and 0.2 mL of thawed SILEC CoA internal standard extract (for a final volume of 1 mL) and vortex. This will generate a standard curve from approximately 100 fmol to 10 pmol of each CoA standard on column.
34. To prepare experimental samples: add 0.8 mL ice cold TCA along with 0.2 mL of the same SILEC internal standard mixture to harvested cell pellets, snap-frozen or lyophilized tissues, or purified extracted cells (platelets, lymphocytes, fibroblasts, etc.)
35. For cell samples, sonicate for 30 sec on ice in a pulsatile manner. For tissue samples, homogenize according to standard protocols. In either case, perform the same processing step for the standard curve samples as well.
36. Spin processed acid extracted lysate at 15000*g* for 5 min to precipitate protein pellet.
37. Perform SPE extraction of CoA species as previously described (steps 10-16).
38. Re-suspend samples in 50 µL 5% SSA.

PAUSE POINT: Samples and standards can be immediately analyzed or frozen at -80°C for future analysis. Since the SILEC CoA internal standards are included, effects on sample stability should be reflected in the internal standards as well.

39. For analysis, inject 10 μL from each sample or standard mix and perform LC-MS/MS analysis using selected reaction monitoring (SRM) mode developed previously.
40. From the raw data, develop a standard curve for each of the CoA species, with the x-axis as the known amount of injected standard and the y-axis as the ratio of unlabeled to labeled integrated peak areas.
41. Use the regression line from this standard curve to calculate the amount of each CoA thioester in samples.

TIMING

Typical times used in our laboratory for the various steps are as follows:

SILEC labeling:

- Expansion: 12-16 days
- Ultra-labeling: 1 day
- Testing of labeling: 3 h
- Customization: 1 h to 12 h
- Testing of labeling: 3 h
- Harvesting and Extraction: 30 min

Application of internal standards

- Sample preparation: approximately 1 h

Analysis: 30 min per sample. One day per experiment, total time: 15-20 days.

3.5 Troubleshooting

3.5.1 Perturbation of cell growth kinetics by SILEC media.

Changes in cell media components may affect a number of cell growth parameters such as doubling times, cell viability, adherence and morphological characteristics. While slightly slower cell growth is expected with SILEC media, if there is severely deranged cell growth or morphological changes, media components should be serially investigated. *Serum.* While serum is necessary for many cell lines, the lack of serum standardization and lot-to-lot variability makes it very challenging to reproducibly scale-up many biosynthetically-generated compounds. Charcoal-stripping is commonly used to standardize serum and csFBS is the optimal serum for our purposes as it dramatically reduces unlabeled pantothenate, which can contaminate the labeled CoA pool. In addition to removing pantothenate, however, charcoal-stripping also removes a number of other serum components including hormones, growth factors and other B vitamins, which can also negatively affect cell growth.[114, 115] One method to overcome this is by either increasing the amount of csFBS or using dFBS during the expansion stage, which may be enough to overcome these effects. Although dFBS would slightly increase the level of unlabeled pantothenate, it still has considerably less pantothenate than undialyzed serum. This may improve cell growth during the expansion phase. If it is found, however, that dFBS is necessary during the ultra-labeling step, the concentration should be substantially reduced and the concentration of pantothenate should be increased to lower the percentage of unlabeled pantothenate in the serum. If both csFBS and dFBS are prohibitive to cell growth, and uFBS is necessary, a different cell line should be considered as the high level of residual pantothenate in uFBS would be difficult to

overcome by simply adding more labeled compound. *Other media components.* Commercial services are available for the production of specialty media such as pantothenate-omitted RPMI 1640 media, which is used in our protocol. However, should you choose to prepare your own SILEC media, make sure all components are dissolved and that your cells show similar growth characteristics when this media is supplemented with standard FBS and the same concentration of pantothenate. Since certain media components can also degrade over time, prepared media should be kept at -20°C for long term storage. Finally, contamination with mycoplasma can slow cell growth. Therefore, thaw fresh cells or perform simple tests for mycoplasma to eliminate this possibility.

3.5.2 Incomplete labeling.

As previously mentioned, a critical aspect to biosynthetic generation of labeled standards is minimizing the unlabeled fraction. Typical SRM chromatograms of CoASH harvested from [$^{13}C_3{}^{15}N_1$]-pantothenate-labeled cells are provided in Figure 3.4. Figure 3.4A shows an example of insufficient labeling, with greater than 5% of the CoASH unlabeled, while Figure 3.4B depicts CoASH from a SILEC batch with more complete labeling (less than 1% unlabeled). There are three underlying causes for incomplete labeling: (1) contaminating unlabeled pantothenate in the media, (2) unlabeled pantothenate in the [$^{13}C_3{}^{15}N$]-pantothenate stock, and (3) insufficient turnover of pantothenate or CoA pool within the cell line. First, determine if there is contaminating unlabeled pantothenate in the media, as this is the most likely cause of the incomplete labeling. For mammalian cell culture, if the pantothenate-omitted media was commercially prepared, verify that pantothenate is not in the formulation. If this was

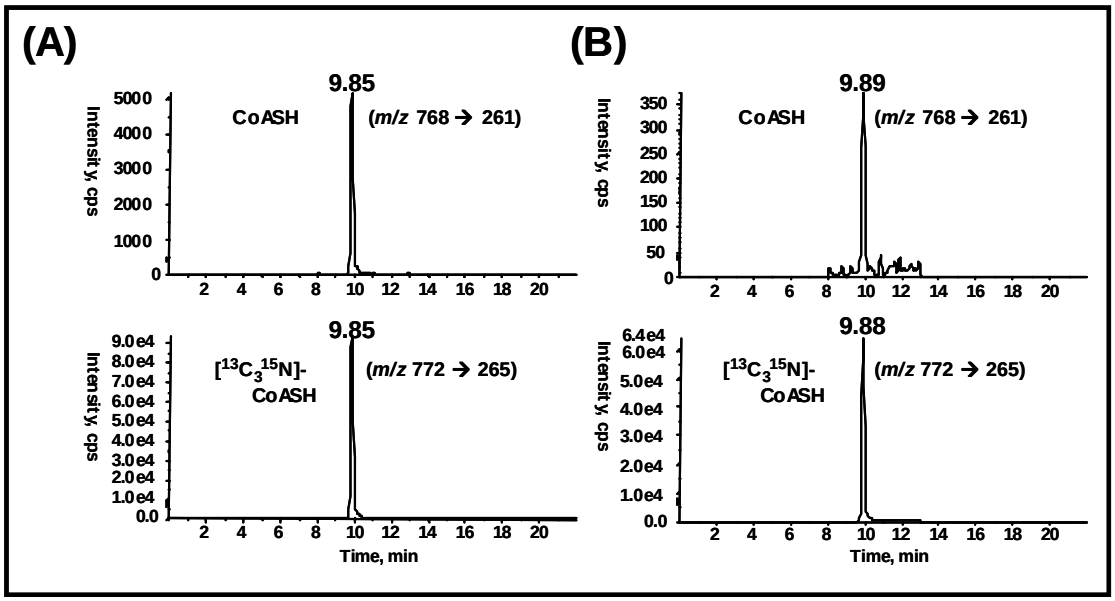

Figure 3.4 Comparison of complete and incomplete labeling. LC-MS (SRM) chromatograms of CoASH harvested from [$^{13}C_3{}^{15}N_1$]-pantothenate-labeled cells. Both unlabeled CoASH (*m/z* 768 → 261) and [$^{13}C_3{}^{15}N_1$]-CoASH (*m/z* 772 → 265) chromatograms are presented to illustrate (A) sub-optimal labeling (>5% unlabeled), and (B) near-complete labeling (<1% unlabeled). Extraction and analysis were performed as specified in the protocol.

prepared in house, verify that the base nutrient mix you are using does not contain any pantothenate. For insect cell culture, Schneider's media contains yeast extract, which contains a variable, though significant level of different B vitamins, including pantothenate. For this reason, a higher concentration of labeled compound is needed for insect SILEC preparation.

If there is incomplete labeling in insect cells, it could very well be coming from increased levels of pantothenate in the yeast extract (yeastolate). To overcome this, the ultra-labeling step can be performed with HBSS media overnight containing 4 mg/L labeled pantothenate which should increase labeling to greater than 99%. More likely, however, the unlabeled pantothenate is originating from the csFBS. While there should be less than 0.1 mg/L of pantothenate remaining in the csFBS[93] (resulting in an effective 0.01mg/L in media containing 10% serum), it is possible that a particular lot of serum may have more, or that a higher concentration of serum is needed for a particular cell line. Adding additional labeled pantothenate to the media should overcome this problem. If this is a newly occurring problem, check the lot of the csFBS, as lot-to lot variability can exist for serum. If a particular lot of csFBS has worked in the past, it may be worth ordering several bottles of this for future use. The serum can be frozen down and stored at -20°C for long-term storage. The second possibility is that the stock itself is contaminated with unlabeled pantothenate. This can be assessed by performing mass spectral analysis of the labeled stock. To do this, reconstitute a small amount of the labeled pantothenate stock and using flow infused syringe injection and SRM analysis. The relative ratio of labeled to unlabeled pantothenate represents the maximal purity that the CoA can be labeled. If this is not acceptable, another source of labeled pantothenate

should be sought. For our experiments, we found that the isotopic purity of the stock was greater than 99.5%. Finally, the last problem that can arise, particularly with suspension culture is that a certain amount of the unlabeled compound is not turning over and remains in the cellular pool due to cell death or senescence. This is more of a problem with SILAC protocols because different proteins turn over at various frequencies and salvage pathways of particular amino acids may cause these unlabeled species to continue to propagate in culture. For CoA species, this turnover is greater and more than 50% of the CoA can turnover in the cell in 24 h,[93] although different CoA species may not turnover as rapidly. To overcome this problem, simply passage the cells two or three more times in the expansion media. If the cells are being split 1:3, less than 0.5% of the original cell mass will remain after 5 passages. While this may add an additional week to the expansion phase, this would replace at least 99.5% of the original cell mass and likewise the original unlabeled CoA. Finally, batch-to-batch variability can arise from the biological variability of cells in different stages of the cell cycle. This effect can be overcome by synchronizing cells with serum-free media prior to the final step of labeling.

3.5.3 Problems in sample preparation and LC-MS

SPE. Oasis HLB columns (Waters) have been found to be optimal for short-chain acyl-CoA extraction, though other methods such as liquid-liquid extraction could be used as well.[67, 93] However, when the experiment involves more complex biological matrix such as in tissue samples, or if a larger amount of biological material is being used (to measure lower abundance analytes), a greater matrix effect may be observed. In our own experience, we have extracted CoA species from liver, brain and adipose tissues. Brain

and liver tissue contain abundant acyl-CoA metabolites, while adipose tissue was found to contain significantly less CoA content, likely due to the decreased cellular content per unit weight of tissue. Also, after homogenization and centrifugation of the adipose tissue, a significant layer of fatty tissue remained on the top of the acid extract. Therefore, the aqueous layer was transferred to a fresh tube, avoiding the lipid layer, and centrifuged again prior to SPE extraction. In each case, repeating the SPE washing step (with water) one or two times may help. Also, using a molecular weight cut off filter prior to SPE extraction may also reduce the matrix effect, though this will increase processing time. Using methanol containing concentrated ammonia may improve elution for all extractions.[67]

LC. While acyl-CoA analysis is generally robust, repeated injections of cell and tissue extracts can lead to build-up of biological materials on the column, which can lead to distortions in peak shape.[69] For this reason, we have added solvent C as a column wash step. If peak distortion is occurring, increasing the wash step as well as slowing down the ramp time for washing can improve column performance, though this will also increase run times. Also lowering the pH of this wash can also improve the ruggedness of the method.

MS. In the case of inadequate sensitivity, use acetonitrile instead of methanol in the mobile phase whenever possible, and decrease formic acid concentration during MS analysis. Also, if LC-SRM/MS analysis is increased to include a large number of species, a proper number of analytical points may not be achieved across each peak and may lead to incorrect quantitation, even with internal standards. To overcome this, SRM dwell time should be reduced so as to increase the number of points across the peak. For

example, if measuring eight CoA species along with their internal standards (16 analytes total), using dwell times of 80-100 milliseconds may be acceptable. However, if the number of analyzed CoA are increased to 20-30 species (40-60 total), shorter dwell times (20-30 ms) may be necessary to achieve enough points across the peak. Also, dividing up the analysis into shorter segments can allow for longer dwell times.

Chapter 4: Development of LC-MS method to monitor CoASSG and its relevance to mitochondrial oxidative stress

4.1 Abstract

Despite technical developments in measuring reactive species in the mitochondria, few markers of mitochondrial oxidative stress are currently available. It has been previously reported that the ratio of CoASH to CoASSG can be used as a marker of intramitochondrial oxidative stress. However, currently analytical methods lack adequate sensitivity for rigorous measurements of CoASSG in cell culture. In this chapter, we present a novel LC-SRM/MS method to measure CoASSG. To accomplish this, CoASSG was first synthesized from CoASH and GSSG. SILEC methodology was used to generate isotopically labeled [$^{13}C_3{}^{15}N_1$]-CoASSG to be used as an internal standard for measuring this compound from cell culture. Menadione and rotenone, both known to generate mitochondrial ROS, were applied to murine heptatoma cells (Hepa 1c1c7) and intracellular levels of CoASH, CoASSG and various short chain acyl-CoA thioesters were quantified using this method. Menadione was found to significantly increase CoASSG and decrease CoASH, the latter likely resulting from arylation of menadione and sequestration of the CoASH pool. Although rotenone had a minimal effect on CoASSG levels, it had a dramatic impact on other CoA thioesters levels at much lower doses, a finding which is further explored in the following chapter. This methodology allowed more rigorous and sensitive measurement of CoASSG and will allow further exploration into its mechanism of formation, as well as aid in finding biomarkers for mitochondrial oxidative stress.

4.2 Introduction

Oxidative stress represents a pathological state in which cellular antioxidant defenses are overwhelmed by oxidative processes arising from endogenous or exogenous sources.[126] During oxidative stress, several highly labile ROS can damage intracellular macromolecules proteins, lipids, and DNA (both nuclear and mitochondrial).[127-130] Accumulation of this damage is believed to contribute to cancer, neurodegenerative diseases and is considered to be a central factor in aging.[131-134] The mitochondria are a major source and target for ROS. Although numerous reports have suggested mitochondrial dysfunction causes increased mitochondrial ROS generation through reverse electron transport,[135-138] an increase in mitochondrial ROS does not necessarily equate to mitochondrial oxidative stress. In fact, under normal conditions of mitochondrial respiration, it has been estimated that as much as 0.1 % and 0.5 % of oxygen consumed the mitochondria is converted to superoxide.[139, 140] In addition, ROS play important physiologic roles in cell signaling.[141, 142] Therefore, despite technical developments in the measurement of reactive species in the mitochondria,[143] increases in ROS or RNS are not necessarily indicative of a pathological state of mitochondrial oxidative stress, for which few markers are currently available.

Glutathione (GSH) is a highly abundant intracellular thiol that serves not only a major reducing agent, but also as an essential detoxifier of xenobiotics and potential damaging electrophiles.[106] Glutathione peroxidase can detoxify intracellular H_2O_2, generating oxidized glutathione (GSSG), which can be reduced back to GSH by the action of glutathione reductase. The redox potential of the cell can be assessed by

measuring the ratio of GSSG: GSH, which is increased during oxidative stress. This can result from GSH-dependent ROS detoxification pathways being compromised or overwhelmed.[107] CoASH is an abundant mitochondrial thiol and like GSH, which can be oxidized to GSSG, CoASH can be oxidized to form CoA-CoA disulfide, [65] or can be converted to CoASSG.[73] Although the exact role of this mixed disulfide is unknown, there is evidence that it has potent vasoconstrictive effects. [46, 50, 51] Like GSSG: GSH, the ratio of CoASSG: CoASH has been shown to increase during states of intramitochondrial oxidative stress, such as in rat models of seizures and hyperoxia,[53, 55] or in response to certain pharmacological agents.[42] However, the primary method to measure CoASSG has been with LC-UV, which requires relatively high concentrations of CoASSG and is inadequate for most practical cell culture applications. In this chapter, we develop a novel LC-SRM/MS method to monitor CoASSG, along with CoASH and other CoA thioesters. This assay was then used to assess mitochondrial oxidative stress generated by menadione, a vitamin K precursor, and rotenone, a classic mitochondrial complex I inhibitor, both known to generate reactive oxygen species in the mitochondria.[135, 144]

4.3 Materials and Methods

4.3.1. Materials

Oxidized glutathione (GSSG), menadione and rotenone and were all purchased from Sigma-Aldrich (St. Louis, MO). Remaining materials were obtained as previously reported.

4.3.2 Synthesis and purification of CoASSG

CoASSG was synthesized using a method developed by Chang and Wilken.[73] Briefly, a 3 mL solution containing 1 mM CoASH and 10 mM GSSG was prepared in a 50 mM sodium phosphate buffer (pH 6.8). Oxygen was bubbled through the mixture at 37°C for 3 h. CoASSG was purified using preparative HPLC using a reversed-phase gradient separation Waters Xbridge C18 column (10 x 250 mm, 5 micron) on a Hitachi HPLC system equipped with a L-7100 pump, L-7400 UV detector (monitoring 254 nm) and D-2500 Chromato-Integtrator. Solvent A was 5mM ammonium acetate in water was and solvent B was 5 mM ammonium acetate in methanol. Gradient conditions (%B) were as follows: 4% for 3 minutes, increased to 50% over 17 minutes, to 80% over 2 minutes, held at 80% for 3 minutes, returned to 4% over 1 min, and re-equilibrated at 4% for 6 minutes. Flow rate was 3 mL/min. Eluting peaks were collected manually and identities of both CoASSG and CoASH were confirmed by LC-tandem MS (MS/MS) analysis on an API 4000 triple quadrupole mass spectrometer (Applied Biosystems).

4.3.2. LC-MS

SILEC standards were prepared as previously described in chapters 2 and 3. LC-MS analysis was also performed as previously described. SRM transitions were determined for CoASSG (*m/z* 1073.1 → 566.1) and isotopically labeled [$^{13}C_3{}^{15}N_1$]-CoASSG was (*m/z* 1077.1 → 570.1). Both transitions were added to the previously described SRM transitions developed for short chain acyl-CoA analysis. Additionally, we monitored BHB-CoA (*m/z* 854.1 → 347.1) and [$^{13}C_3{}^{15}N_1$]- BHB-CoA (*m/z* 858.1 → 351.1). A typical LC-MS chromatogram demonstrating baseline separation of BHB-CoA and malonyl-CoA (isobaric) is provided in the appendix (Figure A.2).

4.3.3 Cell culture and treatments

Murine hepatoma cells (Hepa 1c1c7) were maintained in RPMI media supplemented with 10% FBS, glutamine, penicillin and streptomycin at 37°C, with 5% CO_2. Menadione and rotenone stocks were made fresh in DMSO (1 mM). When cells had reached 80% confluence, they were washed twice with PBS and the media was replaced with HBSS, containing Ca^{2+}, Mg^{2+}, 10 g/L glucose, 25 mM HEPES and either menadione (2 μM and 20 μM), rotenone (2 μM and 20 μM), or DMSO (vehicle). After 1 h, cells were harvested by scraping, processed and analyzed as previously described, with the additional SRM transitions noted above.

4.4 Results

4.4.1 Synthesis and purification of CoASSG

CoASSG was synthesized using modifications to a previously developed method.[73] The disulfide exchange between CoASH and GSSG resulted in the non-enzymatic formation of CoASSG. This was then purified by preparative HPLC-UV, monitoring absorption at 254 nm. Preparative LC-UV chromatograms of GSSG alone, CoASH as well as the reaction mixture are provided in figure 4.1. Four distinct peaks can be observed at 4.00 min (unreacted GSSG), 10.70 min, 11.56 min (unreacted CoASH), and 12.44 min. The remaining two peaks (10.70 min and 12.44 min) were collected and concentrated with nitrogen, and a small aliquot was re-injected to confirm purity. CID MS/MS revealed that peak 2 (10.70 min) was in fact CoASSG, and the product ion spectra for this molecule along with the product ion spectra for CoASH are

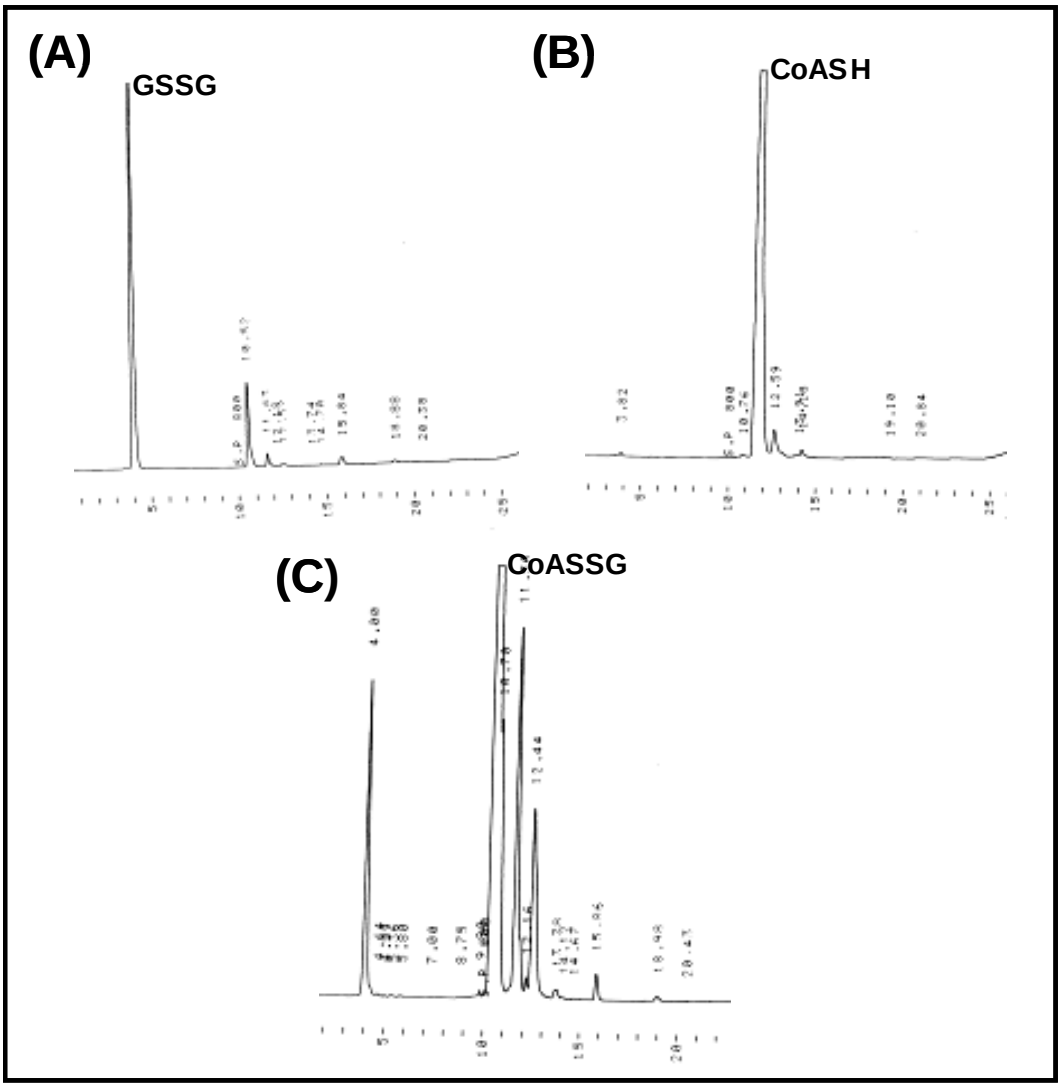

Figure 4.1 Synthesis and purification of CoASSG. CoASSG was synthesized by using thiol exchange reaction of CoASH with GSSG. The reaction mixture was separated and collected using preparative HPLC, monitoring UV absorption at 254 nm. LC-UV chromatograms showing (A) GSSG alone, (B) CoASH alone and (C) reaction mixture of CoASH and GSSG. Peaks were collected, concentrated and identified using CID-MS (Figure 4.2).

provided (Figure 4.2). Like all acyl-CoA thioesters, both CoASH and the mixed disulfide CoASSG were shown to have their most prominent fragment ion to have a neutral loss of 507 amu. For CoASH, the optimal transition was 768.1 → 261.1 (as has been previously shown) while for CoASSG, the optimal transition was 1073.1 → 566.1. The spectra found for CoASSG is consistent with a fast atom bombardment spectra previously published.[42] These transitions were added to the previously developed SILEC method. Figure 4.3 shows a LC-SRM/MS chromatogram of acid extracted CoA species from a mixture of SILEC-labeled and unlabeled Hepa 1c1c7 cells.

4.4.2 Menadione affects CoASSG: CoASH ratio more than rotenone

Hepa 1c1c7 cells were treated with increasing doses of menadione or rotenone for 1 h, and short-chain acyl-CoA species, along with CoASH and CoASSG were analyzed using the described methodology (figure 4.4) Rotenone did not significantly increase levels of CoASSG as we had originally suspected, even at 20 μM. Menadione treatment, on the other hand, resulted in significant decreases in CoASH and increases in CoASSG. We had previously performed an experiment from chapter 3 in which we generated labeled [$^{13}C_3{}^{15}N_1$]-menadione-CoA with treatment of SILEC labeled cells with menadione. We have presented the LC-constant neutral loss/MS spectrum from that study in figure 4.5, which illustrates the increase in [$^{13}C_3{}^{15}N_1$]-menadione CoA as well as a decrease in [$^{13}C_3{}^{15}N_1$]- CoASH with menadione treatment. In addition, changes in short chain acyl-CoA species were also monitored and are presented in figure 4.6.

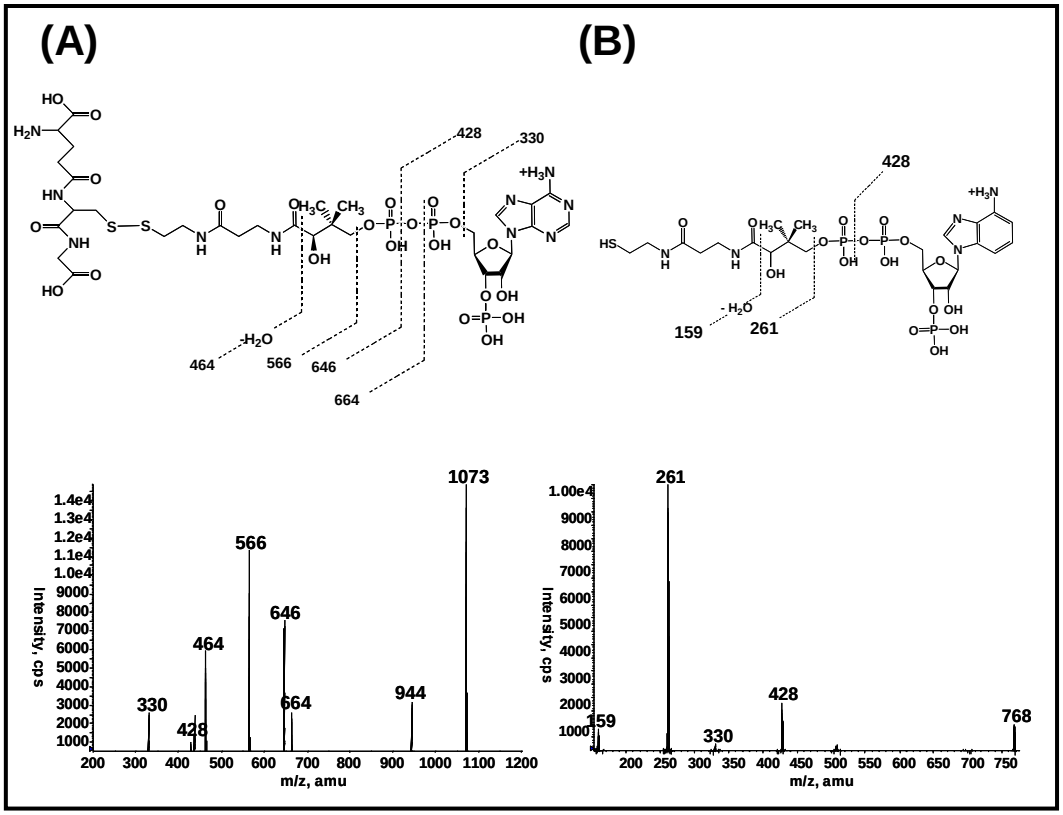

Figure 4.2 Collision-induced dissociation (CID) mass spectra for CoASH and CoASSG. Preparative HPLC effluent corresponding to UV peaks (254 nm) were collected, concentrated and subjected to CID. CID-mass spectra as well as fragmentation schemes for (A) CoASH (MH^+, *m/z* 768), and (B) CoASSG (MH^+, *m/z* 1073).

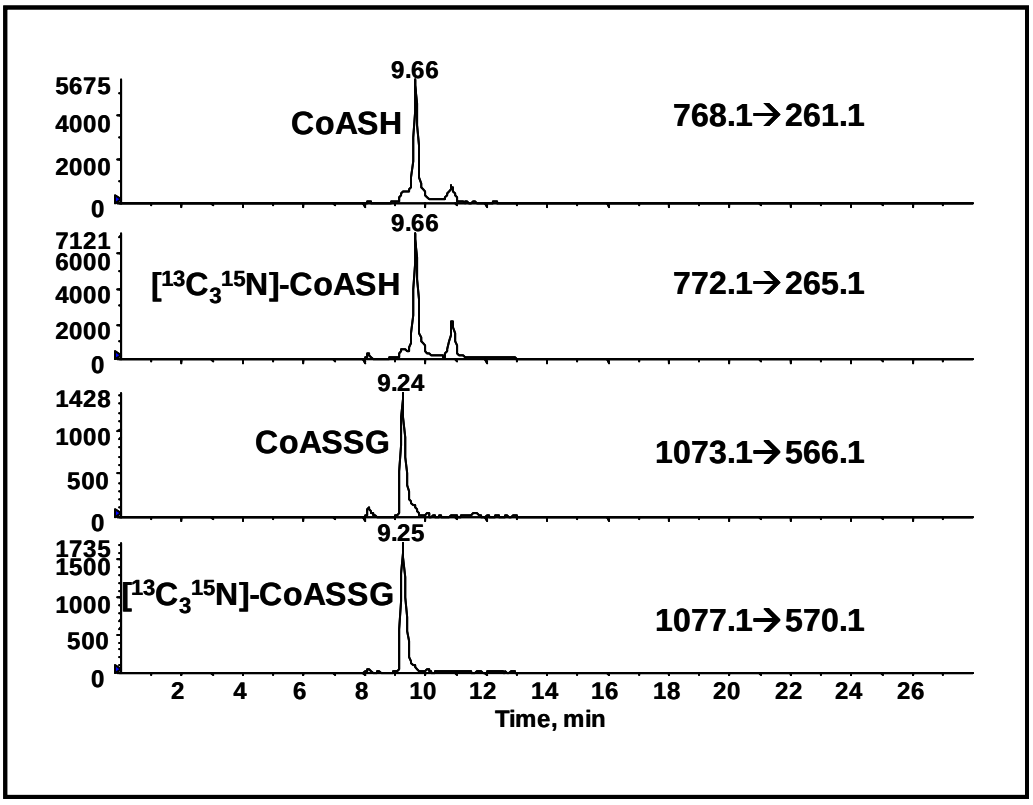

Figure 4.3 LC-SRM/MS chromatograms of CoASH and CoASSG, along with SILEC-labeled stable isotope analogs.

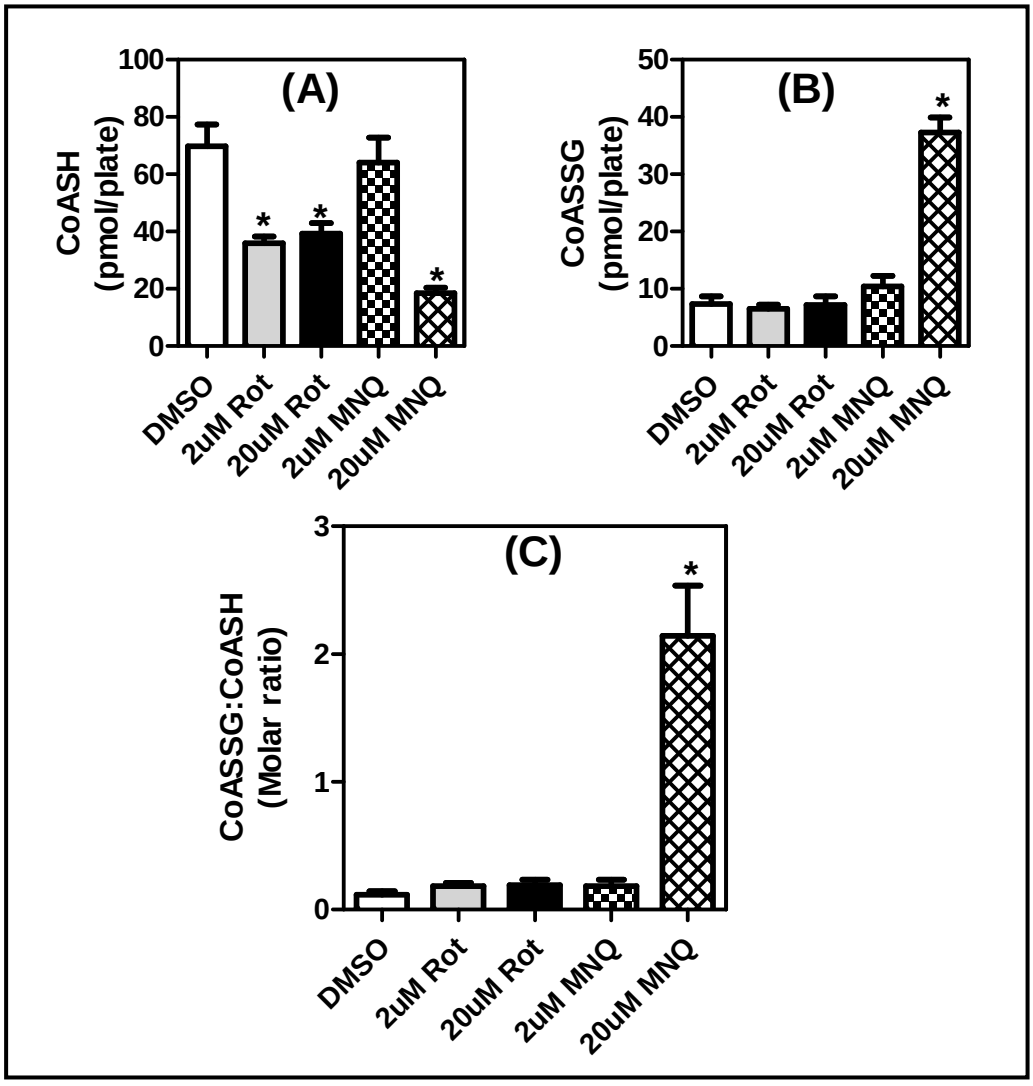

Figure 4.4 Dose-dependent effects of menadione and rotenone on CoASH, CoASSG and CoASSG: CoASH ratio. Hepa 1c1c7 cells treated with rotenone and menadione (2 μM or 20 μM) or DMSO (vehicle) and processed for intracellular levels of (A) CoASH (B) CoASSG (C) and CoASSG: CoASH. Error bars are SEMs for n=4, * $p < 0.005$ compared with DMSO.

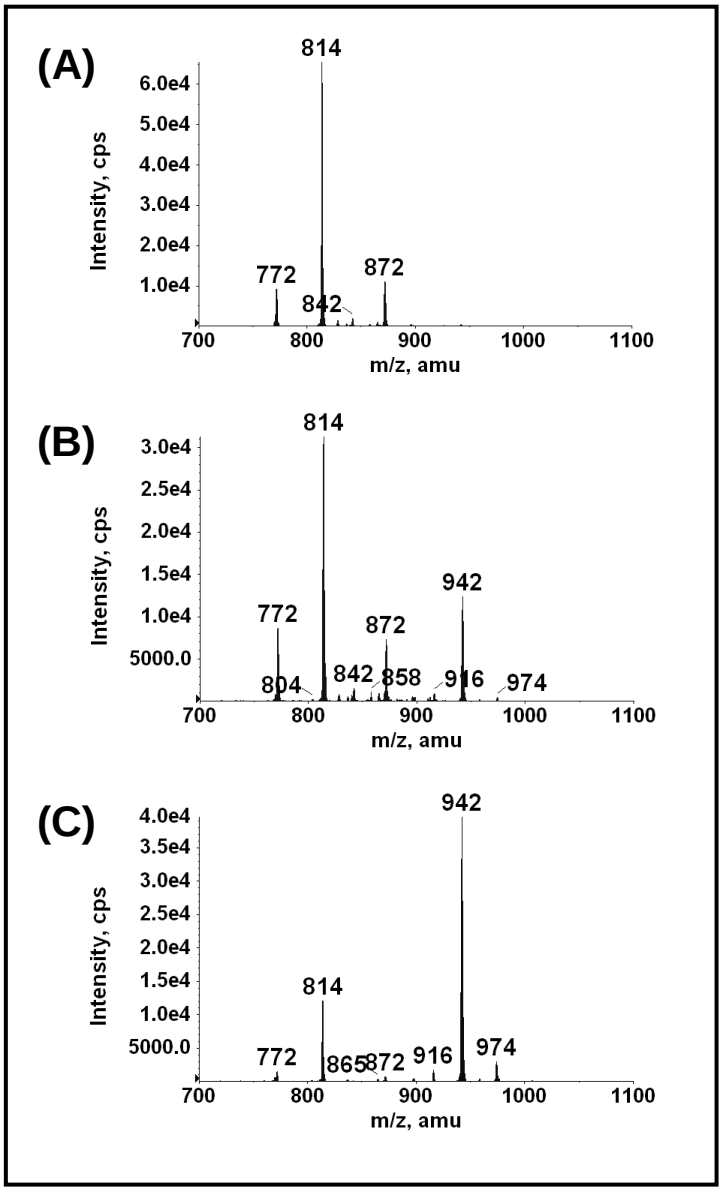

Figure 4.5 LC-constant neutral loss/MS with a neutral loss of *m/z* 507 of SILEC labeled hepatocytes treated with (A) DMSO (vehicle), (B) 10 μM menadione, or (C) 20 μM menadione for 1 h. The parent ions (MH^+) of the observed CoA species are [$^{13}C_3{}^{15}N_1$]-CoASH (MH^+, *m/z* 772), [$^{13}C_3{}^{15}N_1$]-acetyl-CoA (MH^+, *m/z* 814), [$^{13}C_3{}^{15}N_1$]-succinyl-CoA (MH^+, *m/z* 872), [$^{13}C_3{}^{15}N_1$]-HMG-CoA (MH^+, *m/z* 916), and [$^{13}C_3{}^{15}N_1$]-menadione-CoA (MH^+, *m/z* 942).

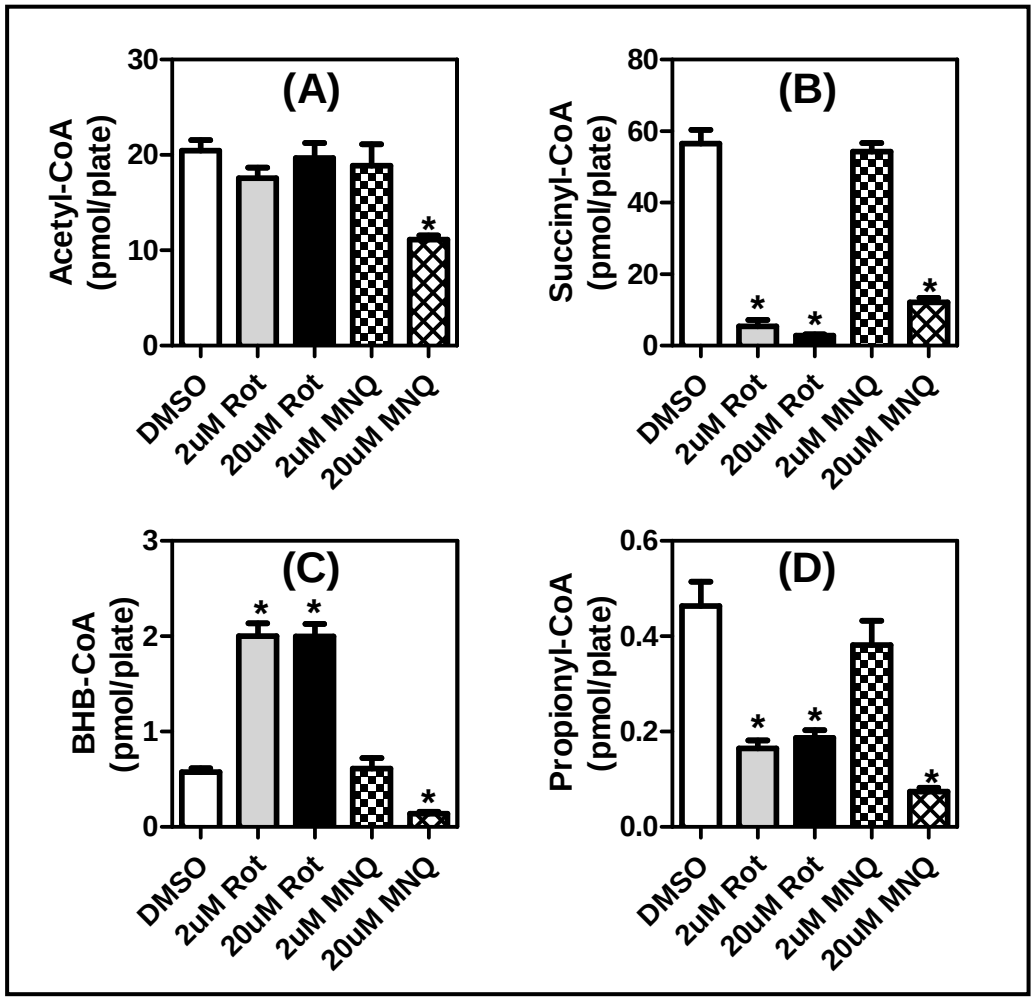

Figure 4.6 Dose-dependent effects of menadione and rotenone on selected short-chain acyl-CoA thioesters. Hepa 1c1c7 cells treated with rotenone and menadione (2 μM or 20 μM) or DMSO (vehicle) and processed for intracellular levels of (A) acetyl-CoA (B) succinyl-CoA (C) BHB-CoA and (D) propionyl-CoA. Error bars are SEMs for n=4, * $p < 0.005$ compared with DMSO.

4.5 Discussion

In this chapter, we have developed for the first time an LC-SRM/MS method to measure CoASSG. Using the previously described SILEC methodology, we are also able to generate isotopically labeled [$^{13}C_3{}^{15}N_1$]-CoASSG, which can be used as an internal standard for measuring this compound from cell culture. This methodology allows more rigorous as well as sensitive analysis of CoASSG in cell culture, where lower concentrations of CoA species limits the application of currently available analytical methods. As CoASSG: CoASH ratio is a purported measure of intramitochondrial oxidative stress, we treated cells with agents known to cause oxidative stress in the mitochondria. Our assay has revealed that menadione, but not rotenone, causes a significant increase in CoASSG, particularly at higher doses.

In addition to increasing intracellular levels of CoASSG, menadione caused decreases in CoASH levels, likely due to arylation of CoASH, as thiols are known to react readily with redox cycling quinones.[145] Additionally, in chapter 3 we demonstrated the generation of [$^{13}C_3{}^{15}N_1$]-menadione-CoA internal standards by treating SILEC labeled cells with menadione. In figure 4.5, we presented the LC-constant neutral loss/MS spectrum from that study, which illustrates the increase in [$^{13}C_3{}^{15}N_1$]-menadione CoA as well as a decrease in [$^{13}C_3{}^{15}N_1$]- CoASH with menadione treatment. Though this was a qualitative rather than a quantitative assessment, a substantially larger m/z 942 peak (corresponding to [$^{13}C_3{}^{15}N_1$]-menadione CoA) is seen with 20 μM compared to 10 μM menadione treatment, as well as a much more substantial decrease in [$^{13}C_3{}^{15}N_1$]-CoASH. A more thorough quantitative dosing analysis to assess the effects of menadione treatment on both menadione-CoA levels and decreases in CoASH levels is needed. This

increase in CoASSG could be a result of the detoxification of menadione, from increased mitochondrial oxidative stress, or a combination of both processes. Although rotenone did not appear to increase CoASSG levels significantly, it did, however, decrease intracellular levels of CoASH, succinyl-CoA and propionyl-CoA and increased BHB-CoA levels even at 2 μM. Further exploration of these changes in human cell lines are described in the following chapter.

Chapter 5: Rotenone-mediated changes in intracellular CoA thioester levels: implications in mitochondrial dysfunction

5.1 Abstract

Rotenone is a natural organic pesticide and potent complex I inhibitor shown to cause Parkinson-like neurodegeneration in rodents and has recently been linked to PD in humans. In this chapter, rotenone-mediated effects on intracellular levels of various CoA thioesters were monitored using a stable isotope dilution LC-MS methodology. LC-SRM/MS analysis with SILEC standards were performed to rigorously quantify dose-dependent effects of rotenone on intracellular short chain acyl-CoA species in various human cell lines, including neuroblastoma (SH-SY5Y), hepatoma (HepG2) and bronchioalveolar carcinoma (H358) cells. To further characterize the temporal nature of these changes in a neuronal cell type, a time course study was performed in SH-SY5Y cells. Finally, stable isotopic tracer analysis using [U-$^{13}C_6$]-glucose was performed in these cells in the presence or absence of rotenone. Rotenone induced a dose-dependent decrease in succinyl-CoA and increase in BHB-CoA in all three cell lines. Isotopic tracer analysis revealed that rotenone inhibited [U-$^{13}C_6$]-glucose-derived acetyl-CoA and succinyl-CoA biosynthesis in SH-SY5Y neuroblastoma cells. These changes may reflect compensatory metabolic changes in response to rotenone.

Portions of this chapter have been previously published (Basu SS, Blair, IA. *Chem Res Toxicol*, 2011).

5.2 Introduction

Numerous studies have suggested a link between pesticide exposure and PD, [146] particularly to rotenone and paraquat, two naturally occurring organic pesticides. A recently published nested case-control study demonstrated a 2.5 fold increase in the relative risk of developing PD amongst farmers exposed to either rotenone or paraquat.[147] Although both pesticides are mitochondrial toxins, they appear to have distinct toxicological mechanisms.[25, 148-150] The focus of this chapter is to explore the effect of rotenone on central metabolic pathways in the cell.[151, 152] The highly lipophilic nature of rotenone allows it to enter the blood brain barrier, freely cross cellular membranes and accumulate in subcellular organelles such as the mitochondria. Once in the mitochondria, rotenone is known to bind to complex I (NADH-ubiquinone oxidoreductase), the first enzyme complex of the mitochondrial respiratory electron-transport chain. Binding of rotenone to complex I prevents the transfer of electrons from iron sulfur clusters to ubiquinone,[135, 153] affecting oxidative phosphorylation and generating potentially damaging ROS.[138, 140, 154] Chronic, low dose administration of rotenone in rats has been shown to result in selective nigrostriatal degeneration and formation of α-synuclein-positive cytoplasmic inclusions (similar to Lewy bodies) in nigral dopaminergic neurons, resulting in neurodegenerative features similar to those seen in PD.[26, 155, 156] Although the majority of research has focused on rotenone-mediated complex I inhibition and ROS formation, rotenone has been shown to have effects independent of complex I inhibition,[157] and also induces significant metabolic alterations both *in vitro* and *in vivo*. Technological developments in both MS and nuclear magnetic resonance (NMR) have produced a growing number of metabolomic assays to assess changes in intracellular and

extracellular metabolites.[158, 159] Using these methodologies, *in vitro* treatment with rotenone was found to induce significant and unique changes in a number of cellular metabolites, including various Krebs cycle organic acid intermediates as well as intermediates and end-products of other major bioenergetic pathways.[160, 161]

In this study, we further explored metabolic changes induced by rotenone by analyzing its effects on intracellular levels on various short chain acyl-CoA thioesters, which are known to be involved in a number of metabolic pathways.[100] To accomplish this, we used stable isotope dilution LC-MS methodology, which allows more rigorous quantification for biomarkers and endogenous metabolites,[91, 93] using the methodology described in Chapters 2 and 3. We analyzed the dose-dependent effects of rotenone on intracellular levels of short chain acyl-CoA species in various human cell lines, including neuroblastoma (SH-SY5Y), hepatoma (HepG2) and bronchioalveolar carcinoma (H358) cells. To further characterize the temporal nature of these changes in a neuronal cell type, a time course study was performed in SH-SY5Y cells. Finally, stable isotopic tracer analysis using [U-$^{13}C_6$]-glucose, [1,2-$^{13}C_2$]-acetate, and [$^{13}C_3{}^{15}N_1$]-pantothenate was performed in these cells in the presence or absence of rotenone. By monitoring the isotopomer distribution pattern in the measured CoA species, the fate of the labeled atoms and consequently their flux through different metabolic pathways was assessed.

5.3 Materials and Methods

5.3.1 Materials

[1,2-$^{13}C_2$]-acetate was purchased from Cambridge Isotopes (Andover, MA). All other materials used in this chapter were obtained as previously reported.

5.3.2 Generation of stable isotope labeled CoA internal standards

Stable isotope CoA and CoA thioester internal standards were generated as described in chapters 2 and 3, with minor modifications as follows. After 30 plates of Hepa 1c1c7 cells were ultra-labeled (overnight incubation in with 3% csFBS and 3 mg/L [$^{13}C_3{}^{15}N_1$]-pantothenate), 10 plates were treated with 10 mM propionate, 10 plates were treated with 10 mM BHB, and 10 plates were left untreated for 1 h. Cells were then harvested and SILEC CoA species were harvested and extracted as described. TCA extracts from all three groups were pooled, aliquoted, frozen, and stored at -80°C.

5.3.3 Cell culture and rotenone treatments

HepG2 and H358 were maintained in RPMI 1640 media and SH-SY5Y cells were maintained in 1:1 F12:DMEM, each media supplemented with 10% FBS, 2 mM L-glutamine, penicillin and streptomycin. Cells were incubated at 37 °C and 95% humidity with 5% CO_2. Rotenone solutions in DMSO were freshly prepared prior to treatment. Serial dilutions of rotenone were made for dosing and time course studies and treatments were performed when cells were approximately 80% confluent and added directly to the plate (DMSO < 1% volume). Control cells were treated with an equal amount of DMSO containing no rotenone. For dosing study, cells were treated for 1 h prior to harvesting.

For time course study, SH-SY5Y cells were treated in the same manner, and harvested at 1, 2, 4, and 6 h after treatment.

5.3.4 Extraction and measurement of CoA using SILEC standards

Analyses of CoASH and CoA thioesters were performed using modifications of methodology previously described. Briefly, after treatment, cells were harvested by scraping, centrifuged at 500*g*, and resuspended in 1 mL ice-cold 10% TCA containing biosynthetically generated stable coenzyme A thioesters (SILEC). Cells were then pulse-sonicated on ice followed by centrifugation to remove protein debris. The supernatant containing the short chain acyl-CoA species were purified by solid-phase extraction using Oasis HLB SPE columns. The eluent was dried down under nitrogen and resuspended in 50 µL 5% SSA. CoA standards were processed in a similar fashion. To determine approximate cell count, a parallel plate of cells split on the same day were counted. Stable isotope dilution LC-MS analysis was performed as previously described.

5.3.5 Isotopic tracer analysis

SH-SY5Y cells were maintained in culture as described above. For isotopic tracer analysis, glucose-free DMEM media was prepared containing 10% csFBS, penicillin, streptomycin, glutamine and supplemented with 1 mg/L of either unlabeled glucose or [U-$^{13}C_6$]-glucose. Cells were washed with PBS and treated for 6 h with labeled media containing 100 nM rotenone or DMSO (control). After treatment, CoA species were extracted as previously described except without SILEC standards. LC-MS methods conducted in the same manner except that in addition to the M0 CoA molecule,

the M1, M2, M3 and M4 isotopomer of each metabolite was also quantified. Label-free cells were used to generate an isotopomer enrichment matrix for acetyl-CoA, succinyl-CoA, BHB-CoA and CoASH. An isotopomer array generated for each sample was multiplied by the inverse of the matrix generated from the label free cells to determine the absolute concentration of each isotopomer and presented as a percentage of the total isotopomers for each CoA derivative as described by Fernandez *et al.*[162] A similar methodology was used to monitor labeling in Krebs cycle organic acids, which were extracted and derivatized with N-tert-Butyldimethylsilyl-N-methyltrifluoroacetamide (MTBSTFA), according to a previously published protocol.[163] An LC-SRM/MS method was developed to measure derivatized citrate, aKG, succinate and malate along with their M0 to M4 isotopomers. For acetate labeling, SH-SY5Y cells were treated in the same media except that instead of 1 mg/mL [U-$^{13}C_6$]-glucose, 10 mM [1,2-$^{13}C_2$]-acetate was used, and cells were incubated in this media for 6 h. For pantothenate isotopic tracer analysis, SILEC media supplemented with 10% csFBS and 3 mg/L [$^{13}C_3{}^{15}N_1$]-pantothenate was used and cells were incubated for 3 or 15 h. In both cases, untreated cells were used for the background isotopomer distribution matrix determination.

5.4 Results

5.4.1 Rotenone dosing study

Rotenone was found to induce a dose-dependent change in the short chain acyl-CoA profile SH-SY5Y, HepG2 and H358 cells. Most notably, there was a significant decrease in levels of succinyl-CoA (Figure 5.1A) and a concomitant increase in

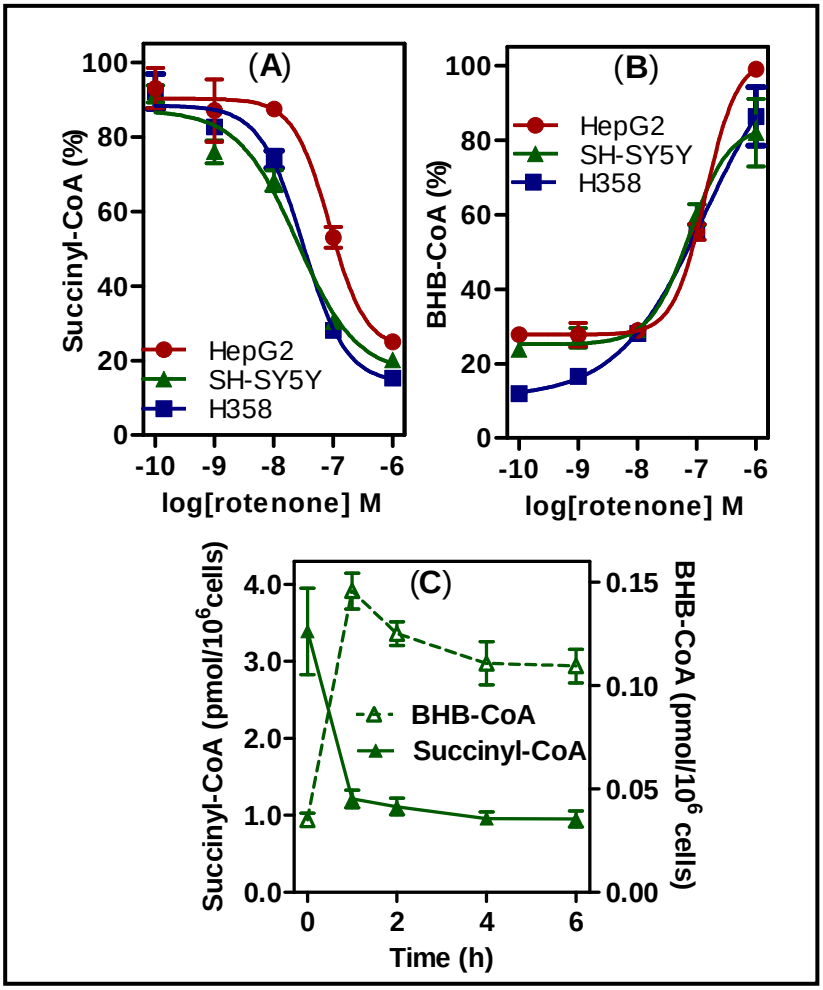

Figure 5.1 Rotenone-mediated changes in intracellular CoA thioester levels. (A) Succinyl-CoA, and (B) BHB-CoA, extracted from SH-SY5Y cells, HepG2 cells, and H358 cells treated with rotenone for 1 h, in triplicate. Values are shown as % of the maximal level for each cell line. (C) Time course of rotenone-mediated changes in intracellular succinyl-CoA and BHB-CoA. SH-SY5Y cells were treated with 100 nM rotenone, harvested at time points up to 6 h, and processed for CoAs. Error bars show SEMs for triplicate determinations. Absolute levels for all measured CoA species are provided in the appendix (Table A.4).

BHB-CoA (Figure 5.1B) after 1 h of treatment with an IC_{50} of < 100 nM in all cell types. There were also significant changes in a number of other acyl-CoA thioesters, which varied among different cell types (appendix, Table A.4). To characterize the temporal nature of these changes, SH-SY5Y cells were treated with 100 nM rotenone and harvested at time points up to 6 h and analyzed for CoA thioesters. The observed changes seen in succinyl-CoA and BHB-CoA persisted for at least 6 h (Figure 5.1C). Overall, these results show that rotenone induces a rapid and persistent metabolic rearrangement in a variety of cell types, similar to changes observed during fasting.[20]

5.4.2 Isotopic tracer analysis

Although the observed changes indicate that rotenone induces a significant metabolic disturbance, absolute CoA measurements represent only a "snapshot" of this metabolic state. To gain additional information on the cumulative flux through different pathways, cells were incubated with [U-$^{13}C_6$]-glucose and isotopomer distribution of the resulting CoA derivatives was analyzed. [U-$^{13}C_6$]-glucose (M6) taken up by cells is converted during glycolysis into two [$^{13}C_3$]-pyruvates (M3), which can subsequently be converted by pyruvate dehydrogenase into [$^{13}C_2$]-acetyl-CoA (M2). Both labeled carbons from acetyl-CoA are then incorporated into citrate and eventually form [$^{13}C_2$]-succinyl-CoA (M2) in the first turn of the Krebs cycle. Additional cycles can result in the M3 and M4 succinyl-CoA isotopomers. It should be noted that isotopic tracer analysis is complex, with numerous intersecting metabolic pathways. For our purposes, however, this simplified interpretation made it possible to asses major changes that were occurring in the cells. SH-SY5Y cells were washed and treated with glucose-free media

supplemented with either unlabeled glucose or [U-$^{13}C_6$]-glucose with or without 100 nM rotenone. The unlabeled cells were used to determine isotopic contributions of unlabeled CoA species to each isotopomer, which were subtracted from the labeled CoA species using a matrix analysis.[162]

Rotenone significantly decreased the incorporation of glucose-derived carbon atoms into acetyl-CoA, from 23% to 5% demonstrating that rotenone inhibited the glucose-derived biosynthesis of acetyl-CoA (Figure 5.2A). Interestingly, while there was a decrease in the % labeled acetyl-CoA, the overall concentration of acetyl-CoA did not change significantly (appendix, Table A.4) Rotenone also significantly decreased the M2, M3 and M4 isotopomers of succinyl-CoA, indicating decreased conversion of glucose to succinyl-CoA. Therefore, the decrease in absolute succinyl-CoA concentration was due, in part, to decreased glucose-derived flux through the Krebs cycle (Figure 5.2A). Lastly, there was no isotopic labeling of CoASH, confirming that the labeling occurred only in the acyl moiety. The decreased flux of glucose-derived carbons was also observed in the Krebs cycle organic acids (Figure 5.2B), confirming the decrease in glucose-derived carbons in the Krebs cycle. There was also a total relative decrease of labeled carbons through the cycle both groups, consistent with the relative number of steps from acetyl-CoA entry into the cycle. Also, rotenone induced increased incorporation of [1,2-$^{13}C_2$]-acetate into acetyl-CoA (Figure 5.3A) and decreased incorporation of labeled [$^{13}C_3{}^{15}N_1$]-pantothenate into CoASH and all of the measured acyl-CoA species at both 3 h and 15 h (Figure 5.3B).

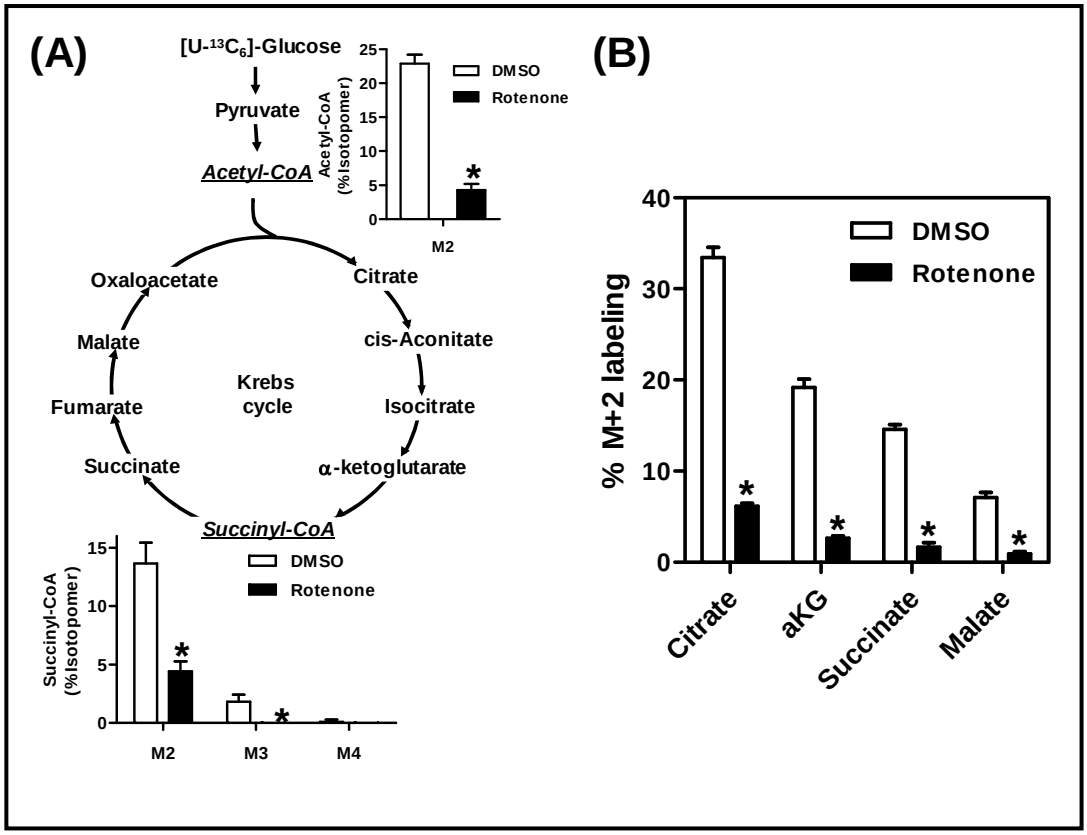

Figure 5.2 Rotenone mediated effects on isotopic labeling of [U-$^{13}C_6$]-glucose. (A) Effect of rotenone on the biosynthesis of glucose-derived acetyl-CoA and succinyl-CoA. SH-SY5Y cells were incubated in media containing [U-$^{13}C_6$]-glucose and 100 nM rotenone or DMSO (vehicle) for 6 h. Isotopomer distributions are shown in relation to the Krebs cycle. Error bars are SEMs for n=5, * $p < 0.005$ compared with DMSO vehicle. (B) Effect of rotenone on the biosynthesis of glucose-derived citrate, aKG, succinate, and malate. SH-SY5Y cells were incubated in media containing [U-$^{13}C_6$]-glucose and 100 nM rotenone or DMSO (vehicle) for 6 h. Error bars are SEMs for n=4, * $p < 0.005$ compared with DMSO.

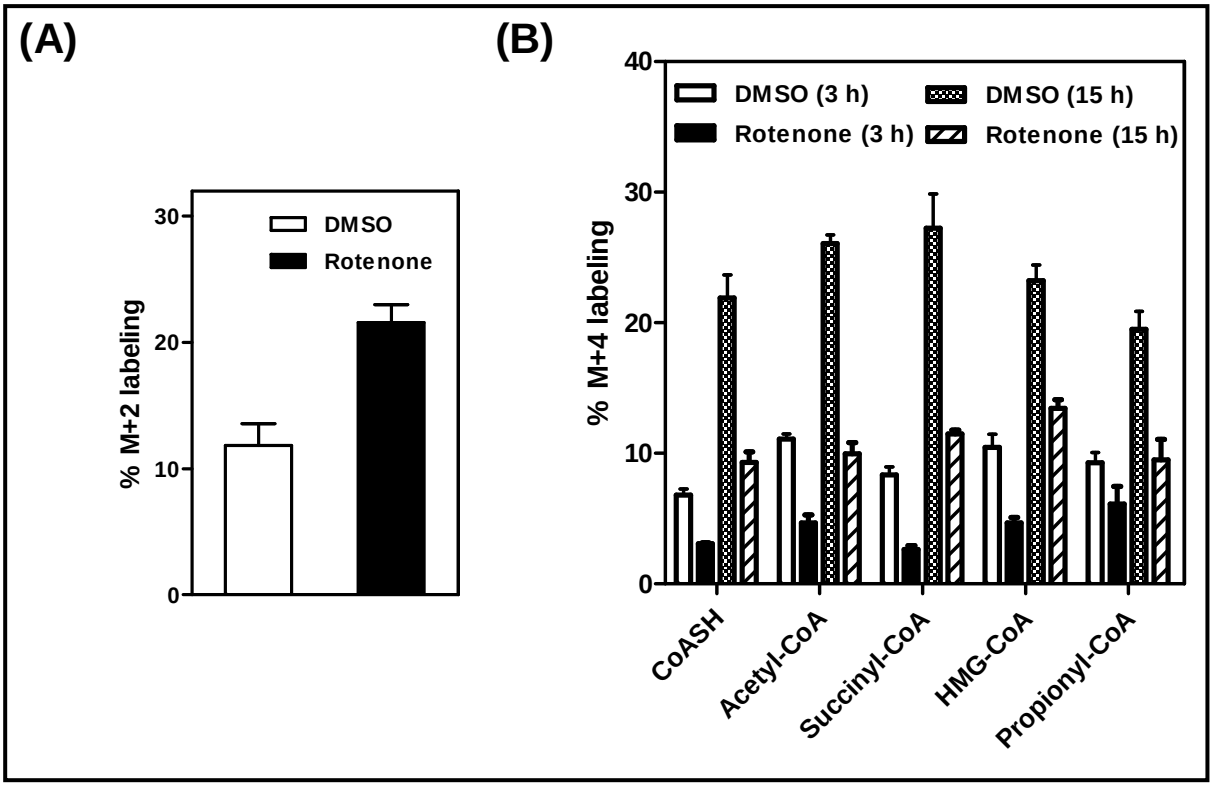

Figure 5.3 Rotenone mediated effects on isotopic labeling of [U-$^{13}C_2$]-acetate and [U-$^{13}C_3$ $^{15}N_1$]-pantothenate. (A) SH-SY5Y cells were incubated in media containing 10 mM [1,2-$^{13}C_2$]-acetate and 100 nM rotenone or DMSO (vehicle) for 6 h. Error bars are SEMs for n=4, * = $p < 0.005$ compared with DMSO vehicle. (B) SH-SY5Y cells were incubated in media containing 3 mg/L [U-$^{13}C_3$ $^{15}N_1$]-pantothenate and 100 nM rotenone or DMSO (vehicle) for 3 h or 15 h. Error bars are SEMs for n=3.

5.5 Discussion

In this chapter, we have shown for the first time that rotenone not only inhibits glucose-derived formation of both acetyl-CoA and succinyl-CoA, it also induces an increase in the formation of BHB-CoA in a number of human cell lines. The decrease in acetyl-CoA labeling would in fact be predicted from the decreased pyruvate dehydrogenase activity that occurs when there is a high NADH/NAD^+ ratio,[164] and is consistent with a recent finding that rotenone causes increased shunting of glycolytic intermediates into lactate.[160] The absence of a decrease in the absolute concentration of acetyl-CoA indicates either an alternate source of acetyl-CoA or an inhibition of acetyl-CoA utilization. The increased labeled acetate incorporation into acetyl-CoA (Figure 5.3A) may also be an attempt by the rotenone treated cells to compensate for the decreased glucose derived acetyl-CoA.

The decrease in succinyl-CoA levels is consistent with a recent study in *Arabidopsis* cells, in which a rapid 50% decrease in aKG, the precursor of succinyl-CoA, was observed after 1 h of rotenone treatment.[161] This may be, in part, due an inhibition of aconitase, which is known to be inhibited by rotenone and ROS formation.[165, 166] The dramatic decrease in intracellular succinyl-CoA (Figure 5.1A) would cause decreased protein succinylation, a post-translational modification with important regulatory implications. For example, 3-hydroxy-3-methyl-glutaryl (HMG)-CoA synthase, the rate-determining enzyme in ketogenesis is inactivated by succinylation, which is, in turn, regulated by succinyl-CoA concentrations.[38] In addition, a recent study has shown that succinylation of lysine residues occurs as a post-translational regulatory modification to certain enzymes such as isocitrate dehydrogenase (Figure 5.2).[167] In addition to

decreased succinyl-CoA biosynthesis, increased conversion of succinyl-CoA to succinate may also contribute to decreased succinyl-CoA levels. The increased succinate could then be used as a complex II substrate. Since complex I and II both ultimately reduce ubiquinone, the increased conversion of succinyl-CoA to succinate may allow for increased complex II activity to compensate for complex I inhibition.

The rotenone-mediated increase in BHB-CoA (Figure 5.1B), an intermediate in fatty acid β-oxidation,[168] together with the minimal incorporation of [U-$^{13}C_6$]-glucose into BHB-CoA (< 5 %) is indicative of a compensatory metabolic rearrangement to maintain cellular bioenergetics, allowing the cell to bypass the inhibition of glucose-derived acetyl-CoA. This would arise through the intermediate 3-hydroxyacyl-CoA dehydrogenase-mediated formation of acetoacetyl-CoA[169] followed by thiolase (ACAT1)-mediated formation of acetyl-CoA.[170]

Finally, the decreased incorporation of pantothenate into CoA (Figure 5.3B) was also quite striking and somewhat surprising, as we expected an increase in CoA utilization and turnover during a state of metabolic stress. This does raise the intriguing possibility that rotenone has effects on the CoA biosynthesis pathway, though this has not been previously documented. Whether any or all of these changes are a pathological result of rotenone toxicity, physiological adaptation to diminished OXPHOS function, or a complex I-independent effect altogether remains to be determined. However, the prolonged reliance on compensatory pathways could play an important role in rotenone toxicity *in vivo* due to differences in the abilities of different tissues or cell types to up-regulate or maintain these metabolic rearrangements.

5.6 Conclusions

In summary, we have shown that SILEC-based stable isotope dilution LC-MS methodology coupled with isotopomer analysis of CoA thioesters can be used *in vitro* to gain insight into the mechanisms involved in the toxicity of environmental agents such as rotenone. Although rotenone does not completely mimic all aspects of PD,[149] it provides an example of an environmental chemical, which causes a systemic defect in mitochondrial function that leads to selective nigrostriatal neurodegeneration.[171] Stable isotope LC-MS approaches along with mass isotopomer experiments make it possible to better characterize the metabolic pathways perturbed by rotenone treatment. Understanding the changes that rotenone induces in disparate cell types will increase our understanding of why rotenone affects certain cell types such as dopaminergic neurons, while sparing other neurons and tissues. These biomarkers might relate specifically to PD but could also be potentially useful for monitoring other neurodegenerative diseases involving mitochondrial dysfunction. By understanding the pathways involved, we will be able to use evidence based prediction of particular pathways to further identify potential pathways for biomarker discovery in other metabolic and neurodegenerative diseases.[23, 131, 134, 172, 173]

Chapter 6: CoA biomarkers in platelets: application in Friedreich's Ataxia

6.1 Abstract

Friedreich's ataxia (FA), the most prevalent inherited form of ataxia, is an autosomal recessive mitochondrial disease, resulting from a tri-nucleotide expansion (GAA) in the gene for frataxin, a protein involved in iron sulfur cluster (ISC) formation. The lack of good FA biomarkers hampers the ability to develop and analyze effective treatments for this disease. There is growing evidence that metabolic dysfunction plays a role in the FA pathogenesis. In this study, changes in acyl-CoA species were characterized using SILEC methodology in a frataxin siRNA knockdown model in HEK293 cells. In addition, the SILEC method was adapted to measure CoA changes in freshly isolated human platelets. Both frataxin knockdown cells and platelets from FA patients were found to have decreased acetyl-CoA: succinyl-CoA ratio compared to controls. This represents the first time platelets have been used as a platform to measure changes in acyl-CoA profiles in FA. In addition to the findings in this study, using LC-MS methodology to measure metabolic changes in platelets may lead to novel biomarkers of FA as well as other metabolic and neurodegenerative diseases.

6.2 Introduction

Friedreich's ataxia (FA) is an autosomal recessive disease of mitochondrial dysfunction and the most common inherited form of ataxia.[174] FA results from a trinucleotide (GAA) expansion repeat in the first intron of the frataxin gene (*FXN),* reducing levels of frataxin protein. While the exact role of frataxin is still unknown, it is believed to be involved in ISC formation.[175-177] This expansion leads to decreased efficiency of ISC-containing enzymes such as those found in complex I-III of the electron transport chain, as well as aconitase, a critical enzyme which converts citrate to isocitrate in the Krebs cycle.[178] Diminished frataxin expression as well as decreased complex I activity occurs in a number of different tissues of FA patients.[179, 180] This leads to loss of dorsal root ganglia neurons accompanied by loss of peripheral nerve sensory fibers.[180]

FA has several characteristic clinical features. The loss of dorsal root ganglia, typically in early childhood or adolescence, leads to degeneration of the dorsal columns, which results in the characteristic ataxia and eventually loss of ambulation. In addition, a large number of patients develop insulin intolerance and diabetes mellitus.[174, 180, 181] In the later stages of FA, hypertrophic cardiomyopathy is often the cause of death.[182] Current therapeutic strategies include the use of coenzyme Q, PPARγ agonists, iron chelators, N-acetylcysteine, idebenone, vitamin E, and ubiquinone, though all have limited efficacy.[174, 175, 179, 183-187] The lack of good biomarkers limits early detection and hampers attempts to rationally design new therapeutic interventions.[188] As a result, most cases are detected clinically, when significant neuronal damage has already occurred. The pervasive multi-organ involvement of this mitochondrial disease, with selective tissue involvement of a severe clinical nature, is similar to that seen with rotenone

treatment in rats,[156] and like with rotenone, may involve an underlying metabolic cause. In fact, a proteomic study in rats with frataxin knockdown, showed large changes in proteins involved in energy homeostasis and alternative energy pathways.[189] Consistent with proteomic changes seen in the animal model, we hypothesized that there could likely be significant metabolic changes that might be observed in both an *in vitro* frataxin knockdown model as well as in FA patients.

LC-MS methodology represents a highly sensitive and specific platform for biomarker development.[91] As demonstrated throughout this thesis, CoA thioesters reflect both short term and long term metabolic changes in physiological, toxicological and pathological settings. Unlike organic acids and acyl-carnitines, which can be found in higher abundance in plasma and urine, CoA species are largely intracellular and as such, require extracts from tissues or cells to be used as biomarkers of disease. Since the primary pathology of FA is in cardiomyocytes and dorsal column neurons,[180] which are located in clinically inaccessible tissues, a surrogate tissue is required for CoA measurements. Surrogate tissues are tissues from an individual that may reflect the disease state, though may not exhibit a pathological phenotype. These can include buccal cells, dermal fibroblasts or blood cells such as red blood cells (RBCs), lymphocytes or platelets. As far as blood cells, RBCs have no mitochondria, and as such do not contain a significant amount of CoA thioesters and therefore would not reflect a mitochondrial pathology. Lymphocytes and platelets represent extractable tissues containing mitochondria that can be used not only to measure baseline metabolic differences for screening, but can also be isolated and subjected to both *ex vivo* challenges to toxins or

isotopic tracer MS analysis to further reveal underlying metabolic and mitochondrial disease.

Since frataxin levels are lower in blood cells including platelets,[190] we hypothesized that platelets might exhibit baseline differences in their CoA profile. In particular, since aconitase activity is decreased in FA,[191, 192] we hypothesized that platelets of FA patients would exhibit altered levels in the intracellular levels of succinyl-CoA compared to healthy individuals. In this chapter, we studied the effects of an *in vitro* frataxin knockdown using siRNA on the intracellular levels of various short chain acyl-CoA species. In addition, we looked at baseline differences among FA patients and age-matched controls in freshly isolated platelets.

6.3 Materials and Methods

6.3.1 Materials

Reagents for LC-MS measurements of short chain acyl-CoA species are described in section 3.3. 8.5 mL acid citrate dextrose Vacutainer tubes (Whole Blood Tube w/ Anticoagulant, ACD Sol A) were purchased from BD Biosciences (REF 364606). Frataxin (144470) and negative control siRNAs were purchased from Ambion.

6.3.2 Cell culture and knockdown experiments

Frataxin knockdown experiments were performed by Eric Deutsch in the lab of David Lynch. HEK293 cells were maintained in minimum essential medium (Invitrogen) supplemented with 7.5%/2.5% FBS/HS (Foundation/GIBCO), 1% pen strep (GIBCO), and 200 nM L-glutamine (GIBCO) at 37C, 5% CO_2. Within 24 h, when cells had

reached 40-50% confluency, cells were transfected for 48 h with frataxin or scramble siRNA. Knockdown success was verified by western blot using an antibody directed toward mature frataxin protein (Mitosciences), and was expressed as a percentage of frataxin in parallel control samples. CoA analysis was performed as previously described.

6.3.3 Short chain acyl- CoA measurements in platelets

FA patients were recruited by the Friedreich Ataxia Research Alliance (FARA) and were seen at the Children's Hospital of Philadelphia as part of an ongoing, multicenter natural history study. In addition, age-matched volunteers were used as controls. All subjects provided written informed consent before participating in study procedures. Blood was collected in 8.5 mL glass acid citrate dextrose Vacutainer tubes and transferred into 15 mL centrifuge tubes. Cells were spun at 129*g* for 15 min with no brakes. The upper platelet rich plasma (PRP) layer was transferred to a fresh tube and spun at 341*g* for 15 min to pellet platelets. Platelets were resuspended and sonicated in 1 mL of 10% TCA and frozen down and stored at -80°C. Prior to SPE purification and LC-MS analysis, samples were thawed and spiked with 0.2 mL acid extracted SILEC standards. SPE extraction of short chain acyl-CoA species as well as LC-MS parameters used in analysis are described in Chapter 3.6. The analysis was performed in two different sets. The first set included 4 FA patients, and 4 healthy controls, while the second study included 8 FA patients and 4 healthy controls. The data from the two studies were combined for meta-analysis. A schematic of the protocol used in platelets is diagrammed in figure 6.1.

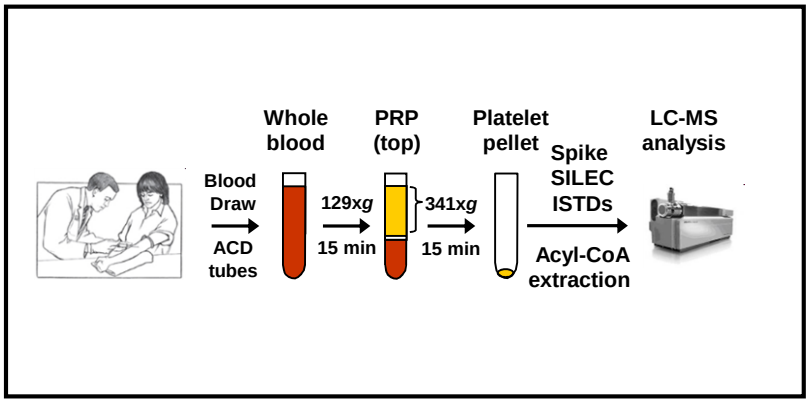

Figure 6.1 Schematic for platelet CoA analysis. PRP: platelet-rich plasma. ISTD: internal standard.

6.4 Results

6.4.1 siRNA knockdown of frataxin[ϕ]

HEK293 cells were transfected with either frataxin siRNA or scramble siRNA (negative control). Western blot analysis of frataxin protein was used to assess knockdown efficiency. Frataxin was knocked down greater than 80% in FA patients as compared to controls after 48 hours (Figure 6.2).

6.4.2 siRNA knckdown results in changes to short chain acyl-CoA profile

Transfected HEK293 cells (48 h) were processed for short chain acyl-CoA as previously described except in 6-well plates instead of 10 cm dishes. As such, only the more abundant CoA species (acetyl-CoA, succinyl-CoA, CoASH) were readily detected and analyzed. There was a significant change in the absolute quantity of acetyl-CoA and succinyl-CoA in the frataxin knockdown cells as compared to the scramble control cells. In particular, when the ratio of acetyl-CoA to succinyl-CoA was assessed, there was a significant decrease in the ratio of acetyl-CoA: succinyl-CoA, contrasting what we observed with rotenone treatment in cell lines.

6.4.3 CoA measurements in freshly isolated human platelets

The SILEC method developed throughout this report was adapted for CoA measurements in platelets. In most *ex vivo* platelet studies, platelets are generally purified from whole blood followed by washing and resuspension in a standardized buffer such as Tyrode's solution. However, we were interested in baseline levels of these

[ϕ] This work was performed by Eric Deutsch in the lab of David Lynch.

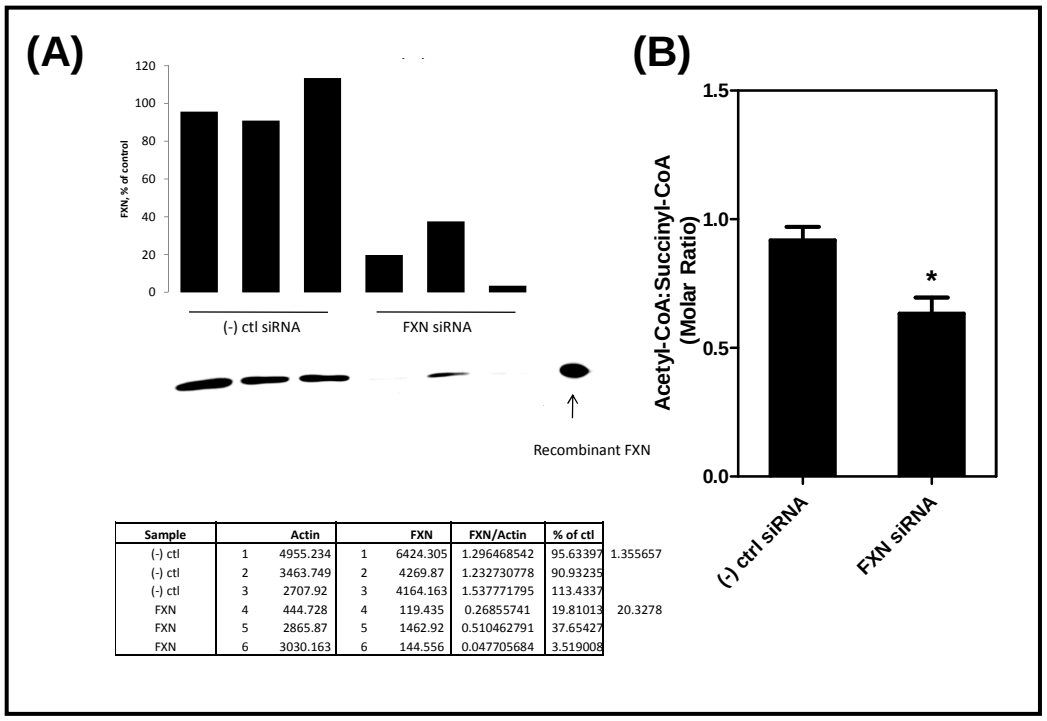

Sample		Actin		FXN	FXN/Actin	% of ctl	
(-) ctl	1	4955.234	1	6424.305	1.296468542	95.63397	1.355657
(-) ctl	2	3463.749	2	4269.87	1.232730778	90.93235	
(-) ctl	3	2707.92	3	4164.163	1.537771795	113.4337	
FXN	4	444.728	4	119.435	0.26855741	19.81013	20.3278
FXN	5	2865.87	5	1462.92	0.510462791	37.65427	
FXN	6	3030.163	6	144.556	0.047705684	3.519008	

Figure 6.2 Frataxin siRNA knockdown. HEK293 cells were transfected with either scrambled siRNA (negative control), or frataxin siRNA for 48 hours. (A) Western blot analysis of frataxin protein siRNA treated cells. (B) Intracellular levels of acetyl-CoA:succinyl-CoA in control and fxn knockdown cells. Each group was performed in triplicate. Error bars are SEMs * $p < 0.05$.

CoA species since we suspected that persistent metabolic stress among FA patients may be reflected in surrogate tissues such as platelets, which are known to have decreased complex I activity. Due to the dynamic nature of metabolites, platelet processing times were reduced as much as possible. To accomplish this, we removed the wash and resuspension steps and simply purified platelets with a two-step centrifugation process, followed by sonication in 10% TCA in the presence of SILEC internal standards. This reduced the amount of time and exogenous stimuli that would affect platelets and deviate from baseline differences. In lieu of normalizing CoA levels to blood volume or platelet counts, which can introduce additional error or increase processing time, we decided to determine absolute counts of the various CoA species and express them as molar ratios to one another, i.e. acetyl-CoA: succinyl-CoA ratio. The advantage of this approach is that it controls for differences in both volume of blood draw and platelet concentration which we found can vary as much as three-fold from one subject to another. In addition to platelets, Ficoll-extracted lymphocytes and brushed buccal cells from the cheek were analyzed. Both lymphocytes and buccal cells were found to have inadequate CoA material, (data not shown), likely due to lower mitochondrial content. Platelets were divided into equal fractions and processed. They were found to have adequate precision for all measured species with RSD < 15% when normalized with SILEC internal standards.

6.4.3 Friedreich's ataxia patients have decreased acetyl-CoA:succinyl-CoA

The method developed for platelets was applied to FA patients and age-matched controls. FA patients were found to have increased levels of succinyl-CoA in their

platelets. In fact, when these were normalized to acetyl-CoA levels, there was a significant decrease in the ratio of acetyl-CoA:succinyl-CoA (Figure 6.3). Other short chain acyl-CoA species were measured, though none appeared to have a significant correlation with FA. This decrease in acetyl-CoA:succinyl-CoA ratio is consistent with changes seen in frataxin knockdown model *in vitro*, though opposite to the changes seen with rotenone treatment, in which succinyl-CoA levels decreased relative to DMSO controls.

6.5 Discussion

In this study, we have demonstrated the application of platelets as a platform to measure baseline acyl-CoA concentrations using stable isotope dilution mass spectrometry. This method was applied to FA, a mitochondrial disease involving metabolic dysfunction. FA patients exhibited significant baseline differences in major short chain acyl-CoA thioester species, consistent with changes exhibited in frataxin knockdown *in vitro*, namely a decrease in the molar ratio of intracellular acetyl-CoA to succinyl-CoA, driven largely by increases in succinyl-CoA. Although we also anticipated that platelets from FA patients would exhibit similar changes to what we had seen with rotenone treatment in cells, the effect we found was actually the opposite of what we expected. That is, rather than a decrease in succinyl-CoA, FA subjects exhibited an increase in succinyl-CoA. Though the underlying cause is not clear, it may signify compensatory changes made by the cells to overcome a metabolic deficiency.[189] This could arise from increased anaplerotic flux from odd chained fatty acids or glutamate.[193] On the other hand, this could be a result of Krebs cycle stalling, resulting in an inhibition

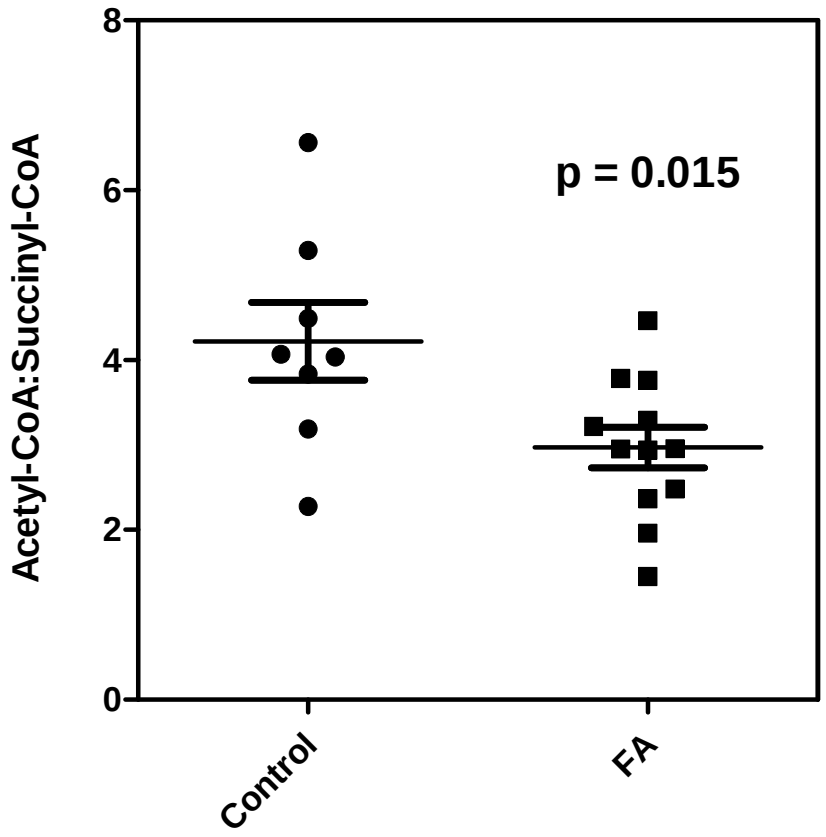

Figure 6.3 Acetyl-CoA: succinyl-CoA ratio in platelets in FA subjects vs. controls. Short chain acyl-CoA species form 12 FA subjects and 8 healthy controls were analyzed using the previously described methods.

and decreased consumption of succinyl-CoA. If this is the case, appropriate *ex vivo* challenges such as galactose treatment rather than glucose may lead to faster or slower metabolic decompensation to reveal an underlying mitochondrial dysfunctional state.[194] Interestingly, although it has been shown that platelets of FA patients have decreased complex I expression and activity, FA patients do not exhibit significant disease at baseline in their blood cells.[190] Moreover, FA patients not generally have any clinically significant deficiencies in hemostasis or platelet function, and yet still displayed differences in platelet metabolites. This further strengthens the hypothesis that the global metabolic changes in FA are occurring in all tissues, however, certain tissues are more or less susceptible to the pathophysiological complications of these changes.[189]

There are several improvements are being considered for this approach. Although significant differences were observed, subjects also showed considerable variability, which may have arisen in various ways. One source is diurnal metabolic variability. Also, levels of various metabolites may widely vary in the blood or urine from the same patient after meals or after a long fast. One potential method of controlling for this variability is by drawing the blood and taking urine samples in the morning, simulating a fasted state, or after a standardized glucose challenge, representing a fed state. Otherwise, to bring out the phenotype, an appropriate challenge may be necessary, such as placing platelets in Tyrode's containing only galactose to make them more reliant on OXPHOS-derived ATP.[194] Then, mitochondrial or OXPHOS dysfunction may be revealed through changes in metabolic or viability parameters. In summary, we have shown that *in vitro* models of mitochondrial dysfunction result in metabolic changes that can be detected in surrogate tissues of diseased individuals with the same genetic defect. Further studies

with *ex vivo* metabolic challenges may further uncover FA phenotypes and lead to functional diagnostic tests for FA, which currently has no clinically practical validated biomarkers.[195] Furthermore, a well-characterized mitochondrial genetic disease such as FA represents an extremely valuable model to characterize the metabolic pathogenesis of mitochondrial dysfunction and the identification of characteristic biomarkers induced by this dysfunction.

Chapter 7: Development of an *ex vivo* metabolic challenge model in platelets to characterize mitochondrial and metabolic physiology

7.1 Abstract

In this chapter, an *ex vivo* metabolic challenge model is developed in freshly isolated human platelets. To achieve this, platelets were isolated and purified from whole blood and treated with propionate, rotenone or stable isotope metabolic tracers ([U-$^{13}C_6$]-glucose, [6-$^{13}C_1$]-glucose [1-$^{13}C_1$]-propionate, [1,2-^{13}C2]-acetate, and [$^{13}C_3{}^{15}$N1]-pantothenate). Subsequently, short chain acyl-CoA species were extracted and analyzed using SILEC standards to determine changes in absolute CoA concentrations, or isotopomer distribution analysis was performed to determine relative flux with metabolic tracers. Platelets treated with 10 mM propionate were found to have a greater than 100-fold increase in propionyl-CoA after 1 h. Also, 1 µM rotenone treatment in platelets resulted in a greater than 90% decrease in succinyl-CoA and a 10 fold increase in BHB-CoA concentration. Both propionate and rotenone-mediated changes were consistent with previous *in vitro* experiments performed on human cell lines. In addition, isotopic tracers were readily incorporated and detected in endogenous platelet CoA thioesters after only one hour of incubation. Remarkably, [1,2-$^{13}C_2$]-acetate labeled more than 70% of acetyl-CoA, HMG-CoA, and BHB-CoA, as well as 30% of succinyl-CoA, when spiked directly into whole blood or after platelet isolation. Therefore, platelets were found to be a viable, metabolically active, *ex vivo* challenge model that can be adapted for diagnostic toxicological and metabolic functional tests. This methodology can be further used to uncover phenotypic differences in mitochondrial and metabolic diseases.

7.2 Introduction

There has been tremendous difficulty in developing and validating biomarkers of disease.[196] Biomarker candidates often show promise pre-clinically, but often have poor performance in predicting disease during later stages of clinical development or when used for larger studies.[197] The two most critical criteria in the success of biomarkers are sensitivity and specificity, with both ideally being greater than 90%.[198] Although many candidate biomarkers have adequate sensitivity, lack of specificity for many of these biomarkers leads to false positives, which decreases the clinical utility of these tests. For metabolomic biomarkers, in particular, the dynamic nature of metabolite levels adds another level of complexity.[199] Unlike proteins, which are often stable for hours or days, endogenous metabolites can turn over in seconds and can also exhibit diurnal variability.[200] In addition, if not properly handled, concentrations of these metabolites can be drastically affected by improper or inconsistent sample collection and processing, due to their dynamic nature. Like urinary and serum metabolites, tissue and cell metabolites such as CoA thioesters can also be affected by these same factors. Moreover, since the measurements are done from cells, which are active biological systems themselves, quenching of cellular and enzymatic activity is also critical during the assay. It is possible that the variability observed in the FA study (chapter 6) may be partly attributed to some of the biological these effects (diurnal variability, sample handling, diet, etc.).

There are various strategies used to overcome or normalize for this variability. One method is using a functional test rather than a traditional biomarker.[201] Traditional biomarkers may include a metabolite or protein that is persistently elevated or reduced in a particular disease state. In a functional test, however, a specific challenge is given,

either *in vivo* or *ex vivo*, to uncover phenotypic differences between healthy and diseased individuals that may not be readily discernible when using baseline measurements. One example of a functional test is a fasting blood glucose test in which glucose measurements are given after overnight fasting, thereby reducing the impact of recent food intake. The level of circulating glucose represents a subject's ability to appropriately regulate insulin and store glucose, and is elevated in diabetes mellitus (Types I and II) as well as certain cancers. A oral glucose tolerance test can also be used, in which the subject is given an oral glucose load followed by sequential blood glucose measurements.[202] Both fasting and oral glucose tests highlight the use of an exogenous challenge to reveal an underlying pathological phenotype, in this case, the inability to properly regulate glucose levels. Most importantly, these types of tests establish an experimental baseline so that all subjects have approximately similar initial conditions. Although HbA1C, a sugar-modified circulating hemoglobin, is a more preferable and predictive biomarker of diabetes progression largely due to its longer half-life in the blood, this type of biomarker is more common in proteomics than in metabolomics due to the longer half-life and stability of proteins in biological systems. [203]

Although both glucose tests are *in vivo* challenges, this approach can be performed *ex vivo* as well. In an *ex vivo* test, a small samples of cells or tissues are extracted and isolated from the subject. These are then challenged with a specified stimulus in hopes of uncovering a particular phenotype.[204] The disadvantage of this method is that a subset of cells is being studies in isolation rather than looking at the system wide physiological effects as is done in a glucose load test. The advantage, however, is that a much larger variety of tests can be used, including pharmacological or

toxicological tests that would be unsafe or unethical to perform *in vivo*, such as rotenone treatment. In addition, since a smaller amount of cells are being tested, a much smaller amount of reagent or testing compound is required for the test as this does not have to become systemically distributed. This is particularly useful for isotopic tracer analysis, in which the reagents may be prohibitively expensive and impractical to perform *in vivo* dosing tests.

We hypothesized that this functional test biomarker approach could be used in platelets *ex vivo* to help diagnose mitochondrial or metabolic diseases such as FA. To achieve this, three methodological approaches are pursued in this chapter. First, freshly isolated platelets were washed and treated with propionate to verify whether platelets could be used as a metabolically viable *ex vivo* surrogate tissue. Second, isolated platelets were subjected to dose-dependent rotenone treatment to determine if the metabolic activity seen in the cells lines (Chapter 5) can be recapitulated in an *ex vivo* toxicological model. Finally, isolated platelets were treated with various isotopic tracer molecules to determine whether metabolic flux could be assessed in this model. A schematic of the experimental protocol is provided in figure 7.1.

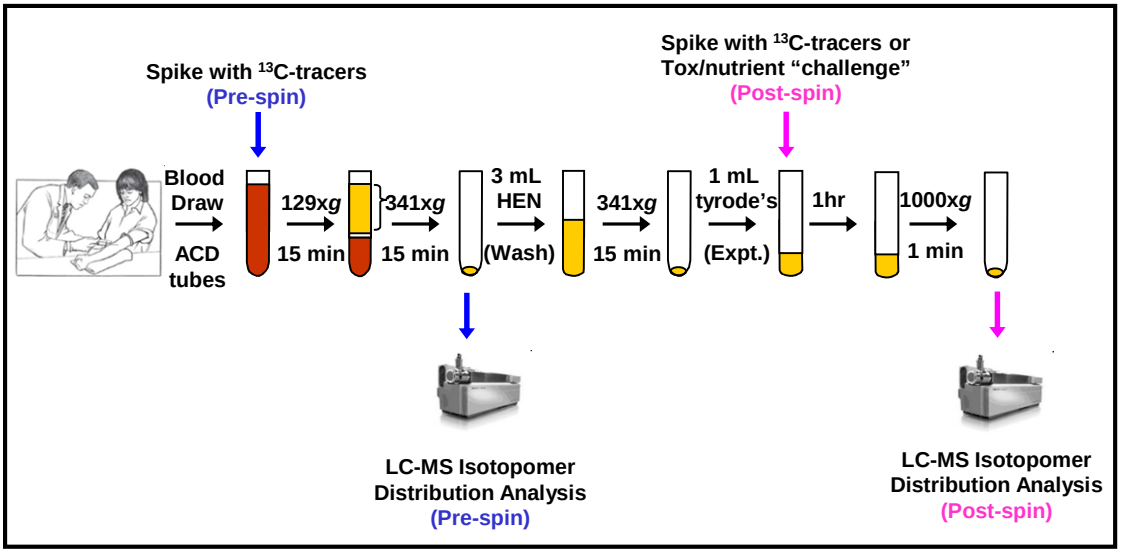

Figure 7.1 Scheme for isotopic tracer analysis and *ex vivo* platelet "challenges."

7.3 Methods

7.3.1 Materials

[6-$^{13}C_1$]-glucose was purchased from Cambridge Isotopes (Andover, MA). All other materials used in this chapter were obtained as previously reported.

7.3.2 Isolation and preparation of human platelets

Platelet extraction was performed similarly to what was presented in Chapter 6, with some modifications. Briefly, whole blood was drawn into 8.5 mL ACD Vacutainer tubes (BD), transferred to 15 mL falcon tubes and spun for 15 min at 129*g* with no brakes. The upper PRP layer was transferred to a fresh tube and spun again at 341*g* for

20 min with no brakes. This pellet was resuspended in 5 mL HEN wash buffer (150 mM NaCl, 1 mM Na_2EDTA, 10 mM HEPES, pH 6.5) and was spun again at 329*g* with no brakes for 15 min. Finally the platelet pellet was resuspended in 1 mL Tyrode's solution (139 mM NaCl, 3 mM KCl, 17 mM $NaHCO_3$, 12 mM glucose, 3 mM $CaCl_2$, 1 mM $MgCl_2$) and transferred to 1.5 mL microcentrifuge tubes. A 10 μL aliquot was transferred for platelet counts which were performed on a BD platelet counter in the laboratory of Dr. Skip Brass.

7.3.2 *Ex vivo platelet "challenges"*

Ex vivo challenges were performed on resuspended platelets in Tyrode's solution. Figure 7.1 illustrates the overall experimental design. Briefly, three different challenge paradigms were performed. (1) Propionate challenge: a stock of 1mM propionate was prepared in water. 10 μL of this solution was added to platelets in Tyrode's solution for a final concentration of 10 mM. 10 μL of water was used as control. Incubations were performed in triplicate. (2) Rotenone challenge: a 10 mM stock of rotenone was freshly prepared in DMSO. Serial 10-fold dilutions were made in DMSO from 1 mM down to 100 pM along with a 5 μM and 500 nM dilution. Platelets from an 8.5 mL blood draw were resuspended in 10 mL of Tyrode's solution and divided into equal 1 mL fractions. 10 μL of each rotenone dilution and DMSO control were then added to each to generate a dosing curve from 1 pM to 100 μM in concentration. (3) Metabolic tracer analysis. Stocks of five different stable isotope labeled metabolic tracers were prepared in water in the following concentrations: [U-$^{13}C_6$]-glucose (100 mg/mL), [U-$^{13}C_1$]-glucose (100 mg/mL), [1-$^{13}C_1$]-propionate (1M), [1,2-$^{13}C_2$]-acetate (1M), and [$^{13}C_3{}^{15}N_1$]-pantothenate

(0.3 mg/mL). 10 μL of each stock was added to different tubes of resuspended platelets (1:100 dilution) for a final concentration of 1 mg/mL, 1 mg/mL, 10 mM, 10 mM, and 3 mg/L, respectively. For all three experiments, platelets were gently mixed by inversion and incubated in the presence of challenge at 37°C for 1 h. After incubation, platelets were spun down and short chain acyl-CoA species were extracted as described in chapter 6. In the case of isotopic tracer analysis, no SILEC standards were used. Finally, we also evaluated the labeling of [1,2-$^{13}C_2$]-acetate spiked directly into whole blood (pre-spin) or into Tyrode's solution after washing and purifying (post-spin). In both cases, we used 1 mM [1,2-$^{13}C_2$]-acetate. In the case of pre-spin labeling, we harvested the platelets in the same fashion as was performed in Chapter 6, (without the HEN wash or Tyrode's solution incubation). This decreased the total time from blood draw to acid extraction down to approximately 45 min.

7.4 Results

7.4.1 Propionate challenge

Freshly isolated human platelets were treated with 10 mM propionate in Tyrode's solution. After 30 minutes, propionyl-CoA levels increased 10-fold and concentrations of acetyl-CoA and succinyl-CoA were significantly decreased (Figure 7.2). These results are consistent with *in vitro* experiments in Hepa 1c1c7 cells (Figure 2.6), in which there was a similar increase in propionyl-CoA and decrease in acetyl-CoA and succinyl-CoA after propionate treatment observed. Therefore, this propionate challenge demonstrated that platelets could be used *ex vivo* as a metabolic functional test platform. This can be further extended to include other fatty acids or nutrients as well.

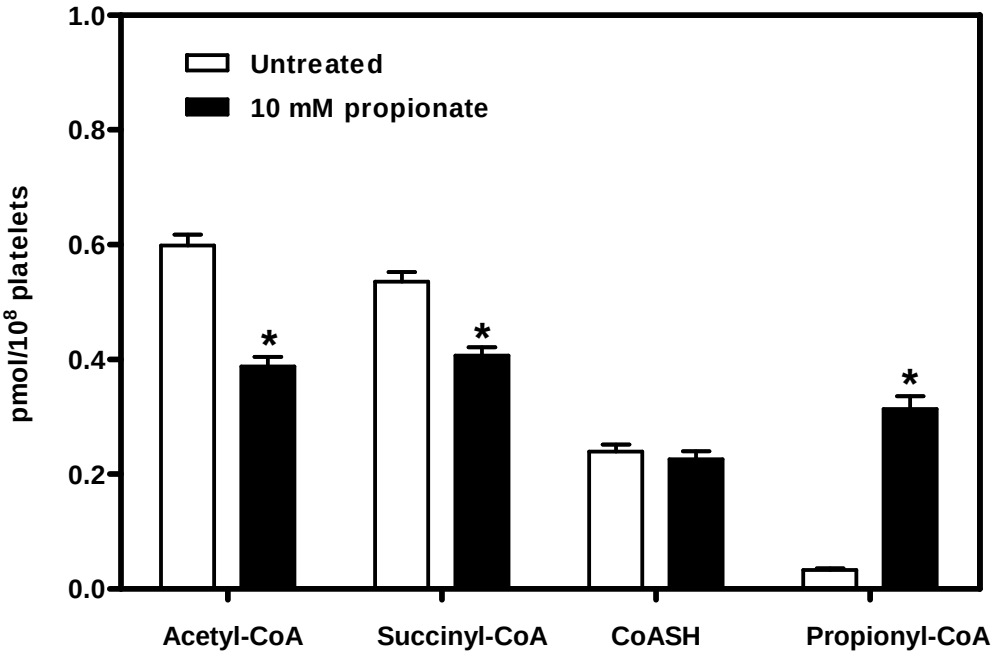

Figure 7.2 Effect of propionate treatment on selected CoA-thioesters in isolated human platelets. Platelets from one healthy subject were isolated, washed and resuspended in either Tyrode's solution or Tyrode's solution containing 10 mM propionate for 30 minutes. Following incubation, platelets were pelleted and processed for short chain acyl-CoA concentrations using SILEC methodology. A small aliquot was taken after resuspension to measure platelet concentration. Each group was performed in triplicate. * $p < 0.005$.

7.4.2 Rotenone challenge

Platelets isolated from an 8.5 mL blood draw were divided into 10 equal fractions and treated with increasing doses of rotenone for 1 h, followed by short chain acyl-CoA thioester analysis (Figure 7.3). Rotenone decreased intracellular succinyl-CoA levels and increased BHB-CoA levels in a dose-dependent manner, both with a IC50 of < 100 nM, consistent with the effect observed in various cell lines. Moreover, the ratio of BHB-CoA: succinyl-CoA was plotted as a function of rotenone dose, demonstrating a likely relationship between these processes (Figure 7.3). These data show that platelets can be used as *ex vivo* toxicological model, and can potentially be used to evaluate the effect of mitochondrial toxins in different disease states.

7.4.3 Isotopic tracer challenge

Platelets were isolated from three different subjects and treated with metabolic tracers for 1 h, followed by CoA extraction. Natural mass isotopomer distribution was calculated in unlabeled platelets and subtracted using a matrix analysis from the labeled cells to determine the relative isotopic labeling of each isotopomer (Figure 7.4). Both [^{13}C]-glucose reagents showed minor labeling. However, with [1,2-$^{13}C_2$]-acetate (10 mM), more than 60% of acetyl-CoA was labeled indicating that acetate may be a more sensitive metabolic tracer to evaluate metabolic flux in the Krebs cycle during shorter incubations. More strikingly, the BHB-CoA gets labeled in M2 and M4, (but not M1 and M3) and HMG-CoA get labeled as the M2, M4 and M6 (not M1, M3 or M5), consistent with incorporation of 2 carbon units from acetate. Also, succinyl-CoA is labeled in M2, M3 and M4 positions indicative of multiple turns of the Krebs cycle. [1-$^{13}C_1$]-propionate

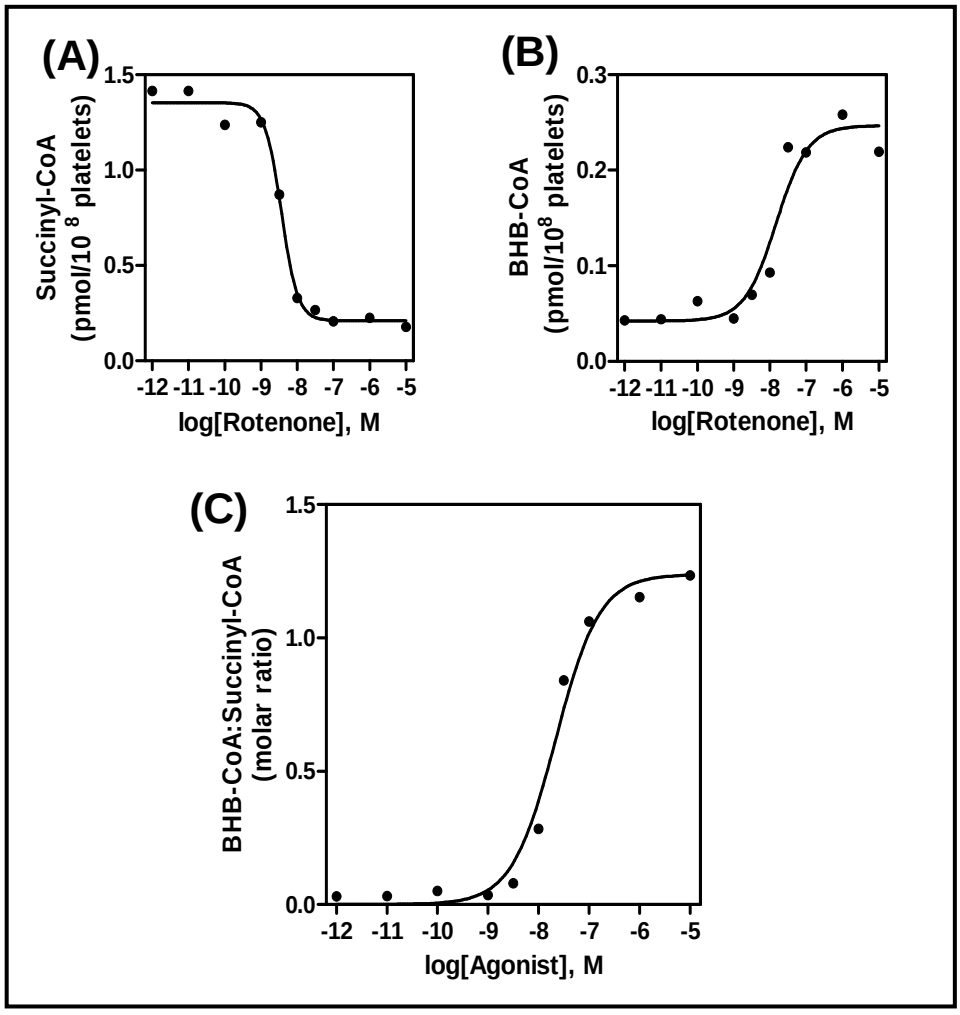

Figure 7.3 Dose-dependent effect of rotenone on succinyl-CoA and BHB-CoA in isolated human platelets. Platelets from one healthy subject were isolated, washed and resuspended in either Tyrode's solution containing an increasing concentration of rotenone for 30 min. Following incubation, platelets were pelleted and processed for short chain acyl-CoA concentrations. A small aliquot was taken after resuspension to measure platelet concentration. Figures (A) and (B) demonstrate intracellular platelet BHB-CoA and succinyl-CoA levels, respectively. Figure (C) demonstrates the ratio of BHB-CoA to succinyl-CoA.

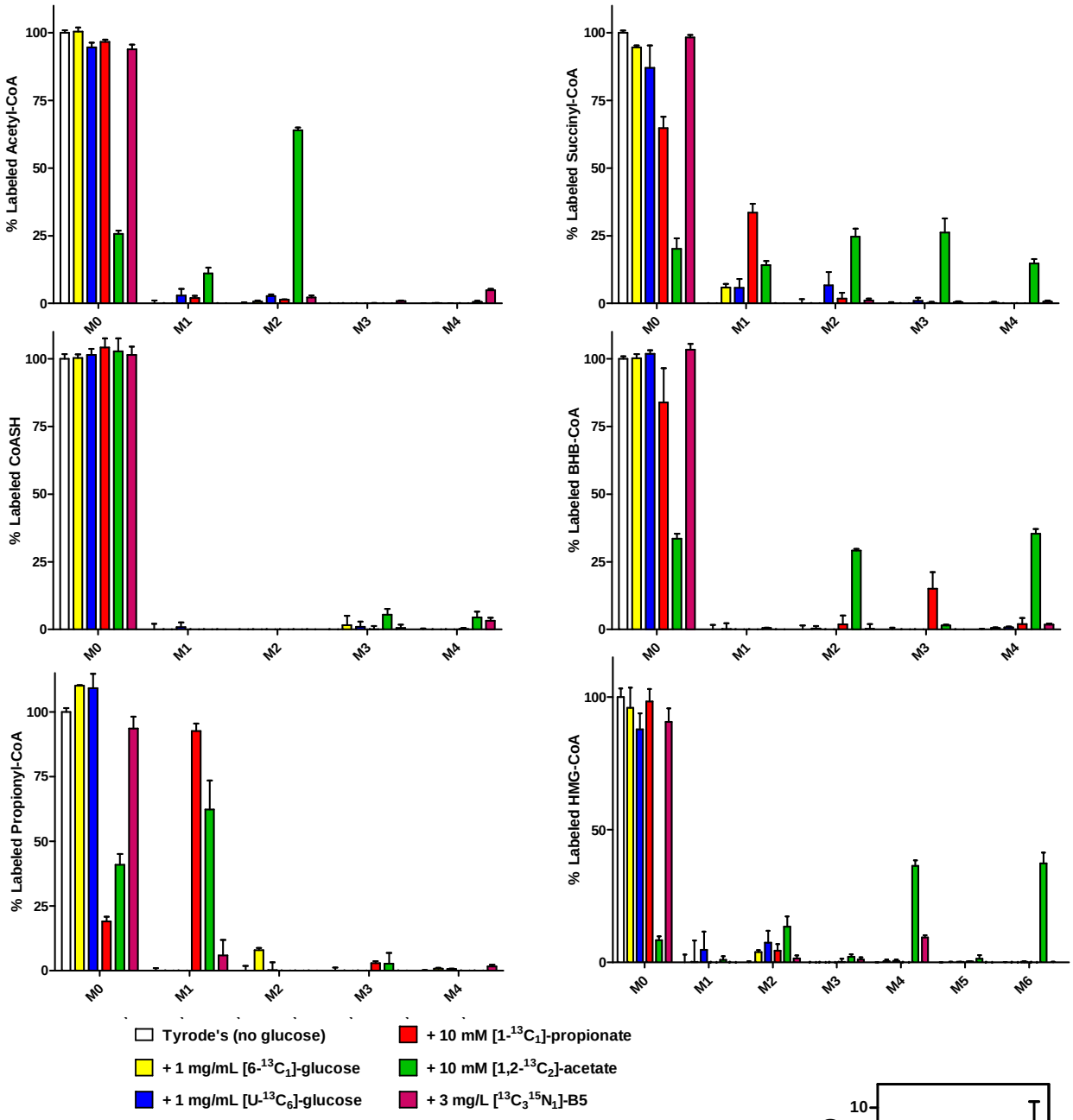

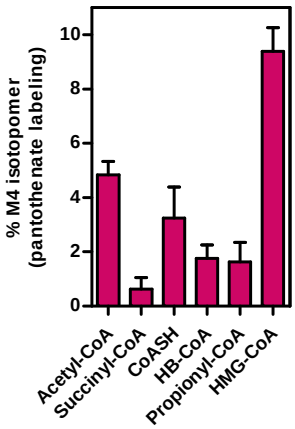

Figure 7.4 Isotopomer distribution of selected CoA thioesters in freshly isolated human platelets treated with various stable isotope metabolic tracers. Platelets from three control subjects were isolated, washed and resuspended in glucose-free Tyrode's solution containing either no glucose, [U-$^{13}C_6$]-glucose (1 mg/mL), [U-$^{13}C_1$]-glucose (1 mg/mL), [1-$^{13}C_1$]-propionate (10 mM), [1,2-$^{13}C_2$]-acetate (10 mM), and [$^{13}C_3$ $^{15}N_1$]-pantothenate (3 mg/L). Following incubation, isotopic distribution of selected CoA species was determined. Pantothenate labeling is also plotted alone (lower right).

was incorporated into [1-$^{13}C_1$]-propionyl-CoA (M1) and was also incorporated into succinyl-CoA (M1), with approximately 30% of the total succinyl-CoA being labeled through this anaplerotic pathway. This reagent could potentially be used as an anaplerotic biomarker by measuring the incorporation of this carbon into succinyl-CoA. Finally, [$^{13}C_3{}^{15}N_1$]-pantothenate (1mg/L) was readily incorporated into each of the measured CoA species, though at different percentages, suggesting different rates of turnover for each CoA thioester. The lack of significant M4 isotopomer from the control cells makes this an ideal labeling reagent for isotopic tracer analysis, as nearly all of the M4 isotopomer comes from the labeling agent. Furthermore, the greater increase in [$^{13}C_3{}^{15}N_1$]-pantothenate labeling (such as seen in HMG-CoA) is indicative of newly formed CoA, and suggests a higher turnover or increased synthesis of this product. Therefore, using [$^{13}C_3{}^{15}N_1$]-pantothenate tracing, in addition to evaluating tracers in the acyl moiety, we can also evaluate the labeling of the CoA backbone. The lack of labeling in CoASH with the remaining tracers confirmed that the isotopic labeling occurred in the acyl group.

Due to the rapid labeling observed with 10 mM [1,2-$^{13}C_2$]-acetate labeling, we evaluated the labeling at 1 mM, to decrease the tendency of the high acetate concentration sequestering the CoA pool. We also evaluated labeling at two different points in the protocol. Either (1) directly into whole blood (pre-spin) or (2) after washing and purification (post-spin), followed by CoA analysis. We found that both pre-spin and post-spin techniques successfully labeled the cells and was relatively consistent among the healthy subjects (Figure 7.5). Many of the findings observed at 10 mM were also seen at 1 mM. Further decreasing the concentration of [1,2-$^{13}C_2$]-acetate or performing a

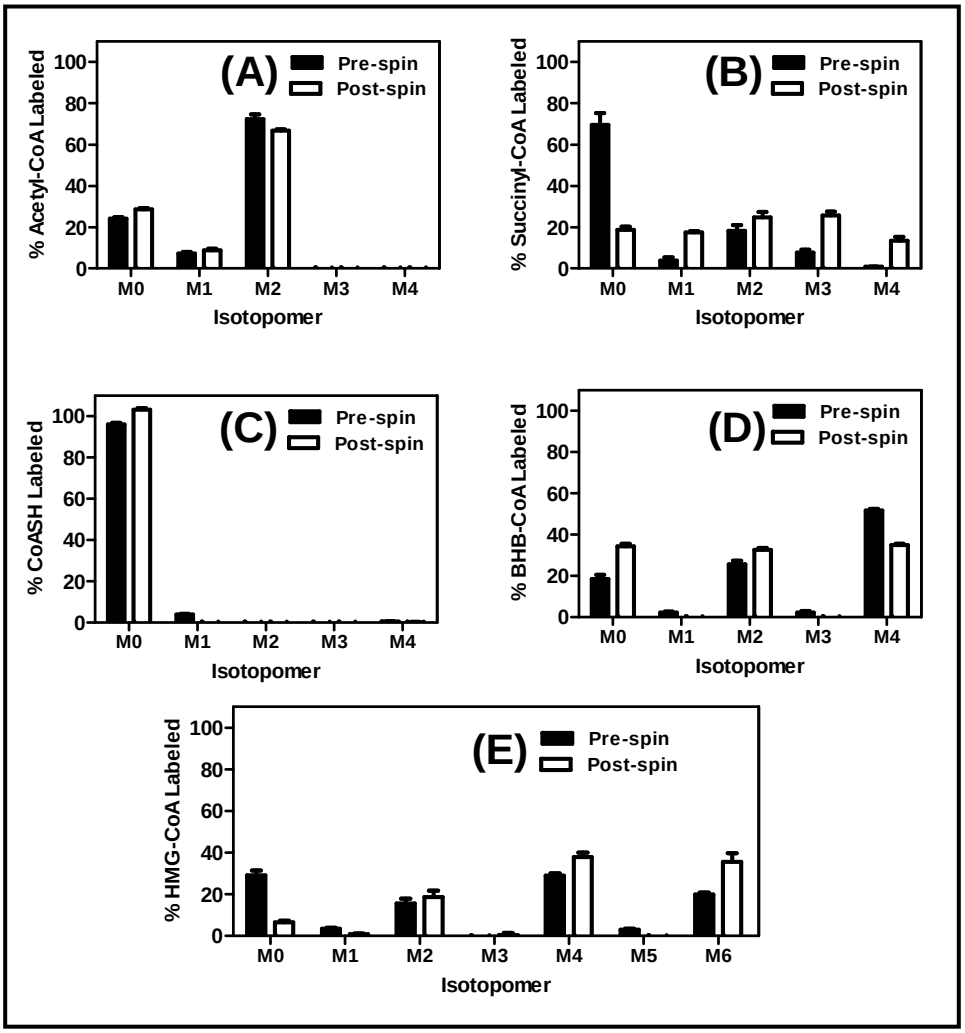

Figure 7.5 [1,2-$^{13}C_2$]-acetate labeling of selected CoA thioesters in freshly isolated human platelets. For pre-spin labeling, whole blood from three different control subjects was spiked with 1 mM [$^{13}C_2$]-acetate, and processed as illustrated in figure 7.1. For post-spin labeling, platelets were isolated, washed and resuspended in 1 mL glucose-free Tyrode's solution containing [$^{13}C_2$]-acetate (1 mM) for 1 h. Following incubation, isotopic distribution of selected CoA species was determined. Unlabeled blood was used in both instances to determine baseline isotopomer distribution.

tracer dosing study should be evaluated. Since the pre-spin application of isotopic tracers was successful in labeling these CoA species, a commercially available blood collection tube containing the labeling reagent of interest dissolved in the buffer represents a powerful and clinically applicable diagnostic tool.

7.5 Discussion

In this chapter, we have shown that freshly isolated human platelets can be used as an *ex vivo* platform for a variety of challenges or functional tests. This type of test could be used to characterize metabolic physiology or uncover metabolic and mitochondrial pathophysiology. First, we demonstrated that in 1 h, an exogenous fatty acid such as propionate can be incorporated into propionyl-CoA in platelets. This could potentially be used as a diagnostic tool for a disease like propionyl-CoA carboxylase deficiency.[205, 206] Insufficient downstream products or a buildup of propionyl-CoA may reveal an enzymatic deficiency.

Second, the rotenone challenge model revealed another potentially powerful application of this method. We demonstrated that rotenone treatment in isolated platelets recapitulates the phenotype seen with cell lines. This not only further strengthens our original findings for rotenone-mediated changes in intracellular CoA species (particularly succinyl-CoA and BHB-CoA), but also demonstrates that platelets are a viable surrogate tissue to study mitochondrial or metabolic dysfunction. In diseases such as FA, where an underlying metabolic disease manifests clinically in certain tissues, this type of approach may be used diagnostically to uncover disease. For instance, FA patients may exhibit increased sensitivity to rotenone, where a lower dose may exacerbate CoA changes due to

a lower toxic threshold. Conversely, FA patients may exhibit decreased sensitivity to rotenone treatment due to metabolic compensation at baseline and increased reliance on glycolysis. These changes must ultimately be determined empirically. This would not only improve diagnostic capabilities, but also help us understand pathological mechanisms that occur in FA. The destruction of a specific group of neuronal cells while sparing nearby cells, is also a distinctive feature of other neurodegenerative diseases such as PD, AD, and ALS in which nigrastriatal, cerebral cortical, and spinal motor neurons are degraded, respectively. Thus, this assay may be useful for other neurodegenerative diseases as well.

Finally, and perhaps the most valuable application of this methodology is the *ex vivo* isotopic tracer analysis. We have demonstrated that in as little as one hour, five different isotopic tracers were incorporated and could be readily detected in the metabolites extracted from freshly isolated platelets. In fact, there are hundreds or even thousands of different stable isotope metabolic tracers that could likewise be used. In addition to the changes in absolute concentrations of these metabolites, this methodology allows characterization of the flux through these pathways as well.[207] This would improve diagnostic capabilities for many metabolic diseases. Nonetheless, the proper tracer, time of application, and sample handling techniques need to be optimized for each disease. For longer incubations, lymphocytes or fibroblasts could be used since platelets cannot be cultured overnight.[204, 208] In fact, there is evidence that platelets from PD, AD and ALS patients as well as fibroblasts from AD patients exhibit decreased glutamate uptake.[209-212] Using the methodology developed here, we would not only be able to more quantitatively analyze glutamate uptake, but by using a labeled glutamate tracer, we

would be able to determine the fate of the labeled glutamate. Since glutamate can serve as an anaplerotic substrate, decreased glutamate uptake may manifest in decreased incorporation of labeled carbons into aKG and downstream metabolites. This is just one of many potential applications of this assay.

There are certain limitations to this approach over classic biomarker approaches. In particular, the requirement of fresh viable cells makes logistical clinical application challenging and also limits any study that proposes using historical or previously collected samples. In addition, rigorous adherence to standardized protocols would be required not only for sample collection, but also for *ex vivo* challenge, extraction and analysis. Additionally, improper or inconsistent handling could result in significant metabolic disturbances which could lead to erroneous conclusions. On the other hand, the ability to collect, wash and resuspend platelets *ex vivo* prior to testing affords increased standardization and reduces variability that may arise from previously described external factors. In total, however, platelets represent not only a novel surrogate tissue to study metabolism, but these approaches provide a methodological advance in biomarker development. By using functional metabolic tests, much richer and more dynamic data sets can be generated than from classical biomarker studies.

Chapter 8: Conclusions and Future Directions

8.1 Conclusions

In this thesis, we have developed a method to generate SILEC-labeled CoA standards and utilized them to rigorously measure short chain acyl-CoA thioester in cell culture, various animal tissues and clinical samples. These not only improved the specificity of CoA measurement, but also improved accuracy and precision of the measurements. By utilizing the lack of a *de novo* biosynthetic pathway, we were able to generate nearly isotopically pure CoA species biosynthetically in both mammalian and insect cell lines. The extracted species were then applied to biological samples to measure changes in CoA molecules. We also improved upon previously developed isotopic tracer analysis to monitor intracellular flux of labeled carbons through different pathways by performing isotopomer distribution analysis on the different CoA species. Together, these methods allowed us to more confidently monitor changes in the absolute concentration of several important CoA species in cell culture, animal tissue and platelet samples as well as the turnover and flux through these species *in vitro*.

Applying these standards to biological samples led to three important findings. First, using a novel LC-SRM/MS method to monitor intramitochondrial oxidative stress by monitoring ratio of CoASSG: CoASH, it was found that these levels increased dramatically at high menadione doses. Similar doses of rotenone, also known to generate ROS in mitochondria, did not appear to increase these levels, suggesting that CoASSG may be involved in the detoxification of xenobiotics and electrophiles within the mitochondria. Second, it was found, that rotenone dramatically changed in the short chain acyl-CoA thioester profile in a number of different cell lines, including

neuroblastoma (SH-SY5Y), hepatoma (HepG2) and bronchioalveolar carcinoma (H358) cells. In particular, rotenone induced a dose-dependent decrease in succinyl-CoA and increase in BHB-CoA. Isotopic tracer analysis revealed that rotenone inhibited [U-$^{13}C_6$]-glucose-derived acetyl-CoA and succinyl-CoA biosynthesis in SH-SY5Y neuroblastoma cells.

Finally, this SILEC method was adapted for use in freshly isolated human platelets. Extracted platelets were used to characterize differences in short chain acyl-CoA concentrations between healthy controls and patients with FA, a mitochondrial disease for which metabolic dysfunction is known to play a role. A significant decrease in the acetyl-CoA: succinyl-CoA concentration was observed in FA patients and was consistent with an *in vitro* frataxin knockdown model. In addition to being used as a surrogate source of CoA and mitochondrial metabolites, we also demonstrated that platelets could be used as a platform for *ex vivo* metabolic and toxicological challenges. In addition, we also demonstrated that platelets could be used to trace isotopically labeled metabolic nutrients through various biochemical pathways.

8.2 Future Directions

8.2.1 Expansion of in vitro, in vivo and ex vivo models

Cancer cell lines were used for the majority of our work with rotenone-induced metabolic derangement. While cancer cell lines are both easier to work with and are more uniform between experiments, they are known to differ metabolically from primary lines. In particular, the Crabtree or Warburg effect, a phenomenon in which cancer cells

become more glycolytic and may derive as much as 95 % of their ATP from glycolysis.[194, 213] Using rotenone to inhibit mitochondrial respiration in highly glycolytic cells may not induce as dramatic a phenotype as cells more reliant on mitochondria for ATP. One method of avoiding this is by replacing glucose with galactose. In the case of galactose, cells do not generate a net gain of ATP through glycolysis and therefore become more reliant on mitochondria for cellular ATP. These OXPHOS-dependent cells are subsequently more sensitive to mitochondrial inhibitors.[194] Another way to overcome this problem is by using primary cell lines, which may more closely resemble the metabolic state of these tissues in rodents and humans. The drawback to using primary cells is the difficulty in isolating a particular cell type. In the case of primary neuronal cells, glial cells often contaminate and complicate the analysis. Nevertheless, a comparison to primary cells will be important in confirming the changes that are observed in the cell lines. Preliminary data indeed demonstrates that the rotenone-mediated metabolic changes observed with the cell lines (Chapter 5) were recapitulated in primary cortical rat neurons.

In addition, application to neuronal tissue is actively being pursued. The rotenone rat model of PD has been widely used and provides a well validated system to study mitochondrial dysfunction in neurodegenerative disease.[152] We hypothesize that chronic low dose treatment of rotenone in rats will lead to compensatory or pathological metabolic derangement that will manifest in a variety of tissues including the brain, though most dramatically in particular regions such as the substantia nigra.

8.2.2 Measuring other organic acids and Krebs cycle intermediates

This thesis was primarily focused on changes in short chain acyl-CoA species. These were important in understanding changes in several metabolites within or proximal to the Krebs cycle. While understanding changes in acyl-CoA species undoubtedly improves our ability to explore pathological changes in numerous metabolic pathways, it only gives us a partial picture. Further studies exploring changes in organic acids such as those in the Krebs cycle can give us a better understanding of these changes. In fact, we are currently developing an LC-MS method to measure changes in numerous organic acids using a derivatization procedure with MTBSTFA, a derivatizing agent commonly used for GC-MS.[163] Using this reagent, we have been able to measure changes and isotopic labeling in citrate, aKG, succinate, fumarate, malate, oxaloacetate and lactate. Measurements in pyruvate, isocitrate, acetoacetate, BHB, glutamate, and many other fatty acid and cellular nutrients are currently being developed. In addition to expanding the number of metabolites measured, a larger panel of isotopic tracers will be developed to further explore the effects of rotenone, FA and other mitochondrial diseases *in vitro* as well as in platelets.

8.2.3 Measuring the human "CoA-balome"

Throughout this thesis, we have primarily focused on measuring short chain acyl-CoA species for a number of reasons. Most importantly, these molecules are involved at the intersection of many central metabolic pathways such as glycolysis, the Krebs cycle and FAO. Nonetheless, they represent only a small fraction of the many CoA-derivatives including medium, long and very long chain acyl-CoA thioesters, not to mention numerous xenobiotic CoA adducts (appendix, Table A.1). In addition, novel CoA

derivatives such as CoA-RNA adducts and CoA-hydroxynonenal adducts have recently been discovered, though the function and mechanism of formation of these molecules remains unclear. [43, 56] Together, all of these species illustrate the complexity as well as the rich abundance of measurable CoA species. Much like the genome has given way to the transcriptome, and the proteome can be further dissected into the phospho-proteome, the human metabolome is also much too complex to be analyzed using a single method. In fact, the multitude of CoA molecules represent a "CoA-balome," the subset of all CoA derivatives, that might require a systems biology approach to study. It is possible, and even likely, that each mitochondrial or metabolic disease would have a unique CoA fingerprint either at baseline or under some experimentally induced stress. This may only be seen in disease-specific tissues, in which case the assays we developed may allow further understanding of the pathogenic mechanisms of these diseases. On the other hand, these may exhibit changes in surrogate tissues as well, as growing evidence suggests underlying metabolic causes for many diseases. The ability afforded by newer software platforms combined with the ability to do perform CoA discovery using neutral loss scanning of CoA (*m/z* 507) would allow a tremendously powerful approach to diagnosing a variety of diseases. By increasing the breadth of this assay to include a larger subset of CoA species, and combining it with isotopic tracer analyses, new disease biomarkers may be discovered for a multitude of diseases.

Appendix

Coenzyme A thioester	MH^+ (amu)	SILEC MH^+ (amu)
CoASH	768	772
Formyl-CoA	796	800
Acetyl-CoA	810	814
Acrylyl-CoA	822	826
Propionyl-CoA	824	828
Methacrylyl-CoA	836	840
Crotonoyl-CoA	836	840
Butyryl-CoA	838	842
Isobutyryl-CoA	838	842
Beta-Alanyl-CoA	839	843
3-Hydroxypropionyl-CoA	840	844
Lactyl-CoA	840	844
Tiglyl-CoA	850	854
3-Methylcrotonyl-CoA	850	854
Acetoacetyl-CoA	852	856
Isovaleryl-CoA	852	856
Pentanoyl-CoA	852	856
2-Methylbutyryl-CoA	852	856
L-3-Aminobutyryl-CoA	853	857
Malonyl-CoA	854	858
3-Hydroxybutyryl-CoA	854	858
(S)-3-Hydroxyisobutyryl-CoA	854	858
trans-2-Hexenoyl-CoA	864	868
trans-3-Hexenoyl-CoA	864	868
2-Methylacetoacetyl-CoA	866	870
Hexanoyl-CoA	866	870
Succinyl-CoA	868	872
S-Methylmalonyl-CoA	868	872
R-Methylmalonyl-CoA	868	872
Methylmalonyl-CoA	868	872
3-Hydroxyisovaleryl-CoA	868	872
2-Methyl-3-hydroxybutyryl-CoA	868	872
Benzoyl-CoA	872	876
Cyclohex-1,5-diene-1-carboxyl-CoA	874	878
Itaconyl-CoA	880	884
Glutaconyl-CoA	880	884
3-Oxohexanoyl-CoA	880	884
2-Methylhexanoyl-CoA	880	884
Heptanoyl-CoA	880	884

Table A.1 CoA-thioesters and derivatives, including unlabeled and SILEC labeled parent ion masses (*m/z* MH^+, amu). Previously published (Basu SS, Blair IA. *Nat Protocols*, 2011).

Coenzyme A thioester	MH^+ (amu)	SILEC MH^+ (amu)
Glutaryl-CoA	882	886
(S)-Hydroxyhexanoyl-CoA	882	886
Malyl-CoA	884	888
Salicyl CoA	886	890
Phenylacetyl-CoA	886	890
4-hydroxybenzoyl-CoA	888	892
3-trans,5-cis-Octadienoyl-CoA	888	892
6-Oxocyclohex-1-ene-1-carboxyl-CoA	890	894
2-trans,4-trans-Octadienoyl-CoA	890	894
6-Hydroxycyclohex-1-ene-1-carboxyl-CoA	892	896
(2E)-Octenoyl-CoA	892	896
S-2-Octenoyl CoA	892	896
3-Methylglutaconyl-CoA	894	898
Valproyl-CoA	894	898
Octanoyl-CoA	894	898
Adipoyl-CoA	896	900
L-Citramalyl-CoA	898	902
4-Hydroxyphenylacetyl-CoA	902	906
2,6-Dimethylheptanoyl-CoA	904	908
3-Oxooctanoyl-CoA	908	912
Nonanoyl-CoA	908	912
(S)-Hydroxyoctanoyl-CoA	910	914
(3S)-3-Hydroxyadipyl-CoA	912	916
3-Hydroxy-3-methylglutaryl-CoA	912	916
2,4-Decadienoyl-CoA	918	922
cis-2-Methyl-5-isopropylhexa-2,5-dienoyl-CoA	918	922
trans-2-Methyl-5-isopropylhexa-2,5-dienoyl-CoA	918	922
(2E)-Decenoyl-CoA	920	924
4-cis-Decenoyl-CoA	920	924
trans-3-Decenoyl-CoA	920	924
trans-D-Decenoyl-CoA	920	924
Decanoyl-CoA (n-C10:0CoA)	922	926
3-Oxopimelyl-CoA	924	928
3-Hydroxypimelyl-CoA	926	930
Pseudoecgonyl-CoA	935	939
3-Hydroxy-2,6-dimethyl-5-methylene-heptanoyl-CoA	936	940
3-Oxodecanoyl-CoA	936	940
Undecanoyl-CoA	936	940
4,8-Dimethylnonanoyl-CoA	936	940

Table A.1 CoA-thioesters and derivatives (cont.)

Coenzyme A thioester	MH^+ (amu)	SILEC MH^+ (amu)
(S)-Hydroxydecanoyl-CoA	938	942
(2E)-Dodecenoyl-CoA	944	948
cis,cis-3,6-Dodecadienoyl-CoA	946	950
trans,cis-Lauro-2,6-dienoyl-CoA	946	950
Trans-2,3-dehydrododecanoyl-CoA	948	952
3Z-dodecenoyl-CoA	948	952
Lauroyl-CoA	950	954
E-Phenylitaconyl-CoA	956	960
(R)-Benzylsuccinyl-CoA	958	962
3(S)-3-hydroxydodecen-(5Z)-oyl-CoA	960	964
(3S)-3-Hydroxydodec-cis-6-enoyl-CoA	960	964
3-Oxododecanoyl-CoA	964	968
(S)-3-Hydroxydodecanoyl-CoA	966	970
(3E,5Z,8Z)-Tetradecatrienoyl-CoA	968	972
(2S,6R,10R)-Trimethyl-2E-hendecenoyl-CoA	972	976
2-Carboxymethyl-3-hydroxyphenylpropionyl-CoA	974	978
(2S,6R,10R)-Trimethyl-hendecanoyl-CoA	974	978
5-cis-8-cis-Tetradecadienoyl-CoA	974	978
(2E)-Tetradecenoyl-CoA	976	980
Tetradecanoyl-CoA	978	982
trans-2-Enoyl-OPC4-CoA	986	990
(3S)-3-Hydroxy-cis-8-tetradecenoyl-CoA	988	992
OPC4-CoA	988	992
3-Oxotetradecanoyl-CoA	992	996
(S)-3-Hydroxytetradecanoyl-CoA	994	998
(4R,8R,12R)-Trimethyl-2E-tridecenoyl-CoA	1000	1004
(2E)-Hexadecenoyl-CoA	1000	1004
Palmitoleyl CoA	1004	1008
Palmitelaidoyl-CoA	1004	1008
Palmitoyl-CoA	1006	1010
(3S)-3-Hydroxy-cis,cis-palmito-7,10-dienoyl-CoA	1014	1018
trans-2-Enoyl-OPC6-CoA	1014	1018
(S)-3-hydroxypalmitoleoyl-CoA	1016	1020
OPC6-CoA	1016	1020
3-Oxohexadecanoyl-CoA	1020	1024
Heptadecanoyl CoA	1020	1024
(S)-3-Hydroxyhexadecanoyl-CoA	1022	1026
Stearidonoyl-CoA	1026	1030
Gamma-linolenoyl-CoA	1028	1032

Table A.1 CoA-thioesters and derivatives (cont.)

Coenzyme A thioester	MH^+ (amu)	SILEC MH^+ (amu)
Alpha-Linolenoyl-CoA	1028	1032
Linoleoyl-CoA	1030	1034
trans-Octadec-2-enoyl-CoA	1032	1036
cis-Vaccenoyl CoA	1032	1036
Oleoyl-CoA	1032	1036
Stearoyl-CoA	1034	1038
(3S)-3-Hydroxylinoleoyl-CoA	1042	1046
trans-2-Enoyl-OPC8-CoA	1042	1046
OPC8-CoA	1044	1048
3-hydroxyoctadecanoyl-CoA	1046	1050
3-Oxooctadecanoyl-CoA	1046	1050
Retinoyl CoA	1050	1054
Timnodonyl CoA	1052	1056
3-Hydroxyhexdecanedioyl-CoA	1052	1056
5Z,8Z,11Z,14Z-eicosatetraenonyl-CoA	1054	1058
Arachidonyl-CoA	1054	1058
Pristanoyl-CoA	1062	1066
Eicosanoyl-CoA	1062	1066
Phytanoyl-CoA	1062	1066
Glutathione-CoA (CoASSG)	1073	1077
2,4,7,10,13,16,19-Docosaheptaenoyl-CoA	1076	1080
Clupanodonyl CoA	1076	1080
2-Hydroxyphytanoyl-CoA	1078	1082
Docosa-4,7,10,13,16-pentaenoyl CoA	1080	1084
Docosanoyl-CoA	1086	1090
8Z,11Z,14Z-eicosatrienoyl-CoA	1096	1100
Trans-2-all-cis-6,9,12,15,18,21-tetracosaheptaenoyl-CoA	1100	1104
Tetracosahexaenoyl CoA	1106	1110
Tetracosatetraenoyl CoA	1110	1114
(3S)-Hydroxy-tetracosa-6,9,12,15,18,21-all-cis-hexaenoyl-CoA	1118	1122
Tetracosanoyl-CoA	1118	1122
Chenodeoxyglycocholoyl-CoA	1142	1146
Chenodeoxycholoyl-CoA	1142	1146
Hexacosanoyl-CoA	1142	1146
Choloyl-CoA	1158	1162
3a,7a-Dihydroxy-5b-cholest-24-enoyl-CoA	1182	1186
3a,7a-Dihydroxy-5b-24-oxocholestanoyl-CoA	1198	1202
3a,7a,12a-Trihydroxy-5b-cholest-24-enoyl-CoA	1198	1202

Table A.1 CoA-thioesters and derivatives (cont.)

Day	Acetyl-CoA	Succinyl-CoA	CoASH	HMG-CoA	Propionyl-CoA
1	5.3	18.3	1.0	0.3	0.2
2	13.0	29.9	2.4	0.5	0.4
3	32.3	80.9	19.1	2.3	1.0
4	110.0	152.9	47.3	8.0	3.7
5	91.9	213.1	91.9	4.0	6.0
6	78.3	108.0	75.8	0.9	2.0
7	68.0	84.5	118.0	0.8	1.9

Table A.2 Amounts of intracellular CoA thioesters formed (pmol/plate) on days after splitting mouse Hepa cells. Previosuly published in Basu et al. *Anal Chem*, 2011, Supporting Information.

		Stable Isotope Internal Standard				
		CoASH	Succinyl-CoA	HMG-CoA	Acetyl-CoA	Propionyl-CoA
CoA	CoASH	**0.9966**	0.9922	0.9877	0.9948	0.9922
	Succinyl-CoA	0.9652	**0.9996**	0.9937	0.9982	0.9991
	HMG-CoA	0.9688	0.9996	**0.9939**	0.9993	0.9983
	Acetyl-CoA	0.8443	0.9978	0.8098	**0.9990**	0.9958
	Propionyl-CoA	0.9585	0.9992	0.9975	0.9983	**0.9999**

Table A.3 Correlation coefficients for linearity of standard curves for various CoA species using SILEC standards (bold) compared with structural analog internal standards (normal). Previosuly published in Basu et al. *Anal Chem*, 2011, Supporting Information.

		Acetyl-CoA	Succinyl-CoA	CoASH	BHB-CoA	Propionyl-CoA	HMG-CoA
SH-SY5Y	DMSO	8.68 ± 0.70	3.37 ± 0.10	2.42 ± 0.17	0.065 ± 0.002	0.047 ± 0.003	0.59 ± 0.01
	10pM	7.05 ± 0.33	2.88 ± 0.30	3.12 ± 1.28	0.065 ± 0.002	0.036 ± 0.006	0.64 ± 0.02
	100pM	8.99 ± 0.33	*2.98 ± 0.07*	2.97 ± 0.87	0.070 ± 0.001	0.042 ± 0.006	0.62 ± 0.07
	1nM	9.53 ± 0.51	**2.48 ± 0.10**	*3.52 ± 0.21*	0.079 ± 0.008	0.049 ± 0.002	0.83 ± 0.12
	10nM	8.21 ± 0.18	**2.23 ± 0.09**	2.13 ± 0.32	**0.086 ± 0.002**	0.041 ± 0.002	0.73 ± 0.06
	100nM	9.54 ± 0.74	**0.99 ± 0.02**	1.93 ± 0.30	**0.177 ± 0.008**	**0.019 ± 0.003**	*1.05 ± 0.16*
	1uM	10.25 ± 0.21	**0.66 ± 0.04**	2.19 ± 0.57	**0.241 ± 0.027**	**0.010 ± 0.003**	1.05 ± 0.21
HepG2	DMSO	11.46 ± 0.44	9.52 ± 0.81	10.76 ± 1.50	0.170 ± 0.008	0.704 ± 0.029	2.02 ± 0.21
	10pM	*8.78 ± 0.72*	6.78 ± *0.35*	6.73 ± 0.43	0.150 ± 0.003	0.601 ± 0.037	1.60 ± 0.04
	100pM	11.49 ± 0.62	7.71 ± 0.45	8.77 ± 1.07	0.164 ± 0.002	0.740 ± 0.049	1.76 ± 0.10
	1nM	9.35 ± 0.85	7.21 ± 0.69	*6.09 ± 0.67*	0.163 ± 0.019	0.586 ± 0.035	1.84 ± 0.20
	10nM	10.13 ± 0.93	*7.25* ± 0.13	6.78 ± 0.35	0.170 ± 0.011	0.783 ± 0.035	2.29 ± 0.08
	100nM	10.51 ± 0.15	**4.39 ± 0.23**	*5.36 ± 0.41*	**0.325 ± 0.012**	0.735 ± 0.018	2.00 ± 0.08
	1uM	12.05 ± 0.46	**2.08 ± 0.06**	*5.42 ± 1.17*	**0.582 ± 0.003**	0.719 ± 0.059	2.10 ± 0.16
H358	DMSO	14.76 ± 0.82	7.48 ± 0.60	5.82 ± 1.12	0.158 ± 0.006	0.157 ± 0.005	2.08 ± 0.19
	10pM	*12.32 ± 0.29*	7.36 ± *0.20*	4.86 ± 0.41	0.160 ± 0.015	0.157 ± 0.011	1.85 ± 0.04
	100pM	12.20 ± 0.43	7.83 ± 0.40	4.44 ± 0.08	0.152 ± 0.006	0.146 ± 0.001	1.83 ± 0.23
	1nM	*10.94 ± 0.91*	7.02 ± 0.12	5.13 ± 0.69	*0.212 ± 0.010*	0.179 ± 0.018	1.62 ± 0.07
	10nM	*11.44 ± 0.16*	6.28 ± *0.20*	5.19 ± 0.42	**0.358 ± 0.002**	*0.222 ± 0.011*	*1.91 ± 0.19*
	100nM	**9.05 ± 0.65**	**2.39 ± 0.13**	3.45 ± 0.19	**0.713 ± 0.006**	0.174 ± 0.005	*1.17 ± 0.11*
	1uM	**10.44 ± 0.34**	**1.30 ± 0.14**	3.87 ± 0.57	**1.103 ± 0.101**	0.150 ± 0.015	*1.36 ± 0.07*

Table A.4. Absolute levels of CoASH and several short chain acyl-CoA thioesters in SH-SY5Y cells treated with rotenone measured using SILEC methodology. Concentrations are presented as pmol/10^6 cells +/- SEM (triplicate). When compared to DMSO controls, $p < 0.05$ (*italics*) and $p < 0.005$ (**bold**). Published in Basu, Blair. *Chem Res Toxicol*, 2011.

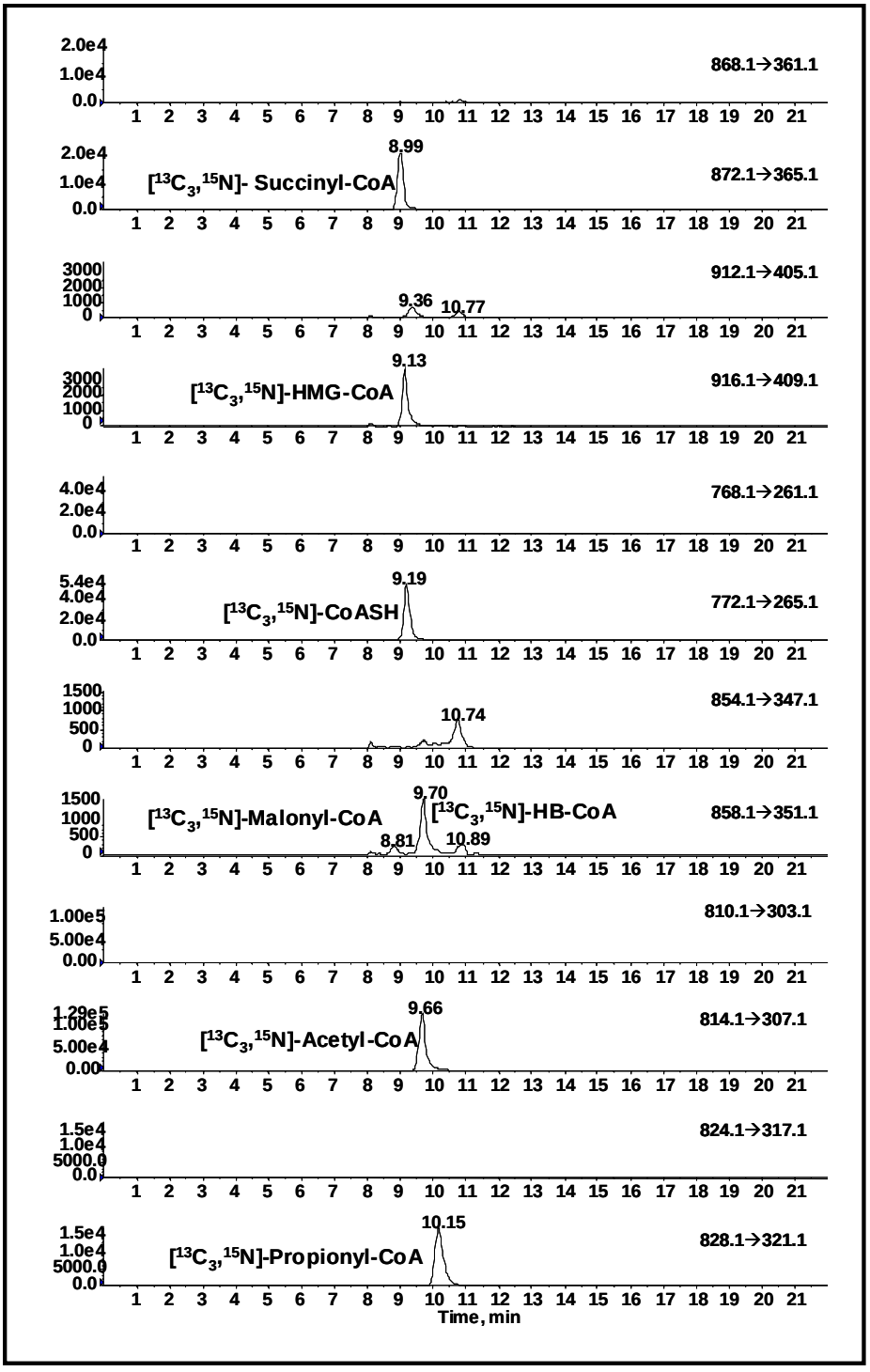

Figure A.1 LC-SRM/MS chromatogram of acid extracted SILEC-labeled short chain acyl-CoA internal standards demonstrating isotopic purity. Previosuly published in Basu et al. *Anal Chem*, 2011, Supporting Information.

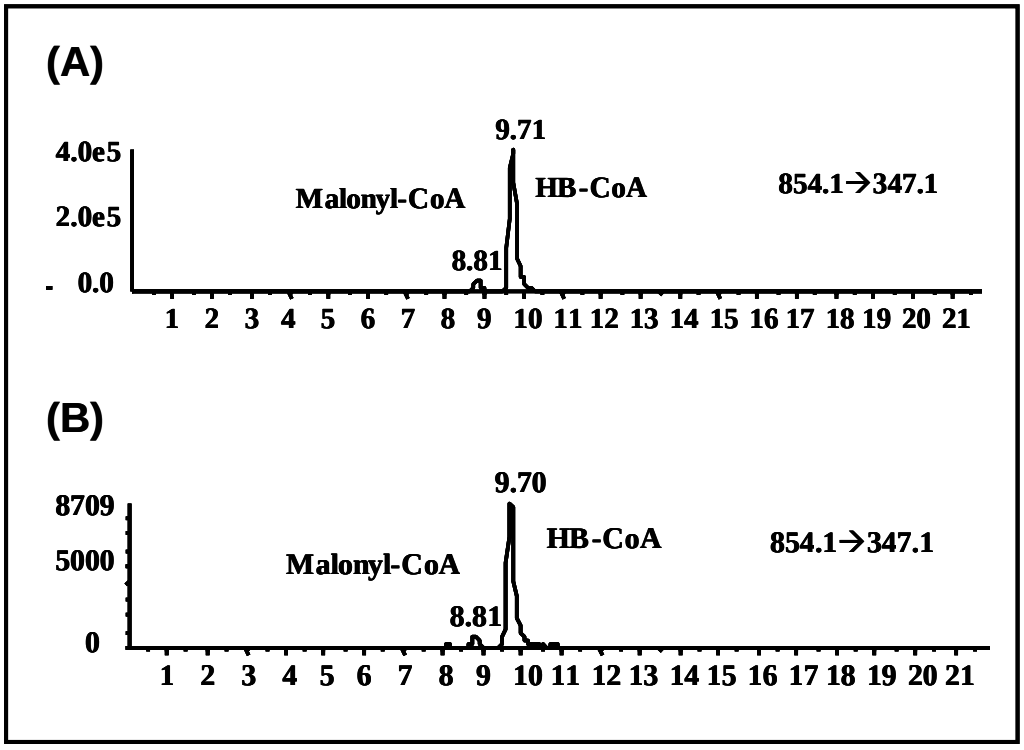

Figure A.2 LC-MS (SRM) chromatograms of (A) malonyl-CoA and BHB-CoA standards (1 pmol each) and (B) acid extracted and SPE CoA species from Hepa 1c1c7 cells.

Reference List

1. Watson,J.D. & Crick,F.H. Molecular structure of nucleic acids; a structure for deoxyribose nucleic acid. *Nature* **171**, 737-738 (1953).

2. Lander,E.S. *et al.* Initial sequencing and analysis of the human genome. *Nature* **409**, 860-921 (2001).

3. Wallace,D.C. A mitochondrial paradigm of metabolic and degenerative diseases, aging, and cancer: a dawn for evolutionary medicine. *Annu. Rev. Genet.* **39**, 359-407 (2005).

4. McFarland,R. & Turnbull,D.M. Batteries not included: diagnosis and management of mitochondrial disease. *J Intern. Med.* **265**, 210-228 (2009).

5. Luft,R. The development of mitochondrial medicine. *Proc. Natl. Acad. Sci. U. S. A* **91**, 8731-8738 (1994).

6. Kristal,B.S., Shurubor,Y.I., Kaddurah-Daouk,R., & Matson,W.R. Metabolomics in the study of aging and caloric restriction. *Methods Mol. Biol.* **371**, 393-409 (2007).

7. Scheffler,I.E. Mitochondria make a come back. *Adv. Drug Deliv. Rev.* **49**, 3-26 (2001).

8. Benard,G. *et al.* Physiological diversity of mitochondrial oxidative phosphorylation. *Am. J Physiol Cell Physiol* **291**, C1172-C1182 (2006).

9. Rocher,C. *et al.* Influence of mitochondrial DNA level on cellular energy metabolism: implications for mitochondrial diseases. *J Bioenerg. Biomembr.* **40**, 59-67 (2008).

10. Wallace,D.C. & Fan,W. The pathophysiology of mitochondrial disease as modeled in the mouse. *Genes Dev.* **23**, 1714-1736 (2009).

11. Camara,B., Hugueney,P., Bouvier,F., Kuntz,M., & Moneger,R. Biochemistry and molecular biology of chromoplast development. *Int. Rev. Cytol.* **163**, 175-247 (1995).

12. Agnati,L.F. *et al.* A new hypothesis of pathogenesis based on the divorce between mitochondria and their host cells: possible relevance for Alzheimer's disease. *Curr. Alzheimer Res.* **7**, 307-322 (2010).

13. Jansen,R.P. Origin and persistence of the mitochondrial genome. *Hum. Reprod.* **15 Suppl 2**, 1-10 (2000).

14. Carelli,V., Ross-Cisneros,F.N., & Sadun,A.A. Mitochondrial dysfunction as a cause of optic neuropathies. *Prog. Retin. Eye Res.* **23**, 53-89 (2004).

15. Poulton,J. & Marchington,D.R. Segregation of mitochondrial DNA (mtDNA) in human oocytes and in animal models of mtDNA disease: clinical implications. *Reproduction.* **123**, 751-755 (2002).

16. Benard,G. *et al.* Functional dynamic compartmentalization of respiratory chain intermediate substrates: implications for the control of energy production and mitochondrial diseases. *Int. J Biochem. Cell Biol.* **40**, 1543-1554 (2008).

17. Kim,J.A., Wei,Y., & Sowers,J.R. Role of mitochondrial dysfunction in insulin resistance. *Circ. Res.* **102**, 401-414 (2008).

18. Shoffner,J.M. & Wallace,D.C. Heart disease and mitochondrial DNA mutations. *Heart Dis. Stroke* **1**, 235-241 (1992).

19. Brandon,M., Baldi,P., & Wallace,D.C. Mitochondrial mutations in cancer. *Oncogene* **25**, 4647-4662 (2006).

20. Yan,S.D., Xiong,W.C., & Stern,D.M. Mitochondrial amyloid-beta peptide: pathogenesis or late-phase development? *J Alzheimers. Dis.* **9**, 127-137 (2006).

21. Lin,T.K. *et al.* Mitochondrial dysfunction and biogenesis in the pathogenesis of Parkinson's disease. *Chang Gung. Med. J.* **32**, 589-599 (2009).

22. Giulivi,C. *et al.* Mitochondrial dysfunction in autism. *JAMA* **304**, 2389-2396 (2010).

23. de Moura,M.B., dos Santos,L.S., & Van,H.B. Mitochondrial dysfunction in neurodegenerative diseases and cancer. *Environ. Mol. Mutagen.* **51**, 391-405 (2010).

24. Suomalainen,A. Mitochondrial DNA and disease. *Ann. Med.* **29**, 235-246 (1997).

25. Gomez,C., Bandez,M.J., & Navarro,A. Pesticides and impairment of mitochondrial function in relation with the parkinsonian syndrome. *Front Biosci.* **12**, 1079-1093 (2007).

26. Sherer,T.B. *et al.* Mechanism of toxicity in rotenone models of Parkinson's disease. *J. Neurosci.* **23**, 10756-10764 (2003).

27. Ulrich,R.G. *et al.* Metabolic, idiosyncratic toxicity of drugs: overview of the hepatic toxicity induced by the anxiolytic, panadiplon. *Chem. Biol. Interact.* **134**, 251-270 (2001).

28. Genschel,U. Coenzyme A biosynthesis: Reconstruction of the pathway in archaea and an evolutionary scenario based on comparative genomics. *Molecular Biology and Evolution* **21**, 1242-1251 (2004).

29. Sim,E., Walters,K., & Boukouvala,S. Arylamine N-acetyltransferases: from structure to function. *Drug Metab. Rev.* **40**, 479-510 (2008).

30. Begley,T.P., Kinsland,C., & Strauss,E. The biosynthesis of coenzyme A in bacteria. *Vitam. Horm.* **61**, 157-171 (2001).

31. Zhang,Y.M. *et al.* Acyl carrier protein is a cellular target for the antibacterial action of the pantothenamide class of pantothenate antimetabolites. *J Biol. Chem.* **279**, 50969-50975 (2004).

32. Webb,M.E., Smith,A.G., & Abell,C. Biosynthesis of pantothenate. *Nat. Prod. Rep.* **21**, 695-721 (2004).

33. Leonardi,R., Zhang,Y.M., Rock,C.O., & Jackowski,S. Coenzyme A: back in action. *Prog. Lipid Res.* **44**, 125-153 (2005).

34. Lobley,C.M. *et al.* Structural insights into the evolution of the pantothenate-biosynthesis pathway. *Biochem. Soc. Trans.* **31**, 563-571 (2003).

35. Brass,E.P. Overview of coenzyme A metabolism and its role in cellular toxicity. *Chem. Biol. Interact.* **90**, 203-214 (1994).

36. Rock,C.O., Calder,R.B., Karim,M.A., & Jackowski,S. Pantothenate kinase regulation of the intracellular concentration of coenzyme A. *J Biol. Chem.* **275**, 1377-1383 (2000).

37. Tahiliani,A.G. & Beinlich,C.J. Pantothenic acid in health and disease. *Vitam. Horm.* **46**, 165-228 (1991).

38. Lowe,D.M. & Tubbs,P.K. Succinylation and inactivation of 3-hydroxy-3-methylglutaryl-CoA synthase by succinyl-CoA and its possible relevance to the control of ketogenesis. *Biochem. J.* **232**, 37-42 (1985).

39. Brown,M.S. & Goldstein,J.L. Multivalent feedback regulation of HMG CoA reductase, a control mechanism coordinating isoprenoid synthesis and cell growth. *J Lipid Res.* **21**, 505-517 (1980).

40. Lipmann,F. Acetylation of Sulfanilamide by Liver Homogenates and Extracts. *J. Biol. Chem.* **160**, 173-190 (1945).

41. Kresge,N., Simoni,R.D., & Hill,R.L. JBC centennial 1905-2005 - 100 years of biochemistry and molecular biology - Fritz Lipmann and the discovery of coenzyme A - Acetylation of sulfanilamide by liver homogenates and extracts (Lipmann, F. (1945) J. Biol. Chem. 160, 173-190). *Journal of Biological Chemistry* **280**, (2005).

42. Rogers,L.K., Valentine,C.J., Szczpyka,M., & Smith,C.V. Effects of hepatotoxic doses of acetaminophen and furosemide on tissue concentrations of CoASH and CoASSG in vivo. *Chem. Res. Toxicol.* **13**, 873-882 (2000).

43. Zhang,G.F. *et al.* Catabolism of 4-hydroxyacids and 4-hydroxynonenal via 4-hydroxy-4-phosphoacyl-CoAs. *J. Biol. Chem.* **284**, 33521-33534 (2009).

44. delCardayre,S.B., Stock,K.P., Newton,G.L., Fahey,R.C., & Davies,J.E. Coenzyme A disulfide reductase, the primary low molecular weight disulfide reductase from Staphylococcus aureus. Purification and characterization of the native enzyme. *J Biol. Chem.* **273**, 5744-5751 (1998).

45. Crane,D., Haussinger,D., & Sies,H. Rise of coenzyme A-glutathione mixed disulfide during hydroperoxide metabolism in perfused rat liver. *Eur. J Biochem.* **127**, 575-578 (1982).

46. Jankowski,J. *et al.* Isolation and characterization of coenzyme A glutathione disulfide as a parathyroid-derived vasoconstrictive factor. *Circulation* **102**, 2548-2552 (2000).

47. Rogers,L.K., Tipple,T.E., Britt,R.D., & Welty,S.E. Hyperoxia exposure alters hepatic eicosanoid metabolism in newborn mice. *Pediatr. Res.* **67**, 144-149 (2010).

48. Luo,J. *et al.* Endogenous coenzyme A glutathione disulfide in human myocardial tissue. *J Endocrinol. Invest* **29**, 688-693 (2006).

49. Gilbert,H.F. Biological disulfides: the third messenger? Modulation of phosphofructokinase activity by thiol/disulfide exchange. *J Biol. Chem.* **257**, 12086-12091 (1982).

50. Schluter,H. *et al.* Coenzyme A glutathione disulfide. A potent vasoconstrictor derived from the adrenal gland. *Circ. Res.* **76**, 675-680 (1995).

51. van der Giet,M. *et al.* CoenzymeA glutathione disulfide is a potent modulator of angiotensin II-induced vasoconstriction. *Am. J Hypertens.* **14**, 164-168 (2001).

52. Ondarza,R.N. Enzyme regulation by biological disulfides. *Biosci. Rep.* **9**, 593-604 (1989).

53. Wong,Y.L., Smith,C.V., McMicken,H.W., Rogers,L.K., & Welty,S.E. Mitochondrial thiol status in the liver is altered by exposure to hyperoxia. *Toxicol. Lett.* **123**, 179-193 (2001).

54. O'Donovan,D.J. *et al.* CoASH and CoASSG levels in lungs of hyperoxic rats as potential biomarkers of intramitochondrial oxidant stresses. *Pediatr. Res.* **51**, 346-353 (2002).

55. Liang,L.P. & Patel,M. Seizure-induced changes in mitochondrial redox status. *Free Radic. Biol. Med.* **40**, 316-322 (2006).

56. Kowtoniuk,W.E., Shen,Y., Heemstra,J.M., Agarwal,I., & Liu,D.R. A chemical screen for biological small molecule-RNA conjugates reveals CoA-linked RNA. *Proc. Natl. Acad. Sci. U. S. A* **106**, 7768-7773 (2009).

57. Beinlich,C.J., Robishaw,J.D., & Neely,J.R. Metabolism of pantothenic acid in hearts of diabetic rats. *J. Mol. Cell. Cardiol.* **21**, 641-649 (1989).

58. MacDonald,M.J. Synergistic potent insulin release by combinations of weak secretagogues in pancreatic islets and INS-1 cells. *J. Biol. Chem.* **282**, 6043-6052 (2007).

59. Bennett,M.J. & Hale,D.E. Medium chain acyl-coenzyme A dehydrogenase deficiency. *N. J. Med.* **89**, 675-678 (1992).

60. Feliz,B., Witt,D.R., & Harris,B.T. Propionic acidemia: a neuropathology case report and review of prior cases. *Arch. Pathol. Lab. Med.* **127**, e325-e328 (2003).

61. Van Hove,J.L. *et al.* D,L-3-hydroxybutyrate treatment of multiple acyl-CoA dehydrogenase deficiency (MADD). *Lancet* **361**, 1433-1435 (2003).

62. Boneh,A. *et al.* VLCAD deficiency: pitfalls in newborn screening and confirmation of diagnosis by mutation analysis. *Mol. Genet. Metab.* **88**, 166-170 (2006).

63. Mitchell,G.A. *et al.* Hereditary and acquired diseases of acyl-coenzyme A metabolism. *Mol. Genet. Metab.* **94**, 4-15 (2008).

64. van Maldegem,B.T., Wanders,R.J., & Wijburg,F.A. Clinical aspects of short-chain acyl-CoA dehydrogenase deficiency. *J. Inherit. Metab. Dis.*(2010).

65. King,M.T. & Reiss,P.D. Separation and measurement of short-chain coenzyme-A compounds in rat liver by reversed-phase high-performance liquid chromatography. *Anal. Biochem.* **146**, 173-179 (1985).

66. King,M.T., Reiss,P.D., & Cornell,N.W. Determination of short-chain coenzyme A compounds by reversed-phase high-performance liquid chromatography. *Methods Enzymol.* **166**, 70-79 (1988).

67. Park,J.W., Jung,W.S., Park,S.R., Park,B.C., & Yoon,Y.J. Analysis of intracellular short organic acid-coenzyme A esters from actinomycetes using liquid chromatography-electrospray ionization-mass spectrometry. *J. Mass Spectrom.* **42**, 1136-1147 (2007).

68. Kasuya,F., Oti,Y., Tatsuki,T., & Igarashi,K. Analysis of medium-chain acyl-coenzyme A esters in mouse tissues by liquid chromatography-electrospray ionization mass spectrometry. *Anal. Biochem.* **325**, 196-205 (2004).

69. Magnes,C., Sinner,F.M., Regittnig,W., & Pieber,T.R. LC/MS/MS method for quantitative determination of long-chain fatty acyl-CoAs. *Anal. Chem.* **77**, 2889-2894 (2005).

70. Mauriala,T., Herzig,K.H., Heinonen,M., Idziak,J., & Auriola,S. Determination of long-chain fatty acid acyl-coenzyme A compounds using liquid chromatography-electrospray ionization tandem mass spectrometry. *J. Chromatogr. B. Analyt Technol. Biomed. Life. Sci.* **808**, 263-268 (2004).

71. Scheffler,I.E. A century of mitochondrial research: achievements and perspectives. *Mitochondrion* **1**, 3-31 (2001).

72. Anson,R.M., Hudson,E., & Bohr,V.A. Mitochondrial endogenous oxidative damage has been overestimated. *FASEB J* **14**, 355-360 (2000).

73. Chang,S.H. & Wilken,D.R. Identity of a bovine liver nucleotide peptide witht the unsymmetrical disulfied of coenzyme A and glutathione. *J. Biol. Chem.* **240**, 3136-3139 (1965).

74. Hayashi,O. & Satoh,K. Determination of acetyl-CoA and malonyl-CoA in germinating rice seeds using the LC-MS/MS technique. *Biosci. Biotechnol. Biochem.* **70**, 2676-2681 (2006).

75. Dalluge,J.J. *et al.* Separation and identification of organic acid-coenzyme A thioesters using liquid chromatography/electrospray ionization-mass spectrometry. *Anal. Bioanal Chem.* **374**, 835-840 (2002).

76. Magnes,C. *et al.* Validated comprehensive analytical method for quantification of coenzyme A activated compounds in biological tissues by online solid-phase extraction LC/MS/MS. *Anal. Chem.* **80**, 5736-5742 (2008).

77. King,R., Bonfiglio,R., Fernandez-Metzler,C., Miller-Stein,C., & Olah,T. Mechanistic investigation of ionization suppression in electrospray ionization. *J. Am. Soc. Mass Spectrom.* **11**, 942-950 (2000).

78. Bonfiglio,R., King,R.C., Olah,T.V., & Merkle,K. The effects of sample preparation methods on the variability of the electrospray ionization response for model drug compounds. *Rapid Commun. Mass Spectrom.* **13**, 1175-1185 (1999).

79. Hsieh,Y. HPLC-MS/MS in drug metabolism and pharmacokinetic screening. *Expert. Opin. Drug Metab Toxicol.* **4**, 93-101 (2008).

80. Brown,S.C., Kruppa,G., & Dasseux,J.L. Metabolomics applications of FT-ICR mass spectrometry. *Mass Spectrom. Rev.* **24**, 223-231 (2005).

81. Hu,Q.Z. *et al.* The Orbitrap: a new mass spectrometer. *J. Mass Spectrom.* **40**, 430-443 (2005).

82. Whalen,K., Gobey,J., & Janiszewski,J. A centralized approach to tandem mass spectrometry method development for high-throughput ADME screening. *Rapid Commun. Mass Spectrom.* **20**, 1497-1503 (2006).

83. Taylor,C.F. *et al.* A systematic approach to modeling, capturing, and disseminating proteomics experimental data. *Nat. Biotechnol.* **21**, 247-254 (2003).

84. Cox,J. *et al.* A practical guide to the MaxQuant computational platform for SILAC-based quantitative proteomics. *Nat. Protoc.* **4**, 698-705 (2009).

85. Madalinski,G. *et al.* Direct introduction of biological samples into a LTQ-Orbitrap hybrid mass spectrometer as a tool for fast metabolome analysis. *Anal. Chem.* **80**, 3291-3303 (2008).

86. Wu,C.C. & Yates,J.R., III The application of mass spectrometry to membrane proteomics. *Nat. Biotechnol.* **21**, 262-267 (2003).

87. Jemal,M. High-throughput quantitative bioanalysis by LC/MS/MS. *Biomed. Chromatogr.* **14**, 422-429 (2000).

88. Remane,D., Wissenbach,D.K., Meyer,M.R., & Maurer,H.H. Systematic investigation of ion suppression and enhancement effects of fourteen stable-isotope-labeled internal standards by their native analogues using atmospheric-pressure chemical ionization and electrospray ionization and the relevance for multi-analyte liquid chromatographic/mass spectrometric procedures. *Rapid Commun. Mass Spectrom.* **24**, 859-867 (2010).

89. Prakash,C., Shaffer,C.L., & Nedderman,A. Analytical strategies for identifying drug metabolites. *Mass Spectrom. Rev.* **26**, 340-369 (2007).

90. Matuszewski,B.K. Standard line slopes as a measure of a relative matrix effect in quantitative HPLC-MS bioanalysis. *J. Chromatogr. B* **830**, 293-300 (2006).

91. Ciccimaro,E. & Blair,I.A. Stable-isotope dilution LC-MS for quantitative biomarker analysis. *Bioanalysis* **2**, 311-341 (2010).

92. Ong,S.E. *et al.* Stable isotope labeling by amino acids in cell culture, SILAC, as a simple and accurate approach to expression proteomics. *Mol. Cell. Proteomics* **1**, 376-386 (2002).

93. Basu,S.S., Mesaros,C., Gelhaus,S.L., & Blair,I.A. Stable isotope labeling by essential nutirents in cell culture for the preparation of labeled coenzyme A and its thioesters. *Anal. Chem.* **83**, 1363-1369 (2011).

94. Bennett,B.D., Yuan,J., Kimball,E.H., & Rabinowitz,J.D. Absolute quantitation of intracellular metabolite concentrations by an isotope ratio-based approach. *Nat. Protoc.* **3**, 1299-1311 (2008).

95. Ong,S.E. & Mann,M. A practical recipe for stable isotope labeling by amino acids in cell culture (SILAC). *Nat. Protoc.* **1**, 2650-2660 (2006).

96. Yan,Y., Weaver,V.M., & Blair,I.A. Analysis of protein expression during oxidative stress in breast epithelial cells using a stable isotope labeled proteome internal standard. *J. Proteome Res.* **4**, 2007-2014 (2005).

97. Shah,S.J., Yu,K.H., Sangar,V., Parry,S.I., & Blair,I.A. Identification and quantification of preterm birth biomarkers in human cervicovaginal fluid by liquid chromatography/tandem mass spectrometry. *J. Proteome Res.* **8**, 2407-2417 (2009).

98. Rangiah,K. *et al.* Differential Secreted Proteome Approach in Murine Model for Candidate Biomarker Discovery in Colon Cancer. *J. Proteome Res.* **8**, 5153-5164 (2009).

99. Geiger,T. *et al.* Use of stable isotope labeling by amino acids in cell culture as a spike-in standard in quantitative proteomics. *Nat. Protoc.* **6**, 147-157 (2011).

100. Robishaw,J.D. & Neely,J.R. Coenzyme A metabolism. *Am. J. Physiol.* **248**, E1-E9 (1985).

101. Li,L.O., Klett,E.L., & Coleman,R.A. Acyl-CoA synthesis, lipid metabolism and lipotoxicity. *Biochim. Biophys. Acta* **1801**, 246-251 (2010).

102. Gao,L. *et al.* Simultaneous quantification of malonyl-CoA and several other short-chain acyl-CoAs in animal tissues by ion-pairing reversed-phase HPLC/MS. *J. Chromatogr. B. Analyt Technol. Biomed. Life. Sci.* **853**, 303-313 (2007).

103. MacDonald,M.J., Smith,A.D., III, Hasan,N.M., Sabat,G., & Fahien,L.A. Feasibility of pathways for transfer of acyl groups from mitochondria to the cytosol to form short chain acyl-CoAs in the pancreatic beta cell. *J. Biol. Chem.* **282**, 30596-30606 (2007).

104. van Grunsven,E.G. *et al.* Peroxisomal D-hydroxyacyl-CoA dehydrogenase deficiency: resolution of the enzyme defect and its molecular basis in

bifunctional protein deficiency. *Proc. Natl. Acad. Sci. U. S. A* **95**, 2128-2133 (1998).

105. Steghens,J.P., Flourie,F., Arab,K., & Collombel,C. Fast liquid chromatography-mass spectrometry glutathione measurement in whole blood: micromolar GSSG is a sample preparation artifact. *J. Chromatogr. B Analyt. Technol. Biomed. Life Sci.* **798**, 343-349 (2003).

106. Blair,I.A. Endogenous glutathione adducts. *Curr. Drug Metab* **7**, 853-872 (2006).

107. Zhu,P., Oe,T., & Blair,I.A. Determination of cellular redox status by stable isotope dilution liquid chromatography/mass spectrometry analysis of glutathione and glutathione disulfide. *Rapid Commun. Mass Spectrom.* **22**, 432-440 (2008).

108. Minkler,P.E., Kerner,J., Kasumov,T., Parland,W., & Hoppel,C.L. Quantification of malonyl-coenzyme A in tissue specimens by high-performance liquid chromatography/mass spectrometry. *Anal. Biochem.* **352**, 24-32 (2006).

109. Brass,E.P. & Beyerinck,R.A. Interactions of propionate and carnitine metabolism in isolated rat hepatocytes. *Metabolism* **36**, 781-787 (1987).

110. Perera,M.A., Choi,S.Y., Wurtele,E.S., & Nikolau,B.J. Quantitative analysis of short-chain acyl-coenzymeAs in plant tissues by LC-MS-MS electrospray ionization method. *J. Chromatogr. B. Analyt Technol. Biomed. Life. Sci.* **877**, 482-488 (2009).

111. Haynes,C.A. *et al.* Quantitation of fatty acyl-coenzyme As in mammalian cells by liquid chromatography-electrospray ionization tandem mass spectrometry. *J. Lipid Res.* **49**, 1113-1125 (2008).

112. Minkler,P.E., Kerner,J., Ingalls,S.T., & Hoppel,C.L. Novel isolation procedure for short-, medium-, and long-chain acyl-coenzyme A esters from tissue. *Anal. Biochem.* **376**, 275-276 (2008).

113. Hosokawa,Y., Shimomura,Y., Harris,R.A., & Ozawa,T. Determination of short-chain acyl-coenzyme A esters by high-performance liquid chromatography. *Anal. Biochem.* **153**, 45-49 (1986).

114. Iwasaki,K. *et al.* Effects of antiprogestins on the rate of proliferation of breast cancer cells. *Mol. Cell. Biochem.* **198**, 141-149 (1999).

115. Cao,Z. *et al.* Effects of resin or charcoal treatment on fetal bovine serum and bovine calf serum. *Endocr. Res.* **34**, 101-108 (2009).

116. Zhang,R., Sioma,C.S., Thompson,R.A., Xiong,L., & Regnier,F.E. Controlling deuterium isotope effects in comparative proteomics. *Anal. Chem.* **74**, 3662-3669 (2002).

117. Huang,Y. *et al.* Quantification of key red blood cell folates from subjects with defined MTHFR 677C>T genotypes using stable isotope dilution liquid chromatography/mass spectrometry. *Rapid Commun. Mass Spectrom.* **22**, 2403-2412 (2008).

118. Evans,J., Wang,T.C., Heyes,M.P., & Markey,S.P. LC/MS analysis of NAD biosynthesis using stable isotope pyridine precursors. *Anal. Biochem.* **306**, 197-203 (2002).

119. Bajad,S.U. *et al.* Separation and quantitation of water soluble cellular metabolites by hydrophilic interaction chromatography-tandem mass spectrometry. *J. Chromatogr. A* **1125**, 76-88 (2006).

120. Cooper,S. Reappraisal of serum starvation, the restriction point, G0, and G1 phase arrest points. *FASEB J.* **17**, 333-340 (2003).

121. Hasan,N.M., Adams,G.E., & Joiner,M.C. Effect of serum starvation on expression and phosphorylation of PKC-alpha and p53 in V79 cells: implications for cell death. *Int. J. Cancer* **80**, 400-405 (1999).

122. Shin,J.S. *et al.* Serum starvation induces G1 arrest through suppression of Skp2-CDK2 and CDK4 in SK-OV-3 cells. *Int. J. Oncol.* **32**, 435-439 (2008).

123. Kawaguchi,A., Yoshimura,T., & Okuda,S. A new method for the preparation of acyl-CoA thioesters. *J. Biochem.* **89**, 337-339 (1981).

124. Olsen,J., Bjornsdottir,I., Tjornelund,J., & Honore,H.S. Chemical reactivity of the naproxen acyl glucuronide and the naproxen coenzyme A thioester towards bionucleophiles. *J. Pharm. Biomed. Anal.* **29**, 7-15 (2002).

125. van Wyk M. & Strauss,E. One-pot preparation of coenzyme A analogues via an improved chemo-enzymatic synthesis of pre-CoA thioester synthons. *Chem. Commun.*398-400 (2007).

126. Biswas,S.K. & Rahman,I. Environmental toxicity, redox signaling and lung inflammation: the role of glutathione. *Mol. Aspects Med.* **30**, 60-76 (2009).

127. Mangal,D. *et al.* Analysis of 7,8-dihydro-8-oxo-2'-deoxyguanosine in cellular DNA during oxidative stress. *Chem. Res. Toxicol.* **22**, 788-797 (2009).

128. Ischiropoulos,H. & Gow,A. Pathophysiological functions of nitric oxide-mediated protein modifications. *Toxicology* **208**, 299-303 (2005).

129. Wood,L.G., Gibson,P.G., & Garg,M.L. Biomarkers of lipid peroxidation, airway inflammation and asthma. *Eur. Respir. J.* **21**, 177-186 (2003).

130. Ledoux,S.P. & Wilson,G.L. Base excision repair of mitochondrial DNA damage in mammalian cells. *Prog. Nucleic Acid Res. Mol. Biol.* **68**, 273-284 (2001).

131. Emerit,J., Edeas,M., & Bricaire,F. Neurodegenerative diseases and oxidative stress. *Biomed. Pharmacother.* **58**, 39-46 (2004).

132. Ladiges,W., Wanagat,J., Preston,B., Loeb,L., & Rabinovitch,P. A mitochondrial view of aging, reactive oxygen species and metastatic cancer. *Aging Cell* **9**, 462-465 (2010).

133. Ohta,S. & Ohsawa,I. Dysfunction of mitochondria and oxidative stress in the pathogenesis of Alzheimer's disease: on defects in the cytochrome c oxidase complex and aldehyde detoxification. *J. Alzheimers. Dis.* **9**, 155-166 (2006).

134. Patten,D.A., Germain,M., Kelly,M.A., & Slack,R.S. Reactive oxygen species: stuck in the middle of neurodegeneration. *J. Alzheimers. Dis.* **20 Suppl 2**, S357-S367 (2010).

135. Koopman,W.J. *et al.* Mammalian mitochondrial complex I: biogenesis, regulation, and reactive oxygen species generation. *Antioxid. Redox. Signal.* **12**, 1431-1470 (2010).

136. Selivanov,V.A. *et al.* Reactive oxygen species production by forward and reverse electron fluxes in the mitochondrial respiratory chain. *PLoS. Comput. Biol.* **7**, e1001115 (2011).

137. Hoffman,D.L. & Brookes,P.S. Oxygen sensitivity of mitochondrial reactive oxygen species generation depends on metabolic conditions. *J. Biol. Chem.* **284**, 16236-16245 (2009).

138. Grivennikova,V.G. & Vinogradov,A.D. Generation of superoxide by the mitochondrial Complex I. *Biochim. Biophys. Acta* **1757**, 553-561 (2006).

139. Giorgio,M., Trinei,M., Migliaccio,E., & Pelicci,P.G. Hydrogen peroxide: a metabolic by-product or a common mediator of ageing signals? *Nat. Rev. Mol. Cell Biol.* **8**, 722-728 (2007).

140. Tahara,E.B., Navarete,F.D., & Kowaltowski,A.J. Tissue-, substrate-, and site-specific characteristics of mitochondrial reactive oxygen species generation. *Free Radic. Biol. Med.* **46**, 1283-1297 (2009).

141. Poyton,R.O., Ball,K.A., & Castello,P.R. Mitochondrial generation of free radicals and hypoxic signaling. *Trends Endocrinol. Metab* **20**, 332-340 (2009).

142. Shiva,S. *et al.* Redox signalling: from nitric oxide to oxidized lipids. *Biochem. Soc. Symp.*107-120 (2004).

143. Mukhopadhyay,P., Rajesh,M., Yoshihiro,K., Hasko,G., & Pacher,P. Simple quantitative detection of mitochondrial superoxide production in live cells. *Biochem. Biophys. Res. Commun.* **358**, 203-208 (2007).

144. Oka,S. *et al.* Two distinct pathways of cell death triggered by oxidative damage to nuclear and mitochondrial DNAs. *EMBO J.* **27**, 421-432 (2008).

145. Flowers-Geary,L., Harvey,R.G., & Penning,T.M. Cytotoxicity of polycyclic aromatic hydrocarbon o-quinones in rat and human hepatoma cells. *Chem. Res. Toxicol.* **6**, 252-260 (1993).

146. Brown,T.P., Rumsby,P.C., Capleton,A.C., Rushton,L., & Levy,L.S. Pesticides and Parkinson's disease--is there a link? *Environ. Health Perspect.* **114**, 156-164 (2006).

147. Tanner,C.M. *et al.* Rotenone, paraquat, and Parkinson's disease. *Environ. Health Perspect.* **119**, 866-872 (2011).

148. Richardson,J.R., Quan,Y., Sherer,T.B., Greenamyre,J.T., & Miller,G.W. Paraquat neurotoxicity is distinct from that of MPTP and rotenone. *Toxicol. Sci.* **88**, 193-201 (2005).

149. Cicchetti,F., Drouin-Ouellet,J., & Gross,R.E. Viability of the rotenone model in question. *Trends Pharmacol. Sci.* **31**, 142 (2010).

150. Uversky,V.N. Neurotoxicant-induced animal models of Parkinson's disease: understanding the role of rotenone, maneb and paraquat in neurodegeneration. *Cell Tissue Res.* **318**, 225-241 (2004).

151. Cicchetti,F., Drouin-Ouellet,J., & Gross,R.E. Environmental toxins and Parkinson's disease: what have we learned from pesticide-induced animal models? *Trends Pharmacol. Sci.* **30**, 475-483 (2009).

152. Greenamyre,J.T., Betarbet,R., & Sherer,T.B. The rotenone model of Parkinson's disease: genes, environment and mitochondria. *Parkinsonism. Relat Disord.* **9 Suppl 2**, S59-S64 (2003).

153. Greenamyre,J.T., Higgins,D.S., & Eller,R.V. Quantitative autoradiography of dihydrorotenone binding to complex I of the electron transport chain. *J. Neurochem.* **59**, 746-749 (1992).

154. Koopman,W.J. *et al.* Human NADH:ubiquinone oxidoreductase deficiency: radical changes in mitochondrial morphology? *Am. J. Physiol Cell Physiol* **293**, C22-C29 (2007).

155. Betarbet,R. *et al.* Chronic systemic pesticide exposure reproduces features of Parkinson's disease. *Nat. Neurosci.* **3**, 1301-1306 (2000).

156. Cannon,J.R. *et al.* A highly reproducible rotenone model of Parkinson's disease. *Neurobiol. Dis.* **34**, 279-290 (2009).

157. Choi,W.S., Kruse,S.E., Palmiter,R.D., & Xia,Z. Mitochondrial complex I inhibition is not required for dopaminergic neuron death induced by rotenone, MPP+, or paraquat. *Proc. Natl. Acad. Sci. U. S. A* **105**, 15136-15141 (2008).

158. Balcke,G.U. *et al.* Linking energy metabolism to dysfunctions in mitochondrial respiration--a metabolomics in vitro approach. *Toxicol. Lett.* **203**, 200-209 (2011).

159. Shaham,O. *et al.* A plasma signature of human mitochondrial disease revealed through metabolic profiling of spent media from cultured muscle cells. *Proc. Natl. Acad. Sci. U. S. A* **107**, 1571-1575 (2010).

160. Xu,Q., Vu,H., Liu,L., Wang,T.C., & Schaefer,W.H. Metabolic profiles show specific mitochondrial toxicities in vitro in myotube cells. *J. Biomol. NMR* **49**, 207-219 (2011).

161. Garmier,M. *et al.* Complex I dysfunction redirects cellular and mitochondrial metabolism in Arabidopsis. *Plant Physiol* **148**, 1324-1341 (2008).

162. Fernandez,C.A., Des,R.C., Previs,S.F., David,F., & Brunengraber,H. Correction of 13C mass isotopomer distributions for natural stable isotope abundance. *J. Mass Spectrom.* **31**, 255-262 (1996).

163. Ward,P.S. *et al.* The common feature of leukemia-associated IDH1 and IDH2 mutations is a neomorphic enzyme activity converting alpha-ketoglutarate to 2-hydroxyglutarate. *Cancer Cell* **17**, 225-234 (2010).

164. Bunik,V.I. 2-Oxo acid dehydrogenase complexes in redox regulation. *Eur. J. Biochem.* **270**, 1036-1042 (2003).

165. Tretter,L. & Adam-Vizi,V. Inhibition of Krebs cycle enzymes by hydrogen peroxide: A key role of [alpha]-ketoglutarate dehydrogenase in limiting NADH production under oxidative stress. *J. Neurosci.* **20**, 8972-8979 (2000).

166. Bulteau,A.L., Ikeda-Saito,M., & Szweda,L.I. Redox-dependent modulation of aconitase activity in intact mitochondria. *Biochemistry* **42**, 14846-14855 (2003).

167. Zhang,Z. *et al.* Identification of lysine succinylation as a new post-translational modification. *Nat. Chem. Biol.* **7**, 58-63 (2011).

168. Houten,S.M. & Wanders,R.J. A general introduction to the biochemistry of mitochondrial fatty acid beta-oxidation. *J. Inherit. Metab Dis.* **33**, 469-477 (2010).

169. Yang,S.Y., He,X.Y., & Schulz,H. 3-Hydroxyacyl-CoA dehydrogenase and short chain 3-hydroxyacyl-CoA dehydrogenase in human health and disease. *FEBS J.* **272**, 4874-4883 (2005).

170. Korman,S.H. Inborn errors of isoleucine degradation: a review. *Mol. Genet. Metab* **89**, 289-299 (2006).

171. Greenamyre,J.T., Cannon,J.R., Drolet,R., & Mastroberardino,P.G. Lessons from the rotenone model of Parkinson's disease. *Trends Pharmacol. Sci.* **31**, 141-142 (2010).

172. Fernandez-Checa,J.C. *et al.* Oxidative stress and altered mitochondrial function in neurodegenerative diseases: lessons from mouse models. *CNS. Neurol. Disord. Drug Targets.* **9**, 439-454 (2010).

173. Mancuso,C. *et al.* Mitochondrial dysfunction, free radical generation and cellular stress response in neurodegenerative disorders. *Front Biosci.* **12**, 1107-1123 (2007).

174. Santos,R. *et al.* Friedreich ataxia: molecular mechanisms, redox considerations, and therapeutic opportunities. *Antioxid. Redox. Signal.* **13**, 651-690 (2010).

175. Lodi,R., Tonon,C., Calabrese,V., & Schapira,A.H. Friedreich's ataxia: from disease mechanisms to therapeutic interventions. *Antioxid. Redox. Signal.* **8**, 438-443 (2006).

176. Rouault,T.A. & Tong,W.H. Iron-sulphur cluster biogenesis and mitochondrial iron homeostasis. *Nat. Rev. Mol. Cell Biol.* **6**, 345-351 (2005).

177. Pandolfo,M. & Pastore,A. The pathogenesis of Friedreich ataxia and the structure and function of frataxin. *J. Neurol.* **256 Suppl 1**, 9-17 (2009).

178. Ye,H. & Rouault,T.A. Human iron-sulfur cluster assembly, cellular iron homeostasis, and disease. *Biochemistry* **49**, 4945-4956 (2010).

179. Schmucker,S. & Puccio,H. Understanding the molecular mechanisms of Friedreich's ataxia to develop therapeutic approaches. *Hum. Mol. Genet.* **19**, R103-R110 (2010).

180. Pandolfo M. Friedreich ataxia: the clinical picture. J Neurol. 256, 3-8. 2009.

Ref Type: Generic

181. Khan,R.J., Andermann,E., & Fantus,I.G. Glucose intolerance in Friedreich's ataxia: association with insulin resistance and decreased insulin binding. *Metabolism* **35**, 1017-1023 (1986).

182. Lynch,D.R., Farmer,J.M., & Wilson,R.B. Mortality in Friedreich's Ataxia. *Tex. Heart Inst. J* **34**, 502-503 (2007).

183. Kearney,M., Orrell,R.W., Fahey,M., & Pandolfo,M. Antioxidants and other pharmacological treatments for Friedreich ataxia. *Cochrane. Database. Syst. Rev.*CD007791 (2009).

184. Tsou,A.Y., Friedman,L.S., Wilson,R.B., & Lynch,D.R. Pharmacotherapy for Friedreich ataxia. *CNS. Drugs* **23**, 213-223 (2009).

185. Babady,N.E. *et al.* Advancements in the pathophysiology of Friedreich's Ataxia and new prospects for treatments. *Mol. Genet. Metab* **92**, 23-35 (2007).

186. Lynch,D.R., Farmer,J.M., Balcer,L.J., & Wilson,R.B. Friedreich ataxia: effects of genetic understanding on clinical evaluation and therapy. *Arch. Neurol.* **59**, 743-747 (2002).

187. Myers,L. *et al.* Antioxidant use in Friedreich ataxia. *J Neurol. Sci.* **267**, 174-176 (2008).

188. Friedman,L.S. *et al.* Measuring the rate of progression in Friedreich ataxia: implications for clinical trial design. *Mov Disord.* **25**, 426-432 (2010).

189. Sutak,R. *et al.* Proteomic analysis of hearts from frataxin knockout mice: marked rearrangement of energy metabolism, a response to cellular stress and altered expression of proteins involved in cell structure, motility and metabolism. *Proteomics.* **8**, 1731-1741 (2008).

190. Selak,M.A. *et al.* Blood cells from Friedreich ataxia patients harbor frataxin deficiency without a loss of mitochondrial function. *Mitochondrion.* **11**, 342-350 (2011).

191. Lu,C. & Cortopassi,G. Frataxin knockdown causes loss of cytoplasmic iron-sulfur cluster functions, redox alterations and induction of heme transcripts. *Arch. Biochem. Biophys.* **457**, 111-122 (2007).

192. Tan,G., Napoli,E., Taroni,F., & Cortopassi,G. Decreased expression of genes involved in sulfur amino acid metabolism in frataxin-deficient cells. *Hum. Mol. Genet.* **12**, 1699-1711 (2003).

193. MacDonald,M.J. Differences between mouse and rat pancreatic islets: succinate responsiveness, malic enzyme, and anaplerosis. *Am. J. Physiol Endocrinol. Metab* **283**, E302-E310 (2002).

194. Marroquin,L.D., Hynes,J., Dykens,J.A., Jamieson,J.D., & Will,Y. Circumventing the Crabtree effect: replacing media glucose with galactose increases susceptibility of HepG2 cells to mitochondrial toxicants. *Toxicol. Sci.* **97**, 539-547 (2007).

195. Deutsch,E.C. *et al.* A rapid, noninvasive immunoassay for frataxin: utility in assessment of Friedreich ataxia. *Mol. Genet. Metab* **101**, 238-245 (2010).

196. Plymoth,A. & Hainaut,P. Proteomics beyond proteomics: toward clinical applications. *Curr. Opin. Oncol.* **23**, 77-82 (2011).

197. Petricoin,E.F. *et al.* Use of proteomic patterns in serum to identify ovarian cancer. *Lancet* **359**, 572-577 (2002).

198. Brower,V. Biomarkers: Portents of malignancy. *Nature* **471**, S19-S21 (2011).

199. Ebeling,P.R. & Akesson,K. Role of biochemical markers in the management of osteoporosis. *Best. Pract. Res. Clin. Rheumatol.* **15**, 385-400 (2001).

200. Brawer,M.K. Laboratory studies for the detection of carcinoma of the prostate. *Urol. Clin. North Am.* **17**, 759-768 (1990).

201. Berk,M., Ebbels,T., & Montana,G. A statistical framework for biomarker discovery in metabolomic time course data. *Bioinformatics.* **27**, 1979-1985 (2011).

202. Beer,S.F., Heaton,D.A., Alberti,K.G., Pyke,D.A., & Leslie,R.D. Impaired glucose tolerance precedes but does not predict insulin-dependent diabetes mellitus: a study of identical twins. *Diabetologia* **33**, 497-502 (1990).

203. Saudek,C.D., Derr,R.L., & Kalyani,R.R. Assessing glycemia in diabetes using self-monitoring blood glucose and hemoglobin A1c. *JAMA* **295**, 1688-1697 (2006).

204. Naydenov,A.V., MacDonald,M.L., Ongur,D., & Konradi,C. Differences in lymphocyte electron transport gene expression levels between subjects with bipolar disorder and normal controls in response to glucose deprivation stress. *Arch. Gen. Psychiatry* **64**, 555-564 (2007).

205. Deodato,F., Boenzi,S., Santorelli,F.M., & Dionisi-Vici,C. Methylmalonic and propionic aciduria. *Am. J. Med. Genet. C. Semin. Med. Genet.* **142C**, 104-112 (2006).

206. Ugarte,M. *et al.* Overview of mutations in the PCCA and PCCB genes causing propionic acidemia. *Hum. Mutat.* **14**, 275-282 (1999).

207. Metallo,C.M., Walther,J.L., & Stephanopoulos,G. Evaluation of 13C isotopic tracers for metabolic flux analysis in mammalian cells. *J. Biotechnol.* **144**, 167-174 (2009).

208. Bradley,J.L., Homayoun,S., Hart,P.E., Schapira,A.H., & Cooper,J.M. Role of oxidative damage in Friedreich's ataxia. *Neurochem. Res.* **29**, 561-567 (2004).

209. Ferrarese,C. *et al.* Reduced platelet glutamate uptake in Parkinson's disease. *J. Neural Transm.* **106**, 685-692 (1999).

210. Ferrarese,C. *et al.* Decreased platelet glutamate uptake in patients with amyotrophic lateral sclerosis. *Neurology* **56**, 270-272 (2001).

211. Ferrarese,C. *et al.* Glutamate uptake is decreased in platelets from Alzheimer's disease patients. *Ann. Neurol.* **47**, 641-643 (2000).

212. Zoia,C.P. *et al.* Fibroblast glutamate transport in aging and in AD: correlations with disease severity. *Neurobiol. Aging* **26**, 825-832 (2005).

213. Ferreira,L.M. Cancer metabolism: the Warburg effect today. *Exp. Mol. Pathol.* **89**, 372-380 (2010).